# UNIVERSITÉ DE STRASBOURG

*ÉCOLE DOCTORALE DES SCIENCES DE LA VIE ET DE LA SANTÉ*

# THÈSE présentée par :


## Valentina PALLOTTINI


soutenue le : **13 novembre 2017**

pour obtenir le grade de : **Docteur de l'université de Strasbourg**

Discipline/ Spécialité : Sciences de la vie - Biologie des organismes : développement et physiologie

# Rôle de la voie mévalonate dans le système nerveux central

**THÈSE dirigée par :**

| | |
|---|---|
| **M. Frank PFRIEGER** | DR2, Université de Strasbourg |

**RAPPORTEURS :**

| | |
|---|---|
| **Mme Lucia CIRANNA** | Professeur, Universita di Catania |
| **Mme Carole ESCARTIN** | CR1 HdR, CEA |

**AUTRES MEMBRES DU JURY :**

| | |
|---|---|
| **M. Hubert SCHALLER** | DR2, Université de Strasbourg |
| **M. Thomas BACH** | Professeur émérite, Université de Strasbourg |
| **M. Gianfranco CARLOMAGNO** | Professionnel, Farmares s.r.l. |
| **M. Emmanuel CAILLAUD** | Professeur, Université de Strasbourg |
| **Mme Anne LAIDEBEUR** | Chargée d'ingénierie, Université de Strasbourg – service VAE |

PhD SCHOOL: LIFE SCIENCES AND HEALTH

BIOLOGY OF ORGANISMS: DEVELOPMENT AND PHYSIOLOGY.

**PhD thesis**

# ROLE OF THE MEVALONATE PATHWAY IN THE CENTRAL NERVOUS SYSTEM

ECOLE DOCTORAL: SCIENCES DE LA VIE ET DE LA SANTÉ

BIOLOGIE DES ORGANISMS: DEVELOPPEMENT ET PHYSIOLOGIE.

Thèse de doctorat

# RÔLE DE LA VOIE DE MEVALONATE DANS LE SYSTÈME NERVEUX CENTRAL


**STUDENT**

**Valentina Pallottini**

**SUPERVISOR**

**Dr. Frank W. Pfrieger**

**Table of content**

*Ad Andrea*
*senza di te tutto questo non sarebbe stato possibile, mi hai sempre incoraggiata e portata per mano là dove non credevo di poter arrivare. Grazie amore mio!*

## Summary in French

La voie biosynthétique du mevalonate (MVA) est une voie métabolique essentielle qui amène à la production de molécules (ex. cholestérol, dolichol, prenil, ubiquinone) qui sont essentielles dans grand nombre de processus physiologiques (Dietschy and Turley, 2004).

Différentes études ont émis l'hypothèse que les produits finaux de cette voie biosynthétique ont un rôle important dans la physiologie du Système Nerveux Central (SNC) (Baytan et al., 2008; Geppert and Sudhof, 1998; Krakowski and Czobor, 2011): En particulier, le cholestérol fournit aux axones l'isolation électrique qui est essentielle pour la conduction saltatoire de l'impulsion, mais qui est aussi fondamentale pour la formation et la stabilité des synapses (Mauch et al., 2001; Pfrieger and Ungerer, 2011) : en outre, l'importance de la voie du MVA dans les processus physiologiques du SNC est ultérieurement soutenue par des études cliniques qui démontrent comment les perturbations de la biosynthétique du MVA sont concomitants avec plusieurs neuropathologies (Valenza and Cattaneo, 2011; Segatto et al., 2014a; Wang, 2014). Malgré toutes ces observations, la plupart des études effectuées sur le rôle physiologique de cet important processus métabolique dans le SNC restent simplement en corrélation. Pour autant, le but des études présentées dans cette thèse a été:

1) évaluer la présence et la régulation des protéines concernées dans le maintien de la voie du MVA dans différentes régions du cerveaux de rat en prenant en considération l'éventuelle modulation selon le sexe et l'âge ;
2) analyser l'impact de l'inhibition du 3-hydroxy-3-méthylglutaryl coenzyme A reductase (HMGCR), enzyme clef et vitesse limitant de la voie biosynthétique du MVA, sur le développement des neurones set sur le comportement des rats;
3) explorer si la voie biosynthétique du MVA est en quelque sorte modifiée dans une pathologie du neurodéveloppement comme l'autisme.

Les résultats obtenus démontrent que la voie biosynthétique du MVA est régulée différemment selon la région du cerveau analysée, ceci probablement dépend du métabolisme de chacune mais surtout de la nécessité des ses produits finals dans chaque région spécifique. La voie biosynthétique est modulée aussi en fonction de l'âge et du sexe dans chaque région cérébrale (Segatto et al., 2012 ; Segatto et al., 2013) : Une partie importante des résultats obtenus durant mon travail de recherche met en lumière comment la voie biosynthétique du MVA revêt un rôle critique dans la modulation physiologique du comportement animal et du

développement des neurones car, l'inhibition pharmacologique du HMGCR induit anxiété sociale et amélioration de la mémoire des rats (Segatto et al., 2014b) et augmente la vitesse d'allongement des néurites dans un modèle *in vitro* (Cartocci et al., 2016). Pour finir, mes données démontrent, dans un modèle expérimental d'autisme, que la voie biosynthétique du MVA est modulée dans plusieurs région du SNC selon l'âge (Cartocci et al., en révision).

Pour conclure, mes études fournissent des nouvelles connaissances sur le rôle de la voie biosynthétique du MVA sur le cerveau, démontrant que ce processus métabolique est exprimé et régulé extrêmement selon la région cérébrale étudiée et qu'il y a des différences très importantes selon le sexe et l 'âge. L'impact de la voie biosynthétique du MVA sur le comportement et sur le développement des neurones, et le fait que cette voie métabolique soit altérée sur le modèle animal d'autisme, nous suggèrent que les différentes protéines impliquées et les produits finaux puissent contribuer à la survenue de pathologies neurologiques et qu'elles puissent être considérées des cibles potentielles moléculaires pour dessiner des nouvelles stratégies thérapeutiques pour le traitement de certains désordres du SNC.

## Summary in English

The mevalonate (MVA) pathway is an essential metabolic pathway that leads to the production of molecules (e.g. cholesterol, dolichol, prenyls, ubiquinone) important in several physiological processes. Notably, these products play pivotal roles in the brain. In particular, cholesterol provides electrical insulation to the axon that is essential for the conduction of rapid saltatory impulse, but it is also critical for synapse formation and stability. Moreover, the importance of cholesterol in CNS processes is further supported by clinical studies, which demonstrate that an imbalance in the MVA pathway is accompanied by the onset of several neuropathological descriptions. Despite these observations, the physiological importance of this metabolic process in the brain has remained unclear. My aim was to study the presence and the regulation of the proteins involved in the MVA pathway in different rat brain areas in a sex- and age-dependent manner, to analyze the impact of the key enzymes on neuronal development and on rat behavior, and to explore whether the MVA pathway is affected in a neurodevelopmental disease such as autism. My results provide clear evidence that the MVA pathway is differently regulated in each brain area, according to the metabolism and the regional requirement of end-products. Moreover, the MVA pathway also undergoes specific age- and sex-dependent modulation in each brain region. My work also highlights a critical role of the MVA pathway in neuronal development and in the physiological modulation of behavior and cognition. Inhibition of the key enzyme of the pathway induced the occurrence of social anxiety-related behaviors and memory improvements in rats and enhanced neurite outgrowth in an in vitro model. Finally, I demonstrated, in an experimental model of autism, that the MVA pathway is modulated in different brain areas in an age-dependent manner.

In conclusion, my studies provide new insights in the physiology of the MVA pathway in the brain. They demonstrate that this metabolic process is expressed and modulated in a highly region-dependent manner and that age and sex induce physiological differences. Notably, the impact of the MVA pathway on behavior and neuronal development suggest that different proteins and enzymatic products may be considered as potential molecular targets when designing novel therapeutic approaches for the treatment of these pathologies.

# Introduction

The mevalonate (MVA) pathway produces several molecules including cholesterol, prenyls, ubiquinone, dolichol that are crucial for a plethora of physiological processes. It has been extensively studied in the liver, where a large fraction of cholesterol is synthesized. However the metabolic pathway is active in all tissues. Clinical studies demonstrate that an imbalance of isoprenoid homoeostasis is accompanied by the onset of several neuropathologies underlining the importance of the end products for the central nervous system (CNS). However, the scientific literature is fragmented and no systematic studies had been performed to investigate the MVA pathway in the CNS. The work I present here addresses this gap, taking into account sex- and age-dependent modulation of the MVA pathway in selected brain areas, and its pathophysiological role in brain.

## Mevalonate pathway

The first committed steps of the MVA pathway (Fig. 1) are the repeated condensation of acetyl-CoA units, resulting in 3β-hydroxy 3β-methylglutharyl coenzyme A (HMG-CoA), and its subsequent reduction to MVA. The reduction utilizes two molecules of NADPH in a two-step reaction that is considered rate-limiting for cholesterol biosynthesis.

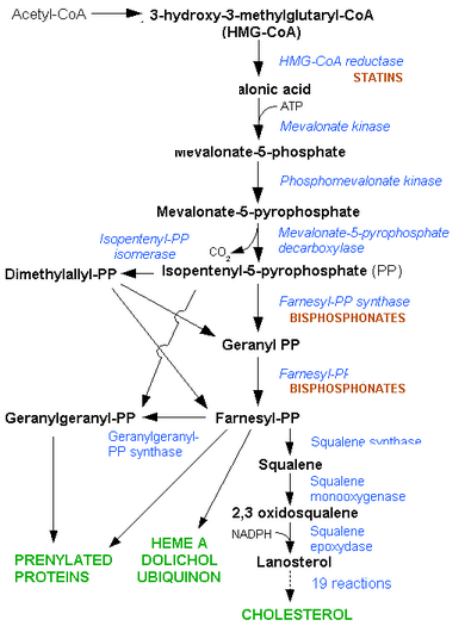


***Figure 1.*** *Schematic representation of the main steps of mevalonate pathway.*

It is mediated by the 3β-hydroxy 3β-methylglutharyl coenzyme A reductase (HMGCR) (Fig. 2), one of the best studied enzymes in biochemistry.

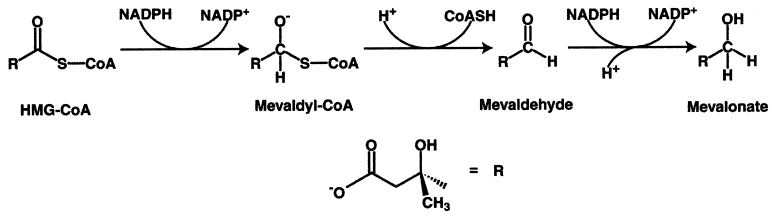


***Figure 2.*** *Transformation of HMG-CoA into MVA. The reductive deacylation of HMG-CoA to MVA is thought to proceed in three steps, with mevaldyl-CoA and mevaldehyde as reaction intermediates (Istvan and Deisenhofer, 2000).*

The following steps are additions of two phospho groups to MVA requiring two molecules of ATP (Istvan and Deisenhofer, 2000). Subsequent dehydration-decarboxylation of MVA-PP results in isopentenyl pyrophosphate (IPP), the building block for the different products of the pathway (Rozman and Monostory, 2010). IPP can be isomerized to dimethylallyl

pyrophosphate by the isopentenyl pyrophosphate isomerase (IPI1). IPP and dimethylallyl pyrophosphate condense to form the C-10 geranyl pyrophosphate, which in turn condenses with another molecule of IPP to produce the C-15 farnesyl pyrophosphate (FPP) by farnesyl pyrophosphate synthase (FDPS) (Rozman and Monostory, 2010). From FPP originates either sterol and non-sterol branches of the pathway. Non-sterol branches produce, among others, ubiquinone, isoprenyls and dolichol. On the other hand, squalene synthase catalyzes the first reaction of the sterol branch producing the C-30 squalene from two molecules of farnesyl pyrophosphate in a reaction that requires NADPH. Cholesterol is finally synthesized by 21 additional reactions (Bentinger et al., 2008).

## The key enzyme and end-products

### HMGCR activity and regulation

HMGCR is a glycoprotein embedded in the endoplasmic reticulum (ER). It consists of three domains: the C-terminal domain of HMGCR contains the catalytic region (residues 460–888) located in the cytosol and a linker domain (residues 340–459) that connects the N- and the C-terminal portions of the protein (Friesen and Rodwell, 2004). The N-terminal domain contains 339 residues, this part of the enzyme spans eight times the ER membrane and contains the Sterol Sensing Domain (SSD). This domain is found in several proteins that are involved in cholesterol homeostasis. The activity of this enzyme is rapidly regulated by phosphorylation/dephosphorylation (Fig. 5 A). The reversible phosphorylation of the residue S872 inhibits the catalytic activity of the enzyme (Beg et al., 1985). AMP-activated Kinase (AMPK) is known to be the main regulator of HMGCR in the liver. AMPK regulates energy homeostasis in response to changes in the cellular AMP/ATP ratio (Hardie et al., 2016). HMGCR dephosphorylation, which re-activates the enzyme, is principally catalyzed by protein phosphatase 2A (PP2A), a serine/threonine phosphatase regulating several cellular processes (Janssens and Goris, 2001). The increase of sterols induces the binding of HMGCR to INSulin Induced Gene (INSIG) that promotes the ubiquitination and proteasomal degradation of the enzyme (Sever et al., 2003) (Fig. 3C).

HMGCR is subjected to transcriptional regulation by an elaborated feedback mechanism that depends, once again, on the cellular level of sterols and that involves several key proteins. Sterol levels are sensed by an ER-embedded protein named Sterol Regulatory Element Binding Protein (SREBP) Cleavage Activating Protein (SCAP), which also contains a SSD. When the sterol content of the ER is low, SCAP binds the transcription factors SREBPs and

transports them from the ER to the Golgi apparatus. Here, the SREBPs are proteolytically cleaved to active fragments (nSREBPs) that enter the nucleus and induce the transcription of their target genes (Brown and Goldstein, 1999). These genes mediate cholesterol synthesis and uptake and include HMGCR and Low Density Lipoprotein receptor (LDLR) (Brown and Goldstein, 1997).

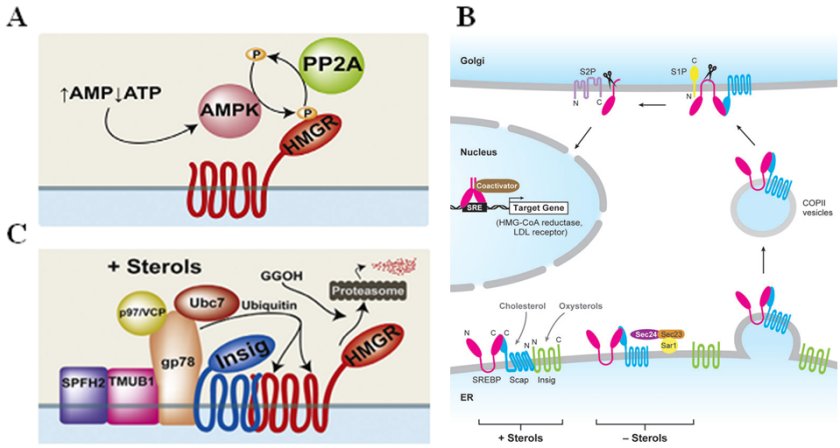


***Figure 3.*** *Schematic illustration of HMGCR short (**A**) and long (**B**, **C**) term regulations. In particular, panel **B** and **C** show the regulation of HMGCR transcription (**B**) and degradation (**C**) as a function of intracellular sterol amount and of cholesterol uptake (Burg and Espenshade, 2011).*

When the sterol content increases in the ER, the SCAP/SREBP complex binds to INSIG and remains in the ER, so the transcription of its target genes declines (Fig. 3 B) (Yang et al., 2002).

Several hormones, such as insulin, glucagon, glucocorticoids, estrogens, and thyroid hormones control the transcription and translation of hepatic HMGCR in mammals. Insulin promotes *HMGCR* transcription and protein activity, whereas glucagon induces the opposite. Both factors also mediate changes of hepatic HMGCR activity during the circadian rhythm (Ness and Chambers, 2000). Thyroid hormones increase hepatic HMGCR levels by enhancing the level and stability of encoding transcripts, whereas glucocorticoids destabilize HMGCR mRNA. The effects of estrogens on HMGCR activity are still debated. Some studies suggest that estrogens increase hepatic HMGCR protein levels by stabilizing mRNA levels and increasing the transcription rate. On the other hand, estrogen deficiency elevates serum cholesterol levels also called hypercholesterolemia (Ness and Chambers, 2000). Studies performed on cell lines and on male rats *in vivo* show that estrogens increase LDLR at the mRNA and protein level, which causes subsequently a decrease in of HMGCR (Messa et al., 2005);(Pallottini et al., 2006).

### *Products of the MVA pathway: Cholesterol*

Cholesterol (Cholest-5-en-3-ol) is the most abundant sterol in vertebrates (Dietschy and Turley, 2004). The main source in the body is endogenous biosynthesis (Fig. 4). Hepatocytes in the liver synthetize a large fraction of cholesterol, but all organs in the body are able to produce significant amounts of this sterol (Dietschy and Turley, 2004). The rate of biosynthesis varies inversely with the amount of cholesterol ingested by the diet (Nervi et al., 1975). During digestion, cholesterol esters are metabolized into unesterified cholesterol and long chain fatty acids. Unesterified cholesterol enters the enterocyte through a transporter located at the apical membrane of the cell, the Niemann-Pick C1-like 1 protein (NPC1L1) (Martini and Pallottini, 2007;Trapani et al., 2011). Within enterocytes, approximately half of cholesterol molecules move to the endoplasmic reticulum, where cholesterol is esterified by acyl-CoA:cholesterol acyltransferase (ACAT) and incorporated into chylomicrons (CMs) that reach the lymph and enter the blood circulation. Unesterified cholesterol is exported from the endosomal-lysosomal system and incorporated into cellular membranes.

Cholesterol synthesized in the liver is delivered to extrahepatic tissues via Very Low Density Lipoproteins (VLDL), which are gradually converted into Intermediate-Density Lipoproteins (IDL) and LDL. When the need of cholesterol is high, cells take up LDL by LDLR-mediated endocytosis (Goldstein et al., 1985). The reverse cholesterol transport from extrahepatic tissues to the liver is mediated by HDLs. While it is being transported, cholesterol is acylated by lecithin cholesterol acyltransferase (LCAT), which facilitates its transport in the core of the lipoproteins. In addition, HDLs promote CM and VLDL turnover by exchanging lipids and apolipoproteins (Nilsson and Duan, 2006).

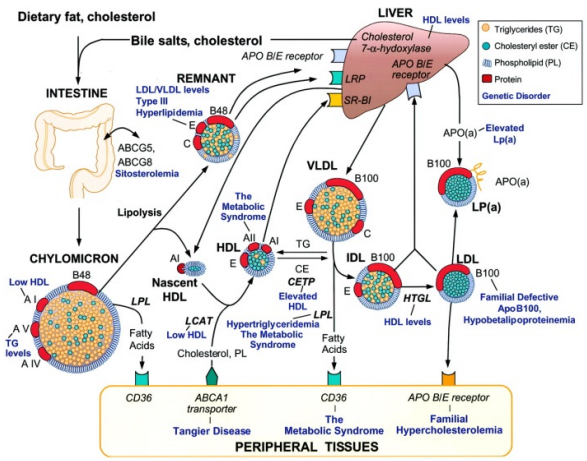


***Figure 4.*** *Schematic illustration of cholesterol metabolism in the whole body. Several genetic mutations can interfere with the maintenance of cholesterol homeostasis, thus leading to the manifestation of a plethora of disorders (Burg and Espenshade, 2011).*

The biological role of cholesterol is dictated by its particular physical and chemical properties. The molecule has three parts (Fig. 5): the rigid and flat lipophilic steroid core mediates its insertion in the lipid bilayer. The apolar hydrocarbon tail anchors the molecule in the lipid bilayer. The polar hydroxyl head group allows for hydrophilic interactions and can be chemically modified, for example by esterification.

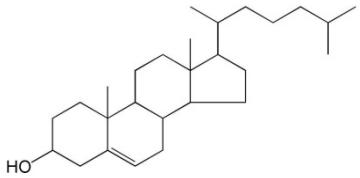


***Figure 5.*** *Structure of cholesterol molecule.*

Cholesterol determines key properties of biological membranes: it modulates their fluidity and permeability and the function of integral proteins. Cholesterol together with other lipids and proteins also forms microdomains called membrane lipid rafts that coordinate the function and the subcellular sorting of several signaling molecules (Tabas, 2002). Rafts are composed of sphingolipids and cholesterol in the outer extracellular leaflet, and connected to phospholipids and cholesterol in the inner cytoplasmic leaflet of the membrane bilayer. Besides its structural role, unesterified cholesterol serves as precursor of several compounds important for mammalian physiology. This includes bile acids, vitamin D and steroid hormones, connecting this fascinating molecule to essential physiologic functions such as nutrition, metabolism, inflammation, immune functions, electrolyte balance and reproduction (Tabas, 2002).

### *Products of the MVA pathway: Ubiquinone (CoQ)*

CoQ consists of a highly substituted benzoquinone ring and an all-*trans* poly-isoprenoid side-chain at carbon 6 (Fig. 6).

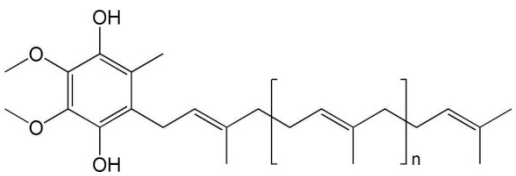


***Figure 6.*** *Structure of CoQ molecule.*

CoQ was originally described as an important component of the mitochondrial respiratory chain, where it serves as electron carrier from complex I and II to complex III (Mitchell, 1975). A reduction of CoQ synthesis can cause dysfunction of the electron transport chain and thereby reduce intracellular ATP levels, which disturbs the energy balance, increases radical production and triggers apoptosis. In addition to its key role in energy metabolism, many more functions have been attributed to this lipid. This includes cell growth and differentiation (Gomez-Diaz et al., 1997), antioxidant (Bentinger et al., 2008), anti-apoptotic (Papucci et al., 2003), anti-inflammatory (Bentinger et al., 2008), anti-atherosclerotic activities (Thomas et al., 1996). Moreover, it was shown that it prevents also endothelial dysfunction (Hamilton et al., 2007).

### *Products of the MVA pathway: Dolichol*

Dolichols are long-chain compounds containing variable numbers of isoprene units. In particular, mammalian cells synthesize chains of 18–21 units of IPP (Fig 7) (Rip et al., 1985; Holstein and Hohl, 2004). The biologic functions of these molecules are debated. It is well accepted that the phosphorylated form of dolichol acts as cofactor in the biosynthesis of glycoproteins. It has been implied in the fusion and differentiation of rat skeletal muscle myoblasts and in the fusion of rat liver microsomes (Belo et al., 1993). Non-phosphorylated dolichol seems to modify the organization and packing of phospholipids in model membranes and to destabilize their structure (Vigo et al., 1984;Parentini et al., 2005). Moreover, dolichol may serve as an indicator of aging (Parentini et al., 2005) and cellular stress (Surmacz and Swiezewska, 2011), it may be involved in intracellular traffic of proteins (Buczkowska et al., 2015) and in cellular defense against adverse environmental conditions (Welti and Hulsmeier, 2014).

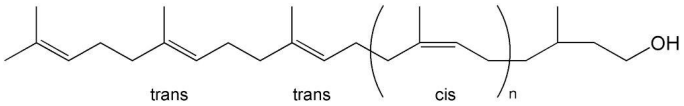


***Figure 7.*** *Structure of dolichol molecule.*

### *Products of the MVA pathway: prenyls*

Prenylation is a post-translational modification of proteins, where 15 (farnesyl) or 20 (geranylgeranyl) isoprenoid units are added to specific cysteines near the *C*-terminus (Fig. 8) (Shepherd et al., 1995). Prenylation requires three steps: the recognition of the “CAAX” box

sequence, proteolysis of the "AAX" sequence, and methyl esterification of the new *C*-terminal cysteine. This type of modification enables attachment of proteins to membranes (Ridker et al., 2001) or interactions with specific targets (Yamazaki et al., 1995). Many signalling pathways require prenylated proteins and 2% of the mammalian proteins are subjected to this modification (Anderson et al., 1995).

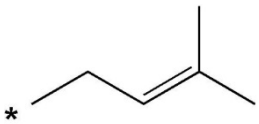

***Figure 8.*** *Generic structure of a prenyl group.*

Prominent targets of prenylation are members of the small G protein family. The Ras family comprising 36 members in mammals mediates cell growth and differentiation, whereas the Rho family with 22 mammalian members is responsible for the cytoskeleton remodelling and for the vesicular transport by regulating the actin dynamics. Rab and Arf proteins with more than 60 members in humans regulate intracellular traffic of vesicular carriers between cellular organelles (Cherfils and Zeghouf, 2013). Small GTPases alternate between two different conformations (Vetter and Wittinghofer, 2001) (Fig. 9). The GDP-bound form is considered inactive, whereas the GTP-bound form switches on downstream pathways by binding effector proteins. The exchange of guanine nucleotides is mediated by socalled guanine nucleotide exchange factors (GEFs) enabling GDP dissociation, and by GTPase activating proteins (GAPs) inducing GTP hydrolysis (Bos et al., 2007). The molecular activation complex contains a small GTPase, a GEF and a GAP.

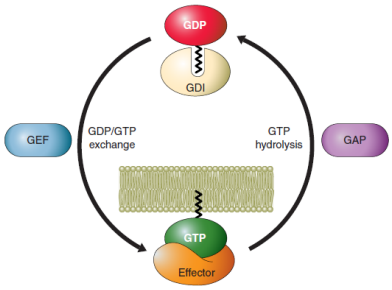


***Figure 9.*** *Regulation of the GDP/GTP switch (inactivation/activation cycle) by GEFs, GAPs, and GDIs (Cherfils and Zeghouf, 2013).*

Guanine dissociation inhibitors (GDIs) can form soluble complexes with prenylated small GTPases that prevent their insertion into the membrane (Takai et al., 2001) (Fig. 9). Prenylation targets the small GTPases to membranes inducing their activation. Ras is

farnesylated, whereas Rab and Rho require two geranylgeranyl groups (Nakagami et al., 2003).

## Role of mevalonate pathway in the brain

Cholesterol is a key molecule for the physiological functions of neurons. Its importance in the CNS is clearly indicated by growing evidence that an imbalance in cholesterol homoeostasis causes or contributes to CNS diseases (Martin et al., 2014; Segatto et al., 2014a; Cartocci et al., 2017). Cholesterol determines the thickness, fluidity (Ohvo-Rekila et al., 2002) and ion permeability of biological membranes (Haines, 2001) and thereby influences the excitability of neurons. Cholesterol is also crucial for the formation and stability of synapses, where is ensures formation of vesicles and the functional integrity of pre- and postsynaptic components like transmitter receptors (Mauch et al., 2001; Martin et al., 2014). Overall, the need of cholesterol in the brain is probably high (Goritz et al., 2005), last not least because it is a key component of myelin, the insulating sheath around axons that is formed by oligodendrocytes (Saher and Stumpf, 2015). In fact, myelin contains up to 70% of all cholesterol in the brain (Snipes and Orfali, 1998). The high content of cholesterol in myelin explains why the brain contains about 25% of the total body cholesterol although it constitutes only 2% of the body weight (Pfrieger, 2003a). In peripheral tissues, the demand for cholesterol is met by local *de novo* biosynthesis and by cellular uptake of cholesterol-containing lipoproteins. In the CNS, the blood brain barrier (BBB) blocks lipoprotein uptake from the circulation, therefore cholesterol must be synthesized *de novo* within this organ (Bjorkhem and Meaney, 2004). A major question is still, which cells produce cholesterol. One hypothesis suggests that postnatally, neurons reduce or even abandon their own synthesis and import cholesterol from astrocytes. According to *in vitro* studies, astrocytes synthesize at least 2- to 3-fold more cholesterol than neurons and fibroblasts (Pfrieger, 2003b; Nieweg et al., 2009). Astrocytes can secrete cholesterol-rich lipoproteins containing apolipoprotein E (APOE) in vitro (Shanmugaratnam et al., 1997). APOE binds to LDLR family members, whose expression is high in neurons and thereby mediates lipoprotein uptake (Pfrieger, 2003b). In addition to LDLR, ATP-binding cassette (ABC) transporters play a key role in shuttling cholesterol from astrocytes to neurons. In particular, ABCA1 is highly expressed in astrocytes and mediates cholesterol transport to extracellular lipid-free APOA1 and APOE (Oram and Heinecke, 2005). This model is further supported by recent results from van Deijk and collaborators (van

Deijk et al., 2017) demonstrating in vivo that astrocyte lipid metabolism is critical for proper development of presynaptic terminals and for hippocampal function.

If neurons depend on cholesterol import, they should also prevent overload. To remove a surplus of cholesterol, the CNS neurons produce 24-S-Hydroxycholesterol (24-OHC) through the action of the enzyme CYP46. 24-OHC is able to cross the BBB, thus preventing accumulation of cholesterol in the CNS (Leoni and Caccia, 2013). It has been demonstrated that 24-OHC is continuously synthesized and released into the systemic circulation both in rats (Bjorkhem et al., 1997) and in humans (Lutjohann et al., 1996). Moreover, 24-OHC is a ligand for LXRs, which in turn activate APOE and ABCA1 expression (Karasinska and Hayden, 2011) (Fig. 10).

Apart from cholesterol, other MVA end-products play also crucial roles in CNS metabolism and functions. CoQ protects brain cells from central neurotoxic damages (Young et al., 2007) and clinical studies suggested that low levels of CoQ10 play a role in the pathophysiology of myalgic encephalomyelitis/chronic fatigue syndrome (Maes et al., 2009). Isoprenylation of specific proteins plays important roles in the CNS. Farnesylated Ras mediates specific aspects of synaptic plasticity and thus contributes to learning and memory processes (Mazzucchelli and Brambilla, 2000). Geranylated RhoA is involved in the structural modulation of synaptic connectivity (Lingor et al., 2007) and its activity has been associated with developmental disabilities such as mental retardation (Ramakers and Storm, 2002). Geranlyated Rab3 is involved in neurotransmitter release by synaptic vesicle exocytosis (Geppert and Sudhof, 1998). Finally, defective dolichol metabolism causes a syndrome presenting cerebellar ataxia (Morava et al., 2011). Together, there is evidence that all end-products of the MVA pathway are important for brain development and function.

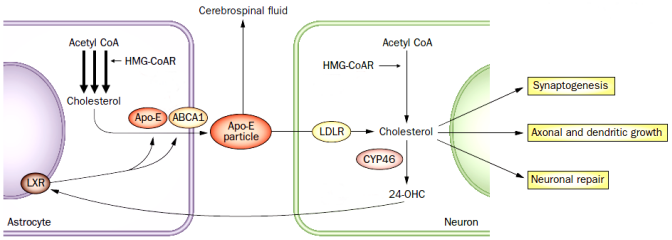


***Figure 10.*** *Cholesterol metabolism and intercellular transport in the brain.*

# Aim

The observations summarized above suggest that the MVA pathway is essential for the function of the CNS, but to date, no systematic studies have been carried out to investigate the physiological modulation of the proteins involved in the homeostasis of this pathway.

My first aim was to perform a methodical study to evaluate the presence and the regulation of this pathway in different areas of the rodent brain and to study the impacts of sex and age. To this end, I used as experimental model, male and female rats of different ages.

My second aim was to analyze the impact of HMGCR on neuronal development and behavior using pharmacologic treatment of cultured neurons and of adult male rats, respectively.

The results of these studies prompted me to explore, in a third aim, whether the MVA pathway is affected in a neurodevelopmental disease using a well-established animal model of autism spectrum disorders (ASDs), rats prenatally exposed to VPA.

## Results

In the following, I will summarize briefly the key findings of my studies. The details can be found in the original articles that are inserted.

My studies addressing the first aim gave rise to two publications (Segatto et al., 2012; Segatto et al., 2013). The results show that the protein levels and the activation state of HMGCR and its regulatory proteins vary among selected brain areas of rats and that they are modulated in a sex- and age-dependent manner.

Two papers addressing the second aim show a functional role of the MVA pathway in the CNS using a pharmacological approach. By using a HMGCR inhibitor, simvastatin, I studied the role of the MVA pathway on emotional reactivity and cognitive performance in rodents. In parallel, I used the same approach to study the impact on neuronal development in vitro. The results demonstrate that HMGCR activity is involved in rodent memory and social interactions (Segatto et al., 2014b). Moreover, inhibition of the enzyme enhances neurite outgrowth and neuronal development (Cartocci et al., 2016). The work addressing the third aim resulted in one publication showing that rats presenting autistic-like symptoms display alterations in key elements of MVA pathway. These changes depend on the age and differ among brain areas (Cartocci et al., 2017, under second revision).

My contribution to the papers was manifold. I obtained funding for the research, I planned the experiments and coordinated the members of my research group and the collaborators. I analyzed data, performed statistical analyses, created the figures and wrote the manuscripts. Being corresponding author on each of the papers, I handled interactions with editors, revised the manuscripts and wrote the responses to the referee comments. On the bench-side, I helped to treat animals, to sacrifice them, and to collect their tissues. Moreover, I performed all the HMGCR activity assays.

ACTA PHYSIOLOGICA

Acta Physiol 2012

# Regulation of cholesterol biosynthetic pathway in different regions of the rat central nervous system

**M. Segatto, L. Trapani, C. Lecis and V. Pallottini**

*Department of Biology, University Roma Tre, Rome, Italy*

Received 30 November 2011,
revision requested 20 February 2012,
revision received 15 March 2012,
accepted 25 April 2012
Correspondence: V. Pallottini, Department of Biology, University Roma Tre, Viale Marconi, 446 00146 Rome, Italy.
E-mail: vpallott@uniroma3.it

**Abstract**

**Aim:** In this study, we investigated the regulatory network of the key and rate-limiting enzyme of cholesterol biosynthetic pathway, the 3-hydroxy 3-methylglutaryl coenzyme A reductase (HMGR) in different brain regions, to add new insight about lipid metabolism and physiology in the central nervous system (CNS).

**Methods:** HMGR levels and activation state and the proteins involved in the enzyme regulatory network were analysed by Western blot in hippocampus, cortex, cerebellum and brain stem of adult male rats.

**Results:** HMGR protein level and phosphorylation state exhibit a specific pattern in each brain area analysed, according to the levels and activation state of the proteins responsible for the short- and long-term regulation of the enzyme. Moreover, low-density lipoprotein receptor expression displays a similar trend to that of HMGR.

**Conclusions:** The obtained data indicate that cholesterol biosynthesis could be differently modulated in each brain region in adult male rat and emphasize marked differences in HMGR and low-density lipoprotein receptor regulation. The results provide new insights into the intricate network that regulates cholesterol homoeostasis in the adult CNS in connection with the regional needs of this molecule.

*Keywords* central nervous system, cholesterol, HMG-CoA reductase.

Cholesterol is one of the most well-known molecules because of its pivotal roles in human physiology and in pathological conditions, such as atherosclerosis, cardiovascular and Alzheimer's disease. Nowadays, we reached a huge knowledge about the biology of cholesterol: it determines the properties of cell membranes and protein components (Yeagle 1985, Burger *et al.* 2000), and represents the precursor of steroid hormones, bile acids and vitamin D (Repa & Mangelsdorf 2000). However, many questions have to be still clarified, especially concerning cholesterol metabolism in the central nervous system (CNS), where this lipid plays crucial roles in several processes such as synapse plasticity and formation, and conduction of the action potential (Dietschy & Turley 2004),

Although the CNS constitutes 2% of the total body weight, it contains five to ten times more cholesterol than any other organ, which corresponds to the 23% of the sterol present in the whole body pool (Pfrieger 2003, Dietschy & Turley 2004). In particular, the greatest amount of unesterified cholesterol is contained in myelin membrane. Currently, there is no evidence for a net transfer of cholesterol from the bloodstream into the CNS or the spinal cord, probably because lipoproteins, which are responsible for intercellular transport of sterols and other lipids, are not able to cross the blood brain barrier (BBB). Thus, it can be assumed that all cholesterol present in the CNS is derived from *in situ* biosynthesis. Cholesterol synthesis reaches the highest rate during brain development, coinciding with the period of major growth and cholesterol-rich myelin formation, but declines at low and constant levels during adulthood (Dietschy & Turley 2004).

3$\beta$-Hydroxy 3$\beta$-methylglutaryl coenzyme A reductase (HMGR) is considered to be the major regulatory enzyme in cholesterol production and is one of the most intensively investigated proteins in biochemistry (Keller *et al.* 1985). HMGR is considered the key and rate-limiting enzyme of cholesterol biosynthetic pathway, catalysing the NADPH-dependent reduction of 3$\beta$-hydroxy 3$\beta$-methylglutaryl coenzyme A (HMG-CoA) to mevalonate, the first committed step in cholesterol biosynthesis (Rozman & Monostory 2010, Trapani *et al.* 2011a). As the central enzyme of cholesterol metabolic pathway, HMGR is tightly regulated (Goldstein & Brown 1990). In particular, the enzyme undergoes both short-term and long-term regulations.

Short-term regulation is achieved by phosphorylation/dephosphorylation cycles, able to affect the enzyme activity. The phosphorylation of enzyme's residue S872 decreases HMGR catalytic activity whereas the removal of the phosphate reactivates the enzyme. AMP-activated kinase (AMPK) appears to be the major HMGR kinase at least in the liver. AMPK is known to be involved in the regulation of energy homoeostasis responding to changes in cellular AMP to ATP ratio (Towler & Hardie 2007). HMGR dephosphorylation (activation) is operated principally by protein phosphatase 2A (PP2A), an abundant cellular serine/threonine phosphatase that regulates a significant network of cellular events (Janssens & Goris 2001).

Aside from short-term regulation, HMGR is subjected to long-term regulation through transcriptional, translational and post-translational control (Xu *et al.* 2005). To monitor levels of membrane sterols cells employ, in addition to HMGR, another membrane-embedded protein of the ER, sterol regulatory element binding protein (SREBP) cleavage activating protein (Scap). Scap is an escort protein for SREBPs, membrane-bound transcription factors able to induce the expression of genes required for cholesterol synthesis and uptake, such as HMGR and low-density lipoprotein receptor (LDLr) respectively (Brown & Goldstein 1997). In sterol-deprived cells, Scap binds SREBPs and escorts them from the ER to the Golgi apparatus where SREBPs are proteolytically processed to yield N-terminal active fragments (nSREBPs) that enter the nucleus and induce the expression of their target genes (Brown & Goldstein 1999). When cholesterol builds up in ER membranes, the Scap/SREBP complex fails to exit the ER, the proteolytic processing of SREBPs is abolished, and the transcription of the target genes declines (Trapani *et al.* 2011b). ER retention of Scap/SREBP is mediated by sterol-dependent binding of Scap/SREBP to Insig (INSulin Induced Gene), an ER resident protein (Yang *et al.* 2002). Moreover, intracellular accumulation of sterols triggers binding of HMGR to Insig, which, in turn, initiates the ubiquitination and the subsequent proteasomal degradation of the enzyme (Sever *et al.* 2003).

The regulation of HMGR is well characterized in the liver, where the highest rate of cholesterologenesis takes place (Goldstein *et al.* 2006). On the contrary, little or nothing is known about the modulation of this key enzyme in the CNS. As far as we know, the rate of cholesterol synthesis during brain development correlates closely with both the rate of cholesterol build-up and the ultimate concentration of this molecule found in each brain region. Thus, the highest biosynthesis is present in those myelin-rich regions, such as the brain stem, that ultimately reach the highest amount of cholesterol (Dietschy & Turley 2004). Moreover, it was recently demonstrated that, in adult rat brain, the transcription factor isoform SREBP-2 shows a specific regional pattern of protein expression (Kim & Ong 2009). This evidence, together with the BBB-derived isolation of brain cholesterol metabolism from any changes in the circulating amounts of lipids, leads to the hypothesis that HMGR could be differently modulated in this organ and that specific regional differences could occur not only in developing but also in mature brain. In this study, we investigated the presence, the protein levels and the activation state of HMGR and its regulatory proteins in four different brain regions of adult rats, to add new insight about cerebral lipid metabolism and physiology of the analysed regions. In particular, the analysis was performed in hippocampus, cortex, cerebellum and brain stem, which differ from neuronal circuits, cytoarchitecture, white matter composition and functions.

## Materials and methods

### *Animals*

Four 3-month-old male Wistar Rattus norvegicus (Harlan Nossan, S. Pietro al Natisone, Italy) were housed under controlled temperature (20 ± 1 °C), humidity (55 ± 10%) and illumination (lights on for 12 h daily, from 7 AM to 7 PM). Food and water were provided *ad libitum*. All rats were held in quarantine for 2 weeks before the experiments. Tubes for tunnelling and nesting materials (paper towels) were daily placed in all cages as environmental enrichment. The experiments were performed according to the ethical guidelines for the conduct of animal research (Ministero della Salute, Official Italian Regulation No. 116/92, Communication to Ministero della Salute no. 391/121). Rats were killed under deep urethane anaesthesia (1.2 g kg$^{-1}$, i.p.) by decapitation, and brains were

immediately removed. Cerebral regions of interest were collected and frozen at −80 °C for subsequent biochemical assays.

### *Lysate preparation*

Total lysates were obtained as follows: 100 mg hippocampus, cortex, cerebellum or brain stem were homogenized in 0.01 M Tris–HCl, 0.001 M $CaCl_2$, 0.15 M NaCl and 0.001 M phenylmethylsulfonyl fluoride (PMSF) (pH 7.5). An aliquot of sample buffer (0.25 M Tris–HCl pH 6.8, containing 20% SDS and protease inhibitor cocktail) was added to the homogenate. The samples were solubilized by sonication and centrifuged for 5 min at 15 600 ***g***, and the supernatant was transferred into microtubes. Protein concentration was determined by the method of Lowry and coll. (Lowry *et al.* 1951). All samples were boiled for 3 min before loading for Western blotting.

### *Protein analysis*

Protein profiles were analysed by Western blotting. Protein (30 $\mu$g) from total lysates was resolved by 12% for Insig-1 (Novus Biologicals, Cambridge, UK) and PP2A (Santa Cruz Biotechnology, Santa Cruz, CA, USA); 10% for P-AMPK$\alpha$, total AMPK$\alpha$ (Cell Signalling Technology, Boston, MA, USA) and Glial fibrillary acidic protein (GFAP) (Synaptic System GmbH, Goettingen, Germany); and 7% for P-HMGR (Millipore, Temecula, CA, USA), HMGR (Upstate, Lake Placid, NY, USA), LDLr ab30532 (Abcam, Cambridge, UK), SREBP-1 (Santa Cruz Biotechnology) and SREBP-2 (Abcam) SDS-PAGE as previously described (Trapani *et al.* 2011b).

### *Statistical analysis*

Data are expressed as means ± SD (standard deviation). The difference in parameters was statistically tested for significance with one-way analysis of variance (ANOVA) followed by Tukey–Kramer post-test. Values of $P < 0.05$ were considered to indicate a significant difference. Statistical analysis was performed using GRAPHPAD INSTAT3 (GraphPad, La Jolla, CA, USA) for Windows.

## Results

This work was aimed at evaluating the presence, the levels and the activation state of HMGR and proteins involved in its regulatory network in different brain regions. HMGR phosphorylation is responsible for the modulation of the enzyme activation state. Thus, Western blot detection of phosphorylated HMGR (P-HMGR) by a specific antibody is a good method to reveal the inactive fraction of the enzyme when compared with the total one. To avoid the full activation of the enzyme by lysosomal phosphatases, sodium fluoride (NaF) was added as phosphatase inhibitor during the preparative procedure. Results in Figure 1 panel (b) show that hippocampus has the highest

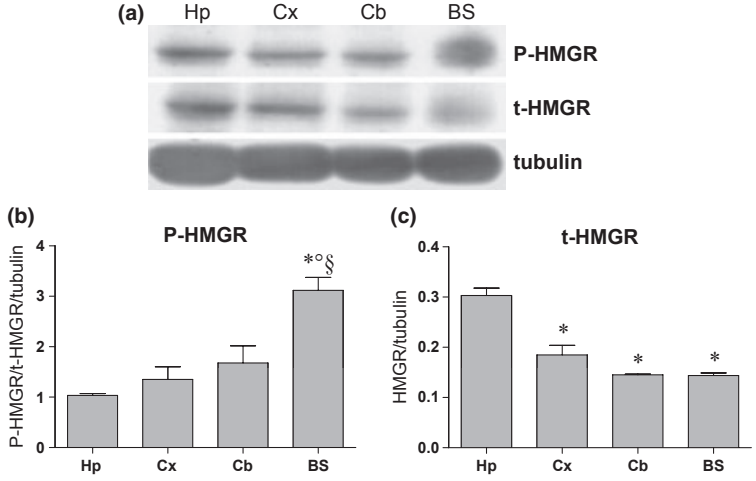


**Figure 1** 3-hydroxy 3-methylglutaryl coenzyme A reductase (HMGR) levels and phosphorylation state in different brain areas. The figure shows a representative Western blot (a) and the densitometric analysis of t-HMGR protein levels (b) and P-HMGR/t-HMGR ratio (c) in hippocampus (Hp), cortex (Cx), cerebellum (Cb) and brain stem (BS). Protein levels were normalized with $\alpha$-tubulin. The data are expressed as arbitrary units obtained analysing protein bands using the software IMAGEJ; for details, see the main text. All the data obtained are reported as the mean ± SD of $n = 4$ independent experiments carried out in duplicate. $P < 0.001$, determined using one-way ANOVA followed by Tukey–Kramer post-test, was compared with hippocampus (*) or cortex (°) or cerebellum (§) values.

HMGR protein expression followed by cortex, cerebellum and brain stem. Moreover, the ratio (activation state) between P-HMGR and total protein expression does not statistically differ between the analysed brain regions except for the brain stem, wherein P-HMGR levels are significantly higher in comparison with hippocampus, cortex and cerebellum (Fig. 1c), suggesting that the enzyme activity could be very low in this cerebral area. The regional differences in expression and activation state of HMGR suggest that each brain region could possess a specific rate of cholesterol biosynthesis.

These results prompted us to evaluate the involvement of the main upstream phosphatase and kinase, which regulate the enzyme phosphorylation state. Results show that PP2A catalytic subunit is expressed at very low levels in brain stem, while a higher and similar amount is present in hippocampus, cortex and cerebellum (Fig. 2a). The reduced PP2A levels in brain stem fit well with the high P-HMGR levels previously detected in the same region. Moreover, as AMPK activation depends on the phosphorylation of its catalytic subunit (Hardie & Sakamoto 2006), both the total levels and phosphorylation state of AMPK$\alpha$ were analysed. As shown in Figure 2a, no differences in total AMPK (t-AMPK) protein levels among the four brain regions were detected. On the contrary, brain cortex exhibits the highest AMPK activation state, as observable from the ratio between the phosphorylated AMPK (P-AMPK) levels and the total when compared with hippocampus, cerebellum and brain stem (Fig. 2b). However, the high AMPK activation does not correlate with the low P-HMGR levels in brain cortex, suggesting that, at least in this case, AMPK seems not to be involved in the modulation of HMGR activity, but likely committed to the regulation of other enzymes.

Once the HMGR activation state was defined and the enzymes involved in HMGR phosphorylation were analysed, the attention was focused on long-term regulation of the enzyme to find an explanation about the different total amount of HMGR found in each brain region. Enzyme levels depend on intracellular cholesterol content, and as the homoeostasis maintenance of cholesterol in the brain is guaranteed by an equilibrium between local biosynthesis and intracellular uptake of cholesterol-rich lipoproteins (Pfrieger 2003), protein levels and maturation of LDLr were checked. We used an anti-LDLr antibody that reacting with both glycosylated and unglycosylated LDLr forms allows us to analyse the expression and the post-translational processing of the receptor. Indeed, LDLr is highly glycosylated through N- and O-linkages, migrating at 100 kDa (neo-synthesized receptor), 130 kDa (intermediate form) and 160 kDa (functional and mature form) on SDS-PAGE, and three specific bands can be detected (Segatto *et al.* 2011). Western blot analysis of LDLr displays a similar distribution to that of HMGR, with the highest levels of neo-synthesized and mature forms detected in hippocampus, followed by cortex, cerebellum and brain stem (Fig. 3). It is interesting to note that LDLr is expressed at very low and barely detectable levels in brain stem. To check whether the region-dependent variations in HMGR and LDLr expression could be related to a

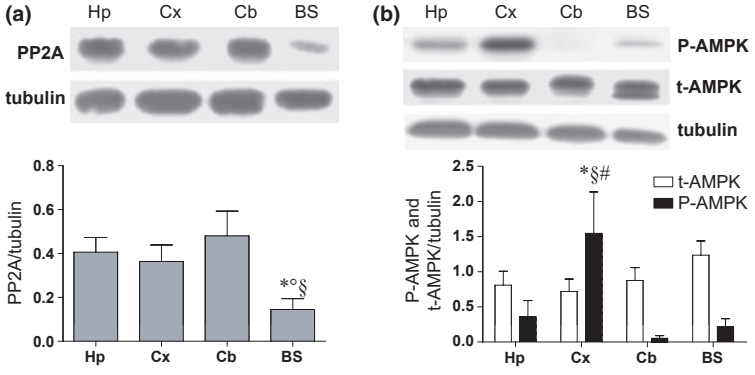


**Figure 2** PP2A level and AMP-activated kinase (AMPK) activation state in different brain areas. (a) shows a representative Western blot (top) and the densitometric analysis (bottom) of PP2A protein levels in hippocampus (Hp), cortex (Cx), cerebellum (Cb) and brain stem (BS). Protein levels were normalized with $\alpha$-tubulin. (b) shows a representative Western blot (top) of both P-AMPK and t-AMPK protein levels in hippocampus (Hp), cortex (Cx), cerebellum (Cb) and brain stem (BS); bottom represents the ratio between the densitometric analysis of each sample analysed. Protein levels were normalized with $\alpha$-tubulin. The data are expressed as arbitrary units obtained analysing protein bands using the software IMAGEJ; for details, see the main text. All the data obtained are reported as the mean ± SD of $n = 4$ independent experiments carried out in duplicate. $P < 0.01$, determined using one-way ANOVA followed by Tukey–Kramer post-test, was compared with hippocampus (*) or cerebellum (§) or cortex (°) or brain stem (#) values.

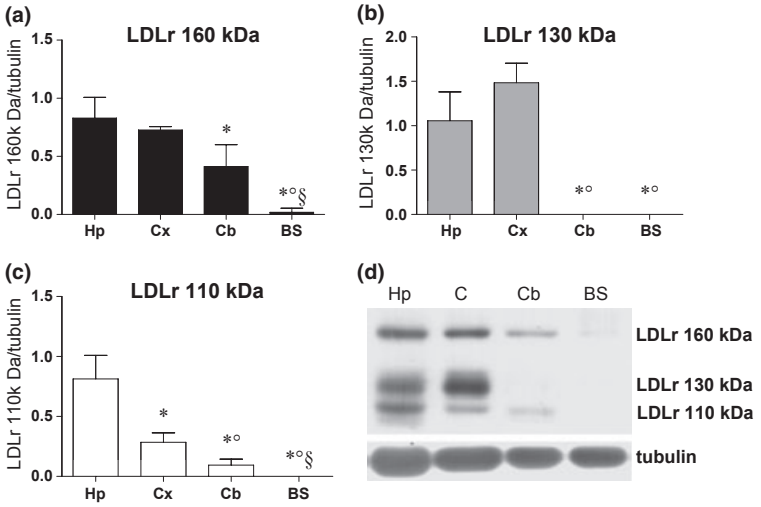


**Figure 3** Low-density lipoprotein receptor (LDLr) levels in different brain areas. The figure shows the densitometric analysis of LDLr glycosylation pattern in hippocampus (Hp), cortex (Cx), cerebellum (Cb) and brain stem (BS). Panel (a) represents 160 kDa LDLr; panel (b), 130 kDa; panel (c), 110 kDa. A representative Western blot is shown in panel (d). Protein levels were normalized with α-tubulin. The data are expressed as arbitrary units obtained analysing protein bands using the software IMAGEJ; for details, see the main text. All the data obtained are reported as the mean ± SD of $n = 4$ independent experiments carried out in duplicate. $P < 0.001$, determined using one-way ANOVA followed by Tukey–Kramer post-test, was compared with hippocampus (*) or cortex (°) or cerebellum (§) values.

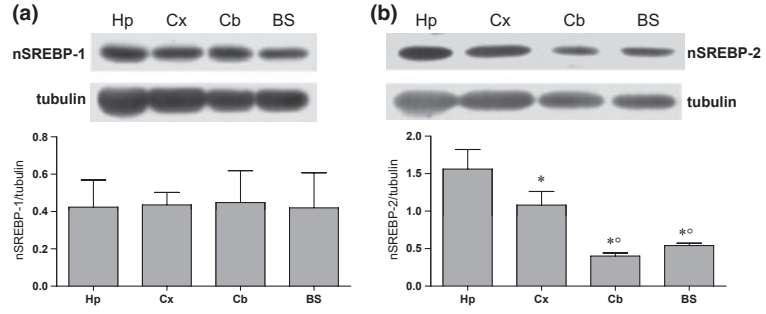


**Figure 4** Levels of sterol regulatory element binding proteins (SREBPs) in different brain areas. (a) shows a representative Western blot (top) and the densitometric analysis (bottom) of nSREBP-1 protein levels in hippocampus (Hp), cortex (Cx), cerebellum (Cb) and brain stem (BS). (b) shows a representative Western blot (top) and the densitometric analysis (bottom) of n-SREBP-2 protein levels in hippocampus (Hp), cortex (Cx), cerebellum (Cb) and brain stem (BS). Protein levels were normalized with α-tubulin. The data are expressed as arbitrary units obtained analysing protein bands using the software IMAGEJ; for details, see the main text. All the data obtained are reported as the mean ± SD of $n = 4$ independent experiments carried out in duplicate. $P < 0.001$, determined using one-way ANOVA followed by Tukey–Kramer post-test, was compared with hippocampus (*) or cortex (°) values.

different activation of their transcription factors, active nSREBPs levels were assessed using antibodies against the cleaved N-terminus of these proteins. Two genes code for three SREBP isoforms, SREBP-1a, SREBP-1c and SREBP-2. SREBP-1a is a powerful activator of all SREBP-responsive genes, including those that mediate the biosynthesis of cholesterol, triglycerides and fatty acids. The functions of SREBP-1c and SREBP-2 are more restricted than that of SREBP-1a: SREBP-1c preferentially enhances the transcription of genes required for fatty acid but not for cholesterol biosynthesis; SREBP-2 mostly activates cholesterol biosynthesis. SREBP-1a and SREBP-2 are the predominant isoforms of SREBP in several cell lines, whereas SREBP-1c and SREBP-2 predominate in the liver and most of other intact tissues (Horton 2002). No differences are detectable in nSREBP-1 levels among the four regions (Fig. 4a). It should be considered that the antibody used for Western blot analysis cannot discriminate between SREBP-1a and -1c; thus, we can assume that both the transcription factor isoforms are equally expressed in all brain areas taken into consideration in this study. On the other hand, nSREBP-2 displays a brain area-specific pattern of protein

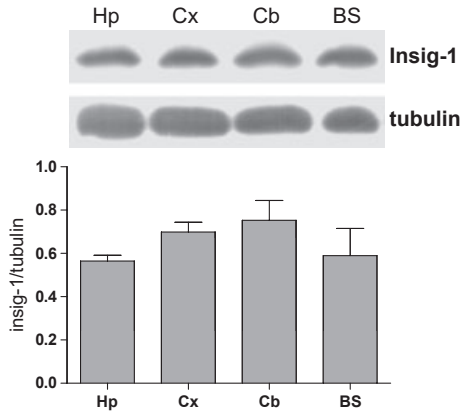


**Figure 5** Insig-1 levels in different brain areas. The figure shows a representative Western blot (top) and the densitometric analysis (bottom) of Insig-1 protein levels in hippocampus (Hp), cortex (Cx), cerebellum (Cb) and brain stem (BS). Protein levels were normalized with α-tubulin. The data are expressed as arbitrary units obtained analysing protein bands using the software IMAGEJ; for details see the main text. All the data obtained are reported as the mean ± SD of $n = 4$ independent experiments carried out in duplicate. Statistical analysis was performed using one-way ANOVA followed by Tukey–Kramer post-test.

expression, with the highest levels found in hippocampus and the lowest ones in cerebellum and brain stem (Fig. 4b), which were consistent with the regional distribution of HMGR and LDLr. As it is well established that Insig-1 binding to HMGR leads to an accelerated degradation of the enzyme (Sever *et al.* 2003), the protein amount of Insig-1 was assessed, to evaluate whether the differences in HMGR protein levels could depend also on degradative processes besides transcriptional ones. However, no significant differences were found among the brain regions analysed (Fig. 5).

Lastly, as astrocytes are the main cell type where cholesterol biosynthesis occurs in the CNS (Pfrieger 2003), to assess whether the differences among the analysed proteins are simply due to the number of astrocytes or to a distinct metabolic regulation, GFAP (astrocyte marker) protein expression was measured. The results indicate that GFAP expression is high in brain stem, low in hippocampus and cortex, and intermediate in cerebellum. Moreover, the calculation of total HMGR/GFAP ratio shows that there is no correlation between the protein expression of the enzyme and the amount of astrocytes found in each brain region (Fig. 6).

## Discussion

Mevalonate pathway is an essential metabolic pathway in the CNS, as it leads to the production of several compounds pivotal for the maintenance of a number of brain functions. Among these end products, cholesterol certainly plays critical roles in CNS physiology (Segatto *et al.* 2011). It fulfils structural tasks into cellular membranes, as an instance influencing membrane thickness and fluidity (Ohvo-Rekila *et al.* 2002) as well as limiting ion leakage by means of cholesterol-rich myelin membranes (Haines 2001), thus providing electrical insulation to the axon that is

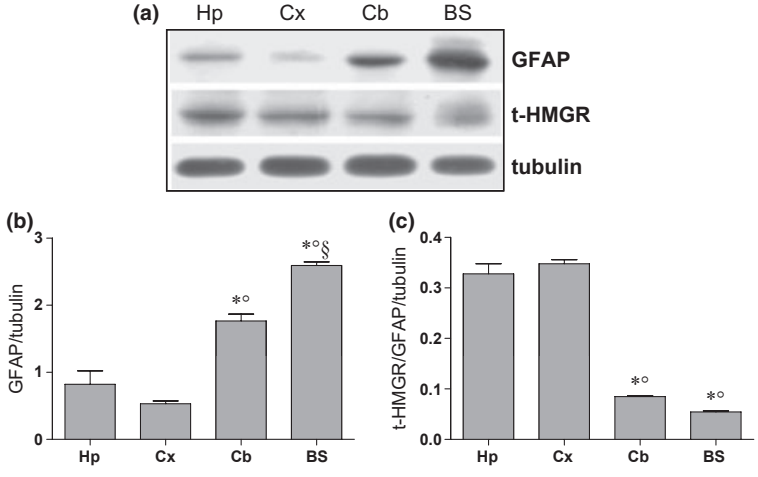


**Figure 6** Glial fibrillary acidic protein expression in different brain areas. The figure illustrates a representative Western blot (a) and the densitometric analysis (b) of GFAP (astrocyte marker) content and t-HMGR/GFAP ratio (c) in hippocampus (Hp), cortex (Cx), cerebellum (Cb) and brain stem (BS). Protein levels were normalized with α-tubulin. The data are represented as arbitrary units obtained analysing protein bands using the software IMAGEJ; for details, see the main text. All the data obtained are reported as the mean ± SD of $n = 4$ independent experiments carried out in duplicate. $P < 0.001$, determined using one-way ANOVA followed by Tukey–Kramer post-test, was compared with hippocampus (*) or cortex (°) or cerebellum (§) values.

essential for the conduction of rapid saltatory impulse (Saher *et al.* 2005). Furthermore, cholesterol is crucial for synapse formation, as it increases the number of synapses by enhancing their stability (Pfrieger 2003). These effects are consistent with the proof that the removal of cholesterol from hippocampal slices through HMGR pharmacological inhibition eliminates the late phase of long-term potentiation (Matthies *et al.* 1997). The importance of cholesterol in CNS processes is also supported by growing clinical studies that demonstrate that imbalance in cholesterol homoeostasis determines several brain pathological descriptions, such as Alzheimer's disease, Niemann–Pick type C disease and multiple sclerosis (Pfrieger 2003, Zipp *et al.* 2007, Segatto *et al.* 2011).

Despite this evidence, available information still remains limited, and no research is addressed to evaluate prospective differences in cholesterol biosynthesis in distinct brain areas, which are known to differ for energy balance, cytoarchitecture and function.

Thus, the current work was aimed at evaluating whether HMGR, the key and rate-limiting enzyme of cholesterol biosynthetic pathway, could undergo brain region-specific regulation.

Our data show that HMGR phosphorylation is high in brain stem, while lower and similar levels are observed in hippocampus, brain cortex and cerebellum, indicating that HMGR activation is less prominent in brain stem. This result is in agreement with PP2A catalytic subunit levels detected in the same area, suggesting that HMGR hyperphosphorylation could be a consequence of the low amount of the phosphatase. No differences are shown about AMPK except for cortex, wherein P-AMPK protein levels are higher than in hippocampus, cerebellum and brain stem. However, these data do not match the HMGR phosphorylation state, suggesting that AMPK could not be involved HMGR short-term modulation we observed. We can not exclude that other kinases, such as protein kinase C (Beg *et al.* 1985), could be involved in. On the other hand, aside the effects on HMGR phosphorylation state, the sustained activation of AMPK in cortex could reflect the energy balance and the metabolic rate of this region.

The evaluation of total HMGR protein content allowed us to analyse the distribution pattern of the enzyme in the CNS. HMGR protein levels in hippocampus are found to be the highest, followed by brain cortex; the lowest ones are expressed in cerebellum and brain stem. The long-term regulation of the enzyme is exerted through transcriptional events: while no differences are revealed in the amount of nSREBP-1, the observed variations in nuclear and transcriptionally active nSREBP-2 are functionally in agreement with brain HMGR trend, according to the classical model well accepted (Goldstein *et al.* 2006, Espenshade & Hughes 2007). nSREBP-2 expression pattern also corroborates with existing literature data, wherein immunoblot analysis showed a dense band corresponding to transcriptionally active SREBP-2 in homogenates from rat hippocampus and cortex, while hardly detectable bands were present in cerebellum and brain stem (Kim & Ong 2009). In this study, the transcriptional regulatory system of HMGR in brain regions operated by SREBP-2 is also supported by LDLr expression, which is strongly and moderately high in hippocampus and cortex, respectively, and extremely low in cerebellum and brain stem.

A variety of findings claim that during development and in mature brain, neurons strongly reduce or even abandon cholesterol synthesis to reserve energy and import cholesterol from astrocytes through lipoproteins. Thus, as the enzymatic machinery to synthesize cholesterol is mainly expressed in astrocytes (Pfrieger 2003), Western blot quantification of a specific astrocyte marker was performed. GFAP determination showed that there is no correlation between the analysed proteins and GFAP protein expression, thus suggesting that the observed differences in HMGR regulation in each brain area are not related to the number of astrocytes, but reflect a distinct metabolic regulation.

When evaluated as a whole, these data emphasize marked functional differences in HMGR and LDLr regulation in brain regions. In particular, hippocampus, followed by cortex, exhibits a lively cholesterol metabolism, as sustained by the highest levels of HMGR and LDLr protein expression. On the contrary, the main cholesterol metabolic pathways seem to be nearly suppressed in brain stem, because of the low HMGR activation and protein levels and the very little LDLr expression. The results do not necessarily indicate that a low cholesterol content is present in these regions, rather than that cholesterol turnover is very low. For instance, the brain stem possesses the highest cholesterol content with respect to the other brain areas analysed (Quan *et al.* 2003). However, it is well known that cholesterol half-life is estimated to be more than 8 months in myelin-rich regions, such as brain stem (Smith & Weyl 1968). Thus, despite the high lipid content, the low basal rate of cholesterol biosynthesis and uptake in this region could reflect the very slow turnover of cholesterol in myelin membranes. This is consistent with *in vivo* experiments, which demonstrate that cholesterol 24-hydroxylase, the main cytochrome P450 involved in brain cholesterol turnover, is principally expressed in neurons of the cortex and hippocampus but not in the white matter of adult CNS (Lund *et al.* 2003).

The physiological relevance of our results, which report a region-specific regulation in LDLr and

HMGR protein expression and activation state, lies in the role of cholesterol in brain processes. For instance, cholesterol is essential for the acquisition of neuronal morphology. The acquisition of neuronal type-specific morphogenesis is a key feature of neuronal differentiation and has important consequences for region-specific functions of the CNS. It was demonstrated that a well-defined intracellular cholesterol profile is responsible for the different regulation of dendrite and axon outgrowths in hippocampal and cortical neurons. Cholesterol content in total homogenate and in lipid rafts of hippocampal neurons is higher than in cortical neurons. The depletion of this molecule strongly induced neurite outgrowth and facilitated the polarity establishment of hippocampal neurons, which showed a similar morphology to that of cortical neurons. On the other hand, variations in the amount of cholesterol in cortical neurons decreased the neurite outgrowth (Ko *et al.* 2005). This finding suggests that an optimal concentration of cholesterol is required to assure the acquisition and the maintenance of a well-defined neuronal morphology. The distribution pattern and the modulation of the main proteins involved in cholesterol homoeostasis evaluated in the present work could represent a good explanation of this phenomena, highlighting for the first time that a deep and tight regional regulation of cholesterol biosynthetic pathway is essential not only during brain development, but also to ensure physiological functions in adult brain.

As cholesterol is pivotal for synapse maturation, the observed differences in the regional expression and activation state of HMGR and LDLr could be also related to the modulation of synaptic plasticity. Hippocampus, together with cerebral cortex, represents a highly dynamic structure because of synaptic plasticity: given the importance of cholesterol in synapse formation/stabilization, this phenomenon could account for an increased cholesterol need in these regions of adult brain, which reflects in a different modulation of proteins and enzymes (such as HMGR and LDLr) responsible for cholesterol homoeostasis maintenance. The tight regulation of cholesterol biosynthesis and its essential role in synaptic plasticity is further supported by the cholesterol disbalance often observed in neurodegenerative pathologies. Indeed, synapses are sensitive to cholesterol content, and interferences in the delivery of this compound from astrocytes to synaptic compartments are at the root of synapse loss and, in turn, of neurodegeneration. Alzheimer's disease (AD), which is characterized by synapse and neuron loss in specific brain regions (such as cortex and hippocampus) could, at least in part, depend on disbalance in cholesterol homoeostasis. In particular, $\beta$-amyloid plaques seem to interfere with cholesterol transport from astrocytes to neurons (Pfrieger 2003). Further evidence that the onset and the progression of AD is related to cholesterol deficit in neurons comes from the observation that neurofibrillary tangles, another AD hallmark, are also present in patients with Niemann–Pick type C disease, a genetic disorder caused by a deregulation of cholesterol storage into cells (Suzuki *et al.* 1995). Even though the underlying mechanisms are still unknown, the puzzling variety of these findings strongly support a link between neurodegenerative pathologies and cholesterol metabolism. For this reason, the results about the tight regional regulation of HMGR in adult brain presented in this work could represent another starting point to better comprehend the involvement of cholesterol metabolism in brain physiology and pathology occurring in specific brain areas, also suggesting that HMGR could be considered as a prospective molecular target for the treatment of a variety of CNS disorders.

Moreover, increasing evidence suggests that statins, powerful HMGR inhibitors widely used in therapies against hypercholesterolaemia, can induce several effects on the CNS, such as mood swings, irritability, depressive syndromes and modulation in cognitive processes (Golomb *et al.* 2004, Baytan *et al.* 2008). Thus, a deep comprehension of cholesterol biosynthetic pathway among the different brain regions could be useful to delve deeper into the molecular mechanisms and the brain areas involved in the onset of these side effects.

In conclusion, the obtained data indicate that marked differences in HMGR and LDLr regulation are present in brain areas analysed. These variations seem to be related to cholesterol turnover, regional myelin content and the modulation of synaptic plastic-

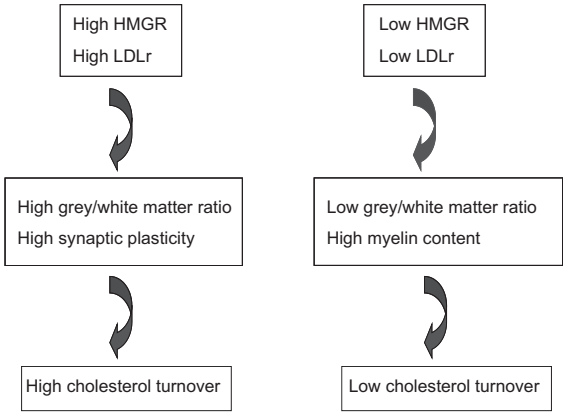


**Figure 7** Potential model to explain the brain region-specific regulation of 3-hydroxy 3-methylglutaryl coenzyme A reductase (HMGR) and low-density lipoprotein receptor (LDLr). Potential model to explain the brain region-specific regulation of HMGR and LDLr.

ity that are specific features of each brain region (Fig 7).

## Conflict of Interest

Authors declare that no conflict of interest exists.

The generous gift of GFAP antibody from Prof. Sandra Moreno (Department of Biology, University Roma Tre) is gratefully acknowledged. This work was supported by grants from the University of 'Roma Tre' CLAR 2010-2011 to V.P.

## References

Baytan, S.H., Alkanat, M., Okuyan, M., Ekinci, M., Gedikli, E., Ozeren, M. & Akgun, A. 2008. Simvastatin impairs spatial memory in rats at a specific dose level. *Tohoku J Exp Med* **214**, 341–349.

Beg, Z.H., Stonik, J.A. & Brewer, H.B. Jr 1985. Phosphorylation of hepatic 3-hydroxy-3-methylglutaryl coenzyme A reductase and modulation of its enzymic activity by calcium-activated and phospholipid-dependent protein kinase. *J Biol Chem* **260**, 1682–1687.

Brown, M.S. & Goldstein, J.L. 1997. The SREBP pathway: regulation of cholesterol metabolism by proteolysis of a membrane-bound transcription factor. *Cell* **89**, 331–340.

Brown, M.S. & Goldstein, J.L. 1999. A proteolytic pathway that controls the cholesterol content of membranes, cells, and blood. *Proc Natl Acad Sci U S A* **96**, 11041–11048.

Burger, K., Gimpl, G. & Fahrenholz, F. 2000. Regulation of receptor function by cholesterol. *Cell Mol Life Sci* **57**, 1577–1592.

Dietschy, J.M. & Turley, S.D. 2004. Thematic review series: brain Lipids. Cholesterol metabolism in the central nervous system during early development and in the mature animal. *J Lipid Res* **45**, 1375–1397.

Espenshade, P.J. & Hughes, A.L. 2007. Regulation of sterol synthesis in eukaryotes. *Annu Rev Genet* **41**, 401–427.

Goldstein, J.L. & Brown, M.S. 1990. Regulation of the mevalonate pathway. *Nature* **343**, 425–430.

Goldstein, J.L., DeBose-Boyd, R.A. & Brown, M.S. 2006. Protein sensors for membrane sterols. *Cell* **124**, 35–46.

Golomb, B.A., Kane, T. & Dimsdale, J.E. 2004. Severe irritability associated with statin cholesterol-lowering drugs. *QJM* **97**, 229–235.

Haines, T.H. 2001. Do sterols reduce proton and sodium leaks through lipid bilayers? *Prog Lipid Res* **40**, 299–324.

Hardie, D.G. & Sakamoto, K. 2006. AMPK: a key sensor of fuel and energy status in skeletal muscle. *Physiology (Bethesda)* **21**, 48–60.

Horton, J.D. 2002. Sterol regulatory element-binding proteins: transcriptional activators of lipid synthesis. *Biochem Soc Trans* **30**, 1091–1095.

Janssens, V. & Goris, J. 2001. Protein phosphatase 2A: a highly regulated family of serine/threonine phosphatases implicated in cell growth and signalling. *Biochem J* **353**, 417–439.

Keller, G.A., Barton, M.C., Shapiro, D.J. & Singer, S.J. 1985. 3-Hydroxy-3-methylglutaryl-coenzyme A reductase is present in peroxisomes in normal rat liver cells. *Proc Natl Acad Sci U S A* **82**, 770–774.

Kim, J.H. & Ong, W.Y. 2009. Localization of the transcription factor, sterol regulatory element binding protein-2 (SREBP-2) in the normal rat brain and changes after kainate-induced excitotoxic injury. *J Chem Neuroanat* **37**, 71–77.

Ko, M., Zou, K., Minagawa, H., Yu, W., Gong, J.S., Yanagisawa, K. & Michikawa, M. 2005. Cholesterol-mediated neurite outgrowth is differently regulated between cortical and hippocampal neurons. *J Biol Chem* **280**, 42759–42765.

Lowry, O.H., Rosebrough, N.J., Farr, A.L. & Randall, R.J. 1951. Protein measurement with the Folin phenol reagent. *J Biol Chem* **193**, 265–275.

Lund, E.G., Xie, C., Kotti, T., Turley, S.D., Dietschy, J.M. & Russell, D.W. 2003. Knockout of the cholesterol 24-hydroxylase gene in mice reveals a brain-specific mechanism of cholesterol turnover. *J Biol Chem* **278**, 22980–22988.

Matthies, H. Jr, Schulz, S., Hollt, V. & Krug, M. 1997. Inhibition by compactin demonstrates a requirement of isoprenoid metabolism for long-term potentiation in rat hippocampal slices. *Neuroscience* **79**, 341–346.

Ohvo-Rekila, H., Ramstedt, B., Leppimaki, P. & Slotte, J.P. 2002. Cholesterol interactions with phospholipids in membranes. *Prog Lipid Res* **41**, 66–97.

Pfrieger, F.W. 2003. Role of cholesterol in synapse formation and function. *Biochim Biophys Acta* **1610**, 271–280.

Quan, G., Xie, C., Dietschy, J.M. & Turley, S.D. 2003. Ontogenesis and regulation of cholesterol metabolism in the central nervous system of the mouse. *Brain Res Dev Brain Res* **146**, 87–98.

Repa, J.J. & Mangelsdorf, D.J. 2000. The role of orphan nuclear receptors in the regulation of cholesterol homeostasis. *Annu Rev Cell Dev Biol* **16**, 459–481.

Rozman, D. & Monostory, K. 2010. Perspectives of the nonstatin hypolipidemic agents. *Pharmacol Ther* **127**, 19–40.

Saher, G., Brugger, B., Lappe-Siefke, C., Mobius, W., Tozawa, R., Wehr, M.C., Wieland, F., Ishibashi, S. & Nave, K. A. 2005. High cholesterol level is essential for myelin membrane growth. *Nat Neurosci* **8**, 468–475.

Segatto, M., Trapani, L., Marino, M. & Pallottini, V. 2011. Age- and sex-related differences in extra-hepatic low-density lipoprotein receptor. *J Cell Physiol* **226**, 2610–2616.

Sever, N., Yang, T., Brown, M.S., Goldstein, J.L. & DeBose-Boyd, R.A. 2003. Accelerated degradation of HMG CoA reductase mediated by binding of insig-1 to its sterol-sensing domain. *Mol Cell* **11**, 25–33.

Smith, W.L. & Weyl, T.C. 1968. The effects of ethosuximide (zarontin) on intellectual functions of children with learning deficits and cortical brain dysfunction. *Curr Ther Res Clin Exp* **10**, 265–269.

Suzuki, K., Parker, C.C., Pentchev, P.G., Katz, D., Ghetti, B., D'Agostino, A.N. & Carstea, E.D. 1995. Neurofibrillary tangles in Niemann-Pick disease type C. *Acta Neuropathol* **89**, 227–238.

Towler, M.C. & Hardie, D.G. 2007. AMP-activated protein kinase in metabolic control and insulin signaling. *Circ Res* **100**, 328–341.

Trapani, L., Segatto, M., Ascenzi, P. & Pallottini, V. 2011a. Potential role of nonstatin cholesterol lowering agents. *IUBMB Life* **63**, 964–971.

Trapani, L., Segatto, M., Simeoni, V., Balducci, V., Dhawan, A., Parmar, V.S., Prasad, A.K., Saso, L., Incerpi, S. & Pallottini, V. 2011b. Short- and long-term regulation of 3-hydroxy 3-methylglutaryl coenzyme A reductase by a 4-methylcoumarin. *Biochimie* **93**, 1165–1171.

Xu, F., Rychnovsky, S.D., Belani, J.D., Hobbs, H.H., Cohen, J.C. & Rawson, R.B. 2005. Dual roles for cholesterol in mammalian cells. *Proc Natl Acad Sci U S A* **102**, 14551–14556.

Yang, T., Espenshade, P.J., Wright, M.E., Yabe, D., Gong, Y., Aebersold, R., Goldstein, J.L. & Brown, M.S. 2002. Crucial step in cholesterol homeostasis: sterols promote binding of SCAP to INSIG-1, a membrane protein that facilitates retention of SREBPs in ER. *Cell* **110**, 489–500.

Yeagle, P.L. 1985. Cholesterol and the cell membrane. *Biochim Biophys Acta* **822**, 267–287.

Zipp, F., Waiczies, S., Aktas, O., Neuhaus, O., Hemmer, B., Schraven, B., Nitsch, R. & Hartung, H.P. 2007. Impact of HMG-CoA reductase inhibition on brain pathology. *Trends Pharmacol Sci* **28**, 342–349.



Acta Physiologica © 2012 Scandinavian Physiological Society, doi: 10.1111/j.1748-1716.2012.02450.x

Journal of Cellular Physiology



# Analysis of the Protein Network of Cholesterol Homeostasis in Different Brain Regions: An Age and Sex Dependent Perspective

MARCO SEGATTO, ANNALAURA DI GIOVANNI, MARIA MARINO, AND VALENTINA PALLOTTINI*

*Department of Sciences, University of Roma Tre, Rome, Italy*

Although a great knowledge about the patho-physiological roles of cholesterol metabolism perturbation in several organs has been reached, scarce information is available on the regulation of cholesterol homeostasis in the brain where this lipid is involved in the maintenance of several of neuronal processes. Currently, no study is available in literature dealing how and if sex and age may modulate the major proteins involved in the regulatory network of cholesterol levels in different brain regions. Here, we investigated the behavior of 3-hydroxy 3-methylglutaryl coenzyme A reductase (HMGR) and low-density lipoprotein receptor (LDLr) in adult (3-month-old) and aged (12-month-old) male and female rats. The analyses were performed in four different brain regions: cortex, brain stem, hippocampus, and cerebellum which represent brain areas characterized by different neuronal cell types, metabolism, cytoarchitecture and white matter composition. The results show that in hippocampus HMGR is lower (30%) in adult female rats than in age-matched males. Differences in LDLr expression are also observable in old females with respect to age-matched males: the protein levels increase (40%) in hippocampus and decrease (20%) in cortex, displaying different mechanisms of regulation. The mechanism underlying the observed modifications are ascribable to Insig-1 and SREBP-1 modulation. The obtained data demonstrate that age- and sex-related differences in cholesterol homeostasis maintenance exist among brain regions, such as the hippocampus and the prefrontal cortex, important for learning, memory and affection. Some of these differences could be at the root of marked gender disparities observed in clinical disease incidence, manifestation, and prognosis.

J. Cell. Physiol. 228: 1561–1567, 2013. 

Highly intricate regulatory systems have evolved for the maintenance of cholesterol homeostasis in the body. Cholesterol fulfills both functional and structural tasks, since it regulates the cell membrane fluidity and stability (Ohvo-Rekila et al., 2002) and constitutes the precursor of bile acids and steroid hormones including vitamin D (Repa and Mangelsdorf, 2000). Although we reached a great knowledge about the patho-physiological roles of cholesterol metabolism perturbation in several organs and tissues, only little information is available on the regulation of cholesterol homeostasis in the central nervous system (CNS) where this lipid is involved in the maintenance of several neuronal functions such as the conduction of the action potential, the stabilization of synapses, and the formation of lipid rafts (Block et al., 2010). Even though the human brain accounts for the 2% of the total body weight, it has been established that approximately 25% of the total content of cholesterol present in humans is found in the CNS (Bjorkhem and Meaney, 2004; Dietschy and Turley, 2004).

There is no proof for a direct transport of cholesterol from the plasma into the CNS or the spinal cord, probably because the blood brain barrier is able to avoid the transit of the lipoprotein–cholesterol from the bloodstream. For this reason, it is widely accepted that almost all the cholesterol found in the CNS is produced from local biosynthesis. Cholesterol synthesis is very high in the developing brain, thus reflecting the synthesis of a large quantity of cholesterol-rich myelin membrane. However, this rate declines at low and constant levels during adulthood (Dietschy and Turley, 2004). Recently, our research group demonstrated that cholesterol biosynthesis could be differently modulated in different brain regions in adult male rat and that parallel differences in the proteins involved in intracellular cholesterol homeostasis maintenance exist (Segatto et al., 2012). Indeed, the 3-hydroxy 3-methyl glutaryl coenzyme A reductase (HMGR) the key and the central regulatory enzyme in cholesterol biosynthesis (Keller et al., 1985; Segatto et al., 2011), and the low density lipoprotein receptor (LDLr), the protein responsible of cellular cholesterol uptake, exhibited a specific brain region pattern of activation state and protein expression (Segatto et al., 2012). Whether this pattern remains constant in both sexes and during ageing is completely unknown.

Age- and sex-dependent regulation of the processes underlying cholesterol homeostasis maintenance has been well demonstrated in rat liver (Pallottini et al., 2003, 2004, 2007; De Marinis et al., 2008; Trapani et al., 2010; Segatto et al., 2011). In elderly male and female rat, HMGR is highly activated; however, the mechanisms driving deregulation of HMGR appear to be gender-dependent (Trapani and Pallottini, 2010). Studies carried out on aged male rats suggest that in males, HMGR

*Abbreviations*: AD, Alzheimer's disease; AMPK, AMP activated kinase; CNS, central nervous system; DMSO, dimethylsulfoxyde; E2, 17-β-estradiol; GFAP, glial fibrillary acidic protein; HMGR, 3-hydroxy 3-methyl glutaryl coenzyme A reductase; Insig, insulin induced gene; LDLr, low-density lipoprotein receptor; PP2A, protein phosphatase 2A; ROS, Reactive oxygen species; SREBPs, sterol regulatory element binding proteins.

Contract grant sponsor: University of Roma Tre;
Contract grant number: CLAR 2010-2011.

*Correspondence to: Valentina Pallottini, Department of Biology, University of Roma Tre, Viale Marconi, 446 00146 Rome, Italy.
E-mail: vpallott@uniroma3.it

Manuscript Received: 9 October 2012
Manuscript Accepted: 19 December 2012

Accepted manuscript online in Wiley Online Library (wileyonlinelibrary.com): 31 December 2012.
DOI: 10.1002/jcp.24315

deregulation is due to the increased ROS-induced protein phosphatase 2A (PP2A) association to HMGR, which results in the increased enzyme activation (Pallottini et al., 2007). On the other hand, studies of aged female rats, in which the levels of the sex steroid hormone estrogen are decreased, suggest that HMGR deregulation is caused by the decreased activation of AMP activated kinase (AMPK) observed during estrogen deficiency inducing, also in this case, an increased activation of the enzyme (Trapani et al., 2010). Sex differences are also observable in the expression of hepatic HMGR in adult rats: these variations seem to be dependent on the estrogen-induced modulation of the proteins involved in HMGR long-term regulation (De Marinis et al., 2008).

Interestingly, literature data support that deregulations of cholesterol homeostasis in the brain could lead to the onset of a variety of neurodegenerative disorders such as Alzheimer's disease (AD) (Pfrieger, 2003), the incidence of which is higher in older women than in age-matched men (Andersen et al., 1999). A number of observations clearly highlight a link between AD and cholesterol metabolism, underlying the pivotal role of this lipid in the brain. In addition, since adult neurons reduce cholesterol biosynthesis and import this molecule from astrocytes through lipoproteins (Pfrieger, 2002), the existence of an intercellular horizontal transport of cholesterol strongly suggests that both LDLr and HMGR may play essential roles in this tissue. Given the importance of HMGR in cholesterol homeostasis maintenance, it is deeply regulated from both short-term and long-term regulations (Goldstein and Brown, 1990).

Short-term regulation is under the control of phosphorylation/dephosphorylation events operated by AMPK and by PP2A that inhibits and activates the enzyme, respectively. The ratio between phosphorylated and total HMGR provides the enzyme phosphorylation state (Pallottini et al., 2006). HMGR also undergoes to long-term regulation by membrane-bound transcription factors, sterol regulatory element binding proteins (SREBPs), able to induce the expression of genes whose products are involved in cholesterol synthesis and uptake, such as HMGR and LDLr (Brown and Goldstein, 1997). SREBP activities depend on cellular sterol content. When sterol concentration falls down into cells, SREBPs migrate from the endoplasmic reticulum (ER) to the Golgi apparatus where SREBPs are proteolytically cleaved by Site-1 and Site-2 proteases. This processing determines the release of the N-terminal transcriptionally active fragments that, once into the nucleus, induce the expression of the genes involved in lipid metabolism (Brown and Goldstein, 1999). When cholesterol accumulates in endoplasmic reticulum membranes, SREBPs are not able to reach the Golgi apparatus because are held into the endoplasmic reticulum by other resident proteins: Insulin induced gene-1 and -2 (Insig-1 and -2); the proteolytic cleavage of SREBPs is avoided and the transcription of the target genes declines (Segatto et al., 2011; Trapani et al., 2011). In addition, Insig proteins, in presence of high cholesterol content, are also able to induce HMGR degradation (Espenshade and Hughes, 2007), reducing cell ability to produce cholesterol.

Up to now, no research is present in literature dealing how and if sex and age may modulate the major proteins involved in the regulatory network of cholesterol levels in different brain regions. In this study we investigated the presence, the protein levels and the activation state of HMGR and LDLr, Insigs and SREBPs in four different brain regions of adult (3-month-old), aged (12-month-old) male and female rats. To verify whether the putative changes of the studied protein could be dependent on estrogen levels, aged (12-month-old) female rats were treated with 17-β estradiol. Twelve months of age can be regarded as the beginning of estropause in rats, characterized by ovarian cycle interruption and reduction in 17-β estradiol (E2) levels; thus 12-month-old female rats could be considered to be in a similar condition to that occurring in women at the onset of menopause (Trapani et al., 2010).

Since cholesterol metabolism in the brain is deeply affected by different factors, such as the amount of myelin and the cell metabolic rate, the analysis were performed in hippocampus, cortex, cerebellum, and brain stem, which are representative brain areas for different neuronal cell types, metabolism, cytoarchitecture, and white matter composition.

## Materials and Methods

### Reagents

All chemicals were obtained from commercial sources and of the highest quality available. Sources not specified were obtained from Sigma–Aldrich (Milan, Italy).

### Ethical approval

The experiments were performed according to the ethical guidelines for the conduct of animal research according Official Italian Regulation No.116/92 and the protocol was approved by the Ethical Review Board of Roma Tre University (protocol n° 18-VI/1.1).

### Animals

Twenty rats, 3- and 12-month-old male and female Wistar *Rattus norvegicus* (Harlan Nossan, S. Pietro al Natisone, Italy) were housed under controlled temperature (20 ± 1°C), humidity (55 ± 10%), and illumination (lights on for 12 h daily, from 7 AM to 7 PM). Food and water were provided ad libitum. All rats were held in quarantine for 2 weeks before the experiments. Nesting materials and tubes for tunneling were placed in all cages as environmental enrichment. Each experimental group was composed by four animals.

Adult female rats (3-month-old) were sacrificed in proestrous. The estrous cycle was determined at 07:00–09:00 using the method described in the organization for economic co-operation and development (OECD) guidance document for the histologic evaluation of endocrine and reproductive test in rodents (OECD, 2008). The cells lining the vagina of the female rat respond to levels of circulating hormones and represent a valuable marker of the stage of preparation of the ovary. To obtain vaginal cell samples, lavage or washing with saline or water from a pipette was used. The stages of the rat estrous cycle were classified according to the presence, absence, or proportions of three cell types in vaginal smears: cornified (keratinized) cells, epithelial cells, and leukocytes. Moreover proestrous was confirmed by plasma 17-β estradiol measurement (Table 1) as already reported (Butcher et al., 1974).

Four 12-month-old female rats were treated with a single intraperitoneal injection of 1 mg/kg 17-β estradiol (E2) or with the same volume of vehicle dimethylsulfoxyde (DMSO) 24 h before the experiment. Rats were sacrificed under deep urethane anesthesia (1.2 g/kg, i.p.) by decapitation and brains were removed. The cerebral regions used in this study were collected and immediately frozen at −80°C for subsequent biochemical assays.

### Lyzate preparation

Total lyzates were obtained as follows: 100 mg hippocampus, cortex, cerebellum, or brain stems were solubilized by sonication

TABLE 1. Plasma 17-β estradiol amount measurement in adult (3-month-old) and aged (12-month-old) female rats

| 3-month-old (vehicle) (pg/ml) | 12-month-old (vehicle) (pg/ml) | 12-month-old (E2) (ns pg/ml) | *P* value |
|---|---|---|---|
| 41.5 ± 2.9 | 31.2 ± 1.9[a] | 42.4 ± 2.3 | $P < 0.001$ |

Aged rats were treated with vehicle (DMSO 1 ml/kg) or 17-β estradiol (1 mg/kg).
[a]As from ANOVA followed by Tukey–Kramer test with respect to 3-month-old female rats.

in sample buffer (0.25 M Tris–HCl pH 6.8, containing 20% SDS and protease inhibitor cocktail). Then, the samples were centrifuged for 5 min at 15,600g, and the supernatant was transferred into microtubes. Protein concentration was determined by the method of (Lowry et al., 1951). All samples were boiled for 3 min before loading for Western blotting.

#### Protein analysis

Protein profiles were analyzed by Western blotting. Protein (30 μg) from total lyzates was resolved by 12% SDS–PAGE for Insig-1 and Insig-2 (Novus Biologicals, Cambridge, UK), 10% SDS–PAGE for glial fibrillary acidic protein (GFAP) (Synaptic System GmbH, Goettingen, Germany), and 7% SDS–PAGE for P-HMGR (Millipore, Temecula, CA), t-HMGR (Upstate, Lake Placid, NY), LDLr ab30532 (Abcam, Cambridge, UK), SREBP-1 (Santa Cruz Biotechnology, Santa Cruz, CA) and SREBP-2 (Abcam) as previously described (Trapani et al., 2011). α-Tubulin (Sigma–Aldrich) was used as housekeeping protein. Hrp-conjugated IgG produced in mouse or in rabbit (Biorad Laboratories, Milan, Italy) were used as secondary antibodies. Bound antibodies were visualized using enhanced chemoluminescence detection (GE Healthcare, Little Chalfont, UK).

#### Statistical analysis

All images derived from Western blotting were analyzed with ImageJ (National Institutes of Health, Bethesda, MD) software for Windows. Each reported value was calculated from the ratio between arbitrary units (a.u.) obtained by the protein band and the respective tubulin. Data are expressed as means ± standard deviation (SD). The significance of differences of parameters was statistically assessed by one-way analysis of variance (ANOVA) followed by Tukey–Kramer post-test. Values of $P < 0.05$ were considered to indicate a significant difference. Statistical analysis was performed using GraphPad Instat3 (GraphPad, Inc., La Jolla, CA) for Windows.

## Results

In order to evaluate prospective age- and sex-related differences of cholesterol metabolism in the CNS, we started to analyze phosphorylated HMGR (P-HMGR) and total HMGR (t-HMGR), the main protein involved in cholesterol synthesis. As illustrated in Figure 1, the phosphorylation state of the enzyme (i.e., ratio P-HMGR/t-HMGR/tubulin) did not show any significant sex- and age-related difference in brain stem (Fig. 1 parts A,B), cerebellum (Fig. 1 parts C,D), brain cortex (Fig. 1 parts E,F), and hippocampus (Fig. 1 parts G,H). It is interesting to note that t-HMGR protein expression (Fig. 1 parts G) was lower in 3-month-old female rats if compared with age-matched males (0.86 ± .0.04 vs. 1.55 ± 0.21; $P < 0.01$) in hippocampus, meaning that HMGR activity is lower with respect to the other experimental groups. This sex-related difference disappears during ageing, since t-HMGR levels rose up to reaching the expression levels of the enzyme found in the other physiological conditions analyzed.

Since cholesterol homeostasis is maintained by biosynthetic processes and extracellular uptake, we turned our attention on LDLr, it is synthesized in a precursor of apparent molecular mass of 110 kDa; this is converted to a mature form of apparent molecular mass of 160 kDa (Tolleshaug et al., 1983): the increase in molecular mass is correlated with extensive *N*- and *O*-glycosylation in the Golgi apparatus and during the vesicular transfer to the cell surface. LDLr contains 18 *O*-linked and two *N*-linked oligosaccharides (Cummings et al., 1983), which result to be essential in the binding affinity of the ligand and in the stability of the receptor (Filipovic, 1989; Reddy and Krieger, 1989). The data obtained in the present work shows that no changes were observed in LDLr content both in brain stem

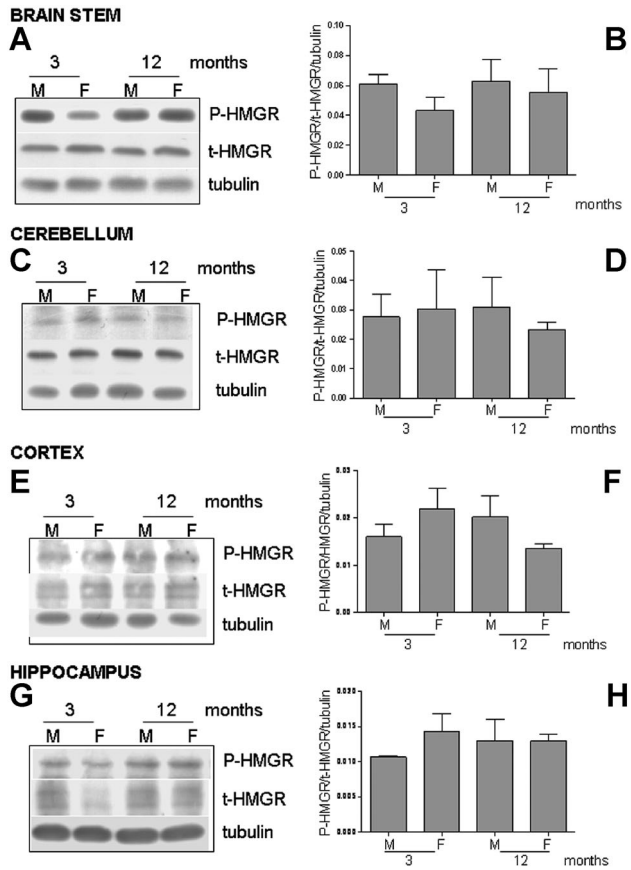


**Fig. 1. HMGR phosphorylation state in different brain areas of adult and aged male and female rats. The figure illustrates the phosphorylation state of HMGR in brain stem (parts A,B), cerebellum (parts C,D), cortex (parts E,F), and hippocampus (parts G,H) of adult (3-month-old) and aged (12-month-old) male and female rats. On the left a typical Western blot of P-HMGR, t-HMGR and tubulin, on the right the densitometric analysis of at least four different experiments performed in duplicate. The graphs show the ratio among P-HMGR/t-HMGR/tubulin arbitrary units obtained analyzing the bands with ImageJ for Windows. For details see the main text.**

(Fig. 2 parts A,B) and in cerebellum (Fig. 2 parts C,D) in all the experimental groups. Differently, a higher content of both the precursor and the mature forms were observable in 12-month-old female hippocampus if compared to age-matched-males (Fig. 2 parts G,H). On the contrary, 12-month-old female cortex showed an expected decrease of LDLr content (Fig. 2 parts E,F), confirming our previous data about the E2-dependent modulation in LDLr expression in aged female rats (Segatto et al., 2011).

The lower t-HMGR observed in adult female hippocampus could depend on a different amount of astrocytes since they represent the main cell pool in producing cholesterol in the adult CNS (Pfrieger, 2003), thus the level of glial fibrillary acidic protein (GFAP), an astrocytic marker, was measured in total hippocampus lysate. Figure 3 shows that GFAP displayed no differences in hippocampal tissue both in male and female adult and aged rats; therefore the proteins involved in the long-term regulation of HMGR were studied. Figure 4 (parts A,B) shows that Insig-1 protein expression was very high in hippocampus of 3-month-old female rats if compared with both age-matched males and 12-month-old animals, while no modifications were

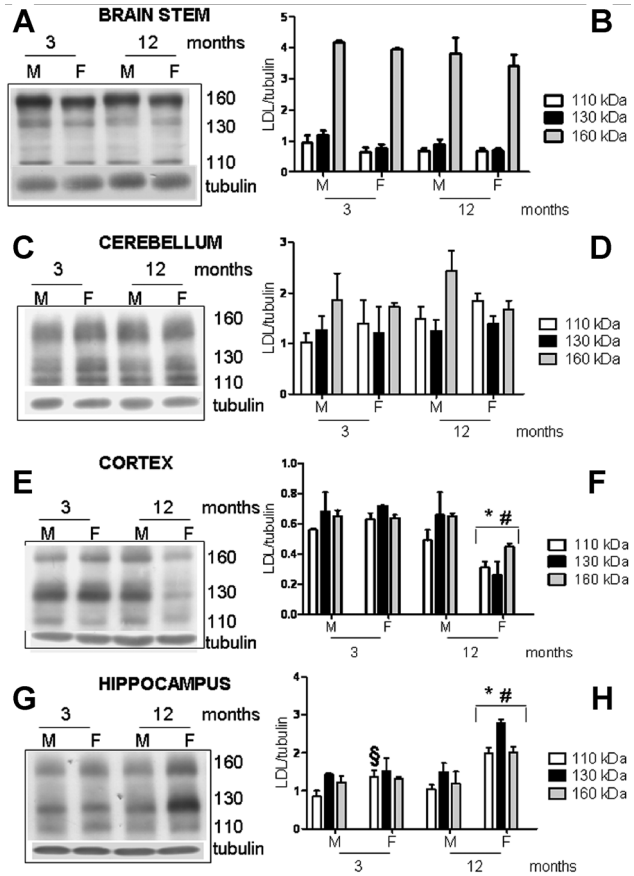


**Fig. 2. LDLr levels in different brain areas of adult and aged male and female rats. The figure illustrates the LDLr glicosylation pattern (110, 130, and 160 kDa) in brain stem (parts A,B), cerebellum (parts C,D), cortex (parts E,F), and hippocampus (parts G,H) of adult (3-month-old) and aged (12-month-old) male and female rats. On the left a typical Western blot of LDLr mature and precursor forms and of tubulin, on the right the densitometric analysis of at least four different experiments performed in duplicate. The graphs show the ratio between LDLr/tubulin arbitrary units obtained analyzing the bands with ImageJ for Windows. For details see the main text. $^{\S}P < 0.005$ as from ANOVA followed by Tukey–Kramer test with respect to 3-month-old males; $^{*}P < 0.001$ as from ANOVA followed by Tukey–Kramer test with respect to 3-month-old females; $^{\#}P < 0.001$ as from ANOVA followed by Tukey–Kramer test with respect to 12-month-old males.**

observable in Insig-2 content (parts C,D). The analyzes of SREBPs showed that the amount of the transcriptionally active fraction of SREBP-1 was higher in hippocampus of aged female rats than in males (Fig. 4 parts E,F). On the contrary, no changes were observed in the protein amount of SREBP-2 (Fig. 4 parts G,H).

Moreover, as sex-dependent differences in hippocampal functions are dependent on activational effects of sex steroid hormones (Swaab and Hofman, 1995), we verified whether the circulating levels of E2 could be related to LDLr and HMGR variations in female hippocampal tissue. To check this hypothesis, plasma E2, LDLr, and HMGR levels were assessed in adult and aged female untreated or treated with 1 mg/kg E2. As expected (Segatto et al., 2011), plasma E2 decreased in aged female rats, and the administration of E2 completely restored the circulating levels of the hormone as a female rat in proestrous (Table 1). However, E2 treatment did not

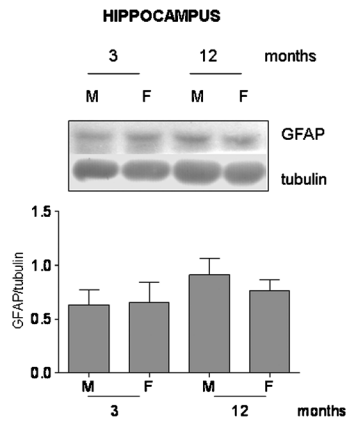


**Fig. 3. GFAP content in hippocampus of adult and aged male and female rats. The figure illustrates GFAP in hippocampus of adult (3-month-old) and aged (12-month-old) male and female rats. On the top a typical Western blot, on the bottom the densitometric analysis of at least four different experiments performed in duplicate. The graphs show the ratio of arbitrary units between GFAP/tubulin obtained by analyzing the protein bands with ImageJ for Windows. For details see the main text.**

re-establish HMGR expression (Fig. 5, part A) and further increased both glicosylated and unglicosylated LDLr forms (Fig. 5, part B).

## Discussion

Cholesterol biosynthetic cascade has to be considered an essential metabolic pathway in the CNS. Beside HMGR, the key and rate-limiting enzyme of this pathway, lipoprotein uptake by LDLr results to be an important event in maintaining cellular cholesterol homeostasis (Segatto et al., 2011). The importance of the physiological regulation of cholesterol metabolism in the CNS is also highlighted by several clinical studies, which demonstrated that impairments in the mechanisms regulating cholesterol homeostasis are linked to a variety of brain pathological pictures, such as Alzheimer's disease, Niemann Pick type C disease, and multiple sclerosis (Pfrieger, 2003; Zipp et al., 2007; Segatto et al., 2011). In addition, recent literature suggests that statins, strong HMGR inhibitors widely used in hypocholesterolemia treatments, can lead to several side effects in the CNS, such as mood changes, irritability, depressive syndromes and modulation in cognition (Golomb et al., 2004; Baytan et al., 2008), suggesting again the key role of cholesterol biosynthetic pathway in the CNS.

Recent data obtained in our laboratory demonstrated that marked differences in HMGR and LDLr expression are observable in the adult CNS of male rats. In fact, the modulation of the key proteins and enzymes responsible for the maintenance of cholesterol homeostasis, in specific brain region, is required in connection with the rate of lipid metabolism and the specific amount of cholesterol needed in each brain area (Segatto et al., 2012). Moreover, these proteins were subjected to both ageing- and sex-dependent regulation in hepatic tissue (De Marinis et al., 2008; Trapani and Pallottini, 2010).

As far as we know, few researches are addressed to evaluate differences from an age and a gender perspective in the regulation of cholesterol homeostasis in different brain areas important for the maintenance of higher-order functions, such as learning and memory (Lebron-Milad and Milad, 2012). It is

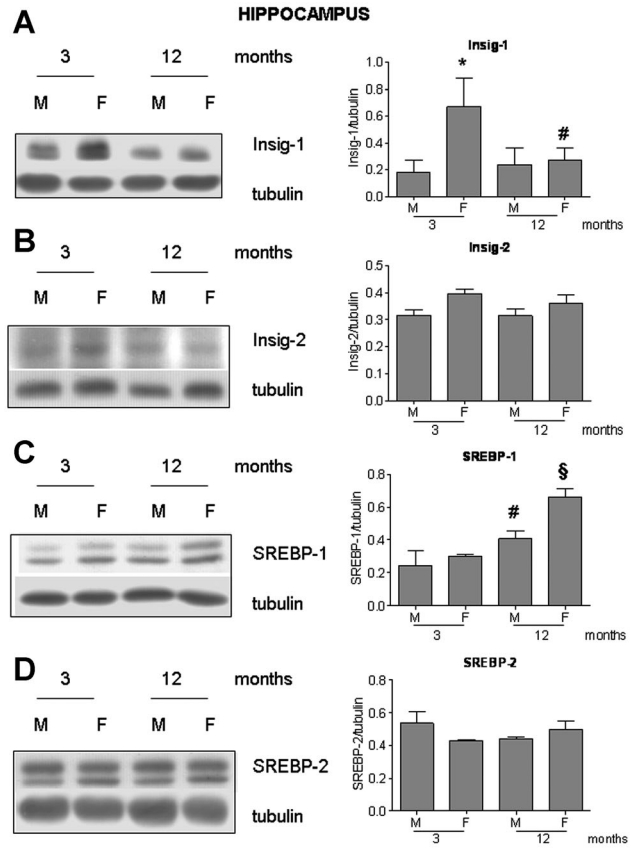


**Fig. 4. Insig-1 and -2, SREBP-1 and -2 levels in hippocampus of adult and aged male and female rats. The figure illustrates Insig-1 content (parts A), Insig-2 content (part B), Srebp-1 content (parts D), and SREBP-2 content (parts E) in the hippocampus of adult (3-month-old) and aged (12-month-old) male and female rats. On the left a typical Western blot of the analyzed proteins and of tubulin, on the right the densitometric analysis of at least four different experiments performed in duplicate. The graphs show the ratio between proteins/tubulin arbitrary units obtained analyzing the bands with ImageJ for Windows. For details see the main text. *$P < 0.001$ as from ANOVA followed by Tukey–Kramer test with respect to 3-month-old males; #$P < 0.001$ as from ANOVA followed by Tukey–Kramer test with respect to 3-month-old females; §$P < 0.001$ as from ANOVA followed by Tukey–Kramer test with respect to 12-month-old males.**

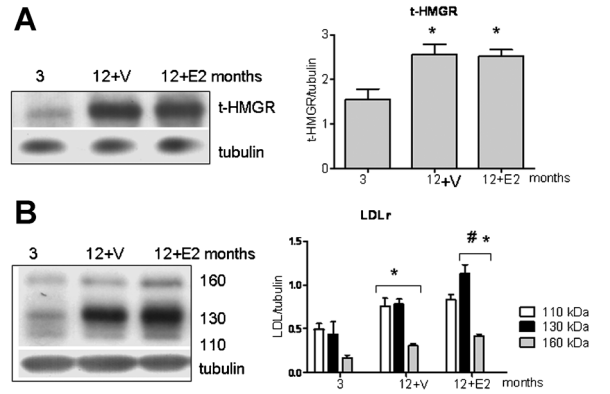


**Fig. 5. t-HMGR and LDLr in hippocampus of adult and E2 treated aged female rats. The figure illustrates t-HMGR content (parts A, B) and LDLr content (part C,D) in the hippocampus of adult female (3-month-old) and aged (12-month-old) female rats treated with vehicle (V) or 1 mg/kg E2 (E2). On the left a typical Western blot of the analyzed proteins and of tubulin, on the right the densitometric analysis of at least four different experiments performed in duplicate. The graphs show the ratio of arbitrary units between proteins/tubulin obtained analyzing the bands with ImageJ for Windows. For details see the main text. *$P < 0.001$ as from ANOVA followed by Tukey–Kramer test with respect to 3-month-old females; #$P < 0.001$ as from ANOVA followed by Tukey–Kramer test with respect to 12-month-old females.**

noticeable that a region-specific study results to be of great importance, since each brain area possess a specific energy balance, cytoarchitecture, function and myelin composition, and all of these distinctive features could be influenced by cholesterol metabolism.

Thus, the present work was aimed at analyzing the proteins involved in cholesterol homeostasis maintenance from a sex and age perspective among different brain regions. The obtained results display that the most relevant differences were observed in the cortex and in the hippocampus. In the cortex, the reported results confirmed what we previously observed showing that LDLr content in aged female rats depends on the plasma E2 decrease during the estropause (Segatto et al., 2011). On the contrary, the results obtained in hippocampus, which displayed both sex- and age-dependent variation in both HMGR and LDLr protein expression, were never reported before.

The low t-HMGR observed in hippocampal tissues of adult female rats, depends neither on a different number of astrocytes nor on a decreased transcription with respect to adult male rats. Instead, the high Insig-1 level supports an increased degradation rate of the protein. The increased amount of t-HMGR in aged female rats, on the contrary, could be ascribable to the modulation of transcriptional events due to the high content of SREBP-1 active fragment present in this physiological state. Moreover, the decrease in Insig-1 protein content in aged female rats with the respect to young ones could also contribute to the rise of t-HMGR. Thus, a different balance of SREBP-1 and Insig-1 is at the root of the low t-HMGR in adult female hippocampus. The high amount of SREBP-1 active fragment observed in aged female hippocampus can also explain the high content of LDLr found in the same samples.

The obtained results led us to exclude the involvement of circulating E2 in the modulations we observed. Indeed, the exogenous E2 treatment was able to restore neither LDLr levels nor HMGR content. In particular, E2 administration did not absolutely affect t-HMGR, while it was able to further enhance the increase in 130 and 160 kDa LDLr, leading to hypothesize that the circulating hormone could have an effect on LDL glycosylation processes. Although E2 could be produced locally, the sex- and age- dependent differences observed both in HMGR and in LDLr in hippocampus are not dependent on circulating E2 levels, and could be explained by an enhanced HMGR degradation operated by Insig-1 in adult female rats, and by an intensified LDLr and HMGR transcription due to the increase in the SREBP-1 transcriptionally active fraction in aged female rats.

When evaluated as a whole, these data confirm marked dissimilarities in HMGR and LDLr regulation in brain regions emphasizing that sex- and age-related differences are present, in particular in the hippocampus. The differences observed between adult male and female support the increasing evidences that physiological dissimilarities are present between sexes in brain areas (Lebron-Milad and Milad, 2012) which maintain cholesterol homeostasis with different mechanisms as reported in other systems (i.e., cardiovascular system) (Pepine et al., 2006; Marino et al., 2011).

Our results obtained from aged rats could be construed on a pathophysiological point of view. The hippocampus and the cerebral cortex are two highly dynamic brain regions in terms of synaptic plasticity: as the importance of cholesterol in the stabilization and the formation of synapses, the differences observed in the presented work may account for the different incidence of those diseases, in connection to different physiological conditions such as age and gender, that could be related to an imbalance in cholesterol homeostasis (Pfrieger, 2003; Zipp et al., 2007; Segatto et al., 2011). It is very interesting to note that deregulation in cholesterol homeostasis in the CNS could be related to the appearance of neurodegenerative disorders such as AD (Pfrieger, 2003), whose incidence is higher in older women than in age-matched men (Andersen et al., 1999) and whose onset is initially charged to the hippocampus, the brain region in which we observed the major imbalances in the studied proteins. A growing number of studies clearly establish a link between AD and cholesterol metabolism, underlying the pivotal role of this lipid in the brain. Indeed, it has been shown that high levels of intracellular cholesterol inhibit α-secretase activity (Bodovitz and Klein, 1996) and increase β-amyloid generation via activation of both β- and γ-secretases (Frears et al., 1999; Xiong et al., 2008) and that diet-induced hypercholesterolemia increases β-amyloid levels in the brain thus accelerating extracellular β-amyloid deposition in a experimental model of AD (Refolo et al., 2000; Shie et al., 2002). In this respect, it is also important to underlie that 12-month-old female rats display an increased plasma cholesterol level that could contribute to the onset of the disease (Trapani et al., 2010). Moreover, several data demonstrate that cellular cholesterol uptake through LDLr may be a very important homeostatic mechanism of clearance as it controls Alzheimer's β-amyloid peptide elimination from the brain (Cao et al., 2006; Zlokovic et al., 2010). Thus the increased hippocampal LDL expression could be a protective mechanism operated by this region to counteract the phyisiological age-related amyloid deposition whose incidence is higher in female (Callahan et al., 2001). On the other hand, it has been recently demonstrated that oligomeric β-amyloid peptide reduces the expression of genes involved in cholesterol synthesis in neurons (Malik et al., 2012), thus suggesting that hippocampal LDLr increase may be not only a neuroprotective event but also a feedback response of the neurons to counteract the prospective reduction in sterol synthesis.

Considering the strong divergences in the regional modulation of the proteins involved in cholesterol metabolism assessed in this work, it is possible to speculate that each brain area can be considered as a unique structure with a specific cellular context, able to respond in a different way to the same stimuli (i.e., E2 treatment).

There are now extensive data in scientific literature indicating that structural, cellular and molecular differences exist between male and female brains, especially in regions that are important for learning, memory and affection, such as the hippocampus and the prefrontal cortex. Some of these differences may have clinical relevance, as marked disparities in disease incidence, manifestation, prognosis and treatment have been observed between the sexes. The results obtained can be inserted in this context adding a new piece in the complicated puzzle of physiological sex differences and in the changes that occur in dependence of ageing.

## Acknowledgments

The generous gift of GFAP antibody from Prof. Sandra Moreno (Department of Biology, University of Roma Tre) is gratefully acknowledged. This work was supported by grants from University of "Roma Tre" CLAR 2010-2011 to V.P.

## Literature Cited

Andersen K, Launer LJ, Dewey ME, Letenneur L, Ott A, Copeland JR, Dartigues JF, Kragh-Sorensen P, Baldereschi M, Brayne C, Lobo A, Martinez-Lage JM, Stijnen T, Hofman A. 1999. Gender differences in the incidence of AD and vascular dementia: The EURODEM Studies. EURODEM Incidence Research Group. Neurology 53:1992–1997.

Baytan SH, Alkanat M, Okuyan M, Ekinci M, Gedikli E, Ozeren M, Akgun A. 2008. Simvastatin impairs spatial memory in rats at a specific dose level. Tohoku J Exp Med 214:341–349.

Bjorkhem I, Meaney S. 2004. Brain cholesterol: Long secret life behind a barrier. Arterioscler Thromb Vasc Biol 24:806–815.

Block RC, Dorsey ER, Beck CA, Brenna JT, Shoulson I. 2010. Altered cholesterol and fatty acid metabolism in Huntington disease. J Clin Lipidol 4:17–23.

Bodovitz S, Klein WL. 1996. Cholesterol modulates alpha-secretase cleavage of amyloid precursor protein. J Biol Chem 271:4436–4440.

Brown MS, Goldstein JL. 1997. The SREBP pathway: Regulation of cholesterol metabolism by proteolysis of a membrane-bound transcription factor. Cell 89:331–340.

Brown MS, Goldstein JL. 1999. A proteolytic pathway that controls the cholesterol content of membranes, cells, and blood. Proc Natl Acad Sci USA 96:11041–11048.

Butcher RL, Collins WE, Fugo NW. 1974. Plasma concentration of LH, FSH, prolactin, progesterone, and estradiol-17 beta throughout the 4-day estrous cycle of the rat. Endocrinology 94:1704–1708.

Callahan M, Lipinski W, Bian F, Durham R, Pack A, Walker L. 2001. Augmented senile plaque load in aged female beta amyloid precursor protein-transgenic mice. Am J Pathol 158:1173–1177.

Cao D, Fukuchi K, Wan H, Kim H, Li L. 2006. Lack of LDL receptor aggravetes learning deficits and amyloid deposits in Alzheimer transgenic mice. Neurobiol Ageing 27:1632–1643.

Cummings RD, Kornfeld S, Schneider WJ, Hobgood KK, Tolleshaug H, Brown MS, Goldstein JL. 1983. Biosynthesis of *N*- and *O*-linked oligosaccharides of the low-density lipoprotein receptor. J Biol Chem 258:15261–15273.

De Marinis E, Martini C, Trentalance A, Pallottini V. 2008. Sex differences in hepatic regulation of cholesterol homeostasis. J Endocrinol 198:635–643.

Dietschy JM, Turley SD. 2004. Thematic review series: Brain Lipids. Cholesterol metabolism in the central nervous system during early development and in the mature animal. J Lipid Res 45:1375–1397.

Espenshade PJ, Hughes AL. 2007. Regulation of sterol synthesis in eukaryotes. Annu Rev Genet 41:401–427.

Filipovic I. 1989. Effect of inhibiting *N*-glycosylation on the stability and binding activity of the low-density lipoprotein receptor. J Biol Chem 264:8815–8820.

Frears ER, Stephens DJ, Walters CE, Davies H, Austen BM. 1999. The role of cholesterol in the biosynthesis of beta-amyloid. Neuroreport 10:1699–1705.

Goldstein JL, Brown MS. 1990. Regulation of the mevalonate pathway. Nature 343:425–430.

Golomb BA, Kane T, Dimsdale JE. 2004. Severe irritability associated with statin cholesterol-lowering drugs. QJM 97:229–235.

Keller GA, Barton MC, Shapiro DJ, Singer SJ. 1985. 3-Hydroxy-3-methylglutaryl-coenzyme A reductase is present in peroxisomes in normal rat liver cells. Proc Natl Acad Sci USA 82:770–774.

Lebron-Milad K, Milad MR. 2012. Sex differences, gonadal hormones and the fear extinction network: Implications for anxiety disorders. Biol Mood Anxiety Disord 2:3.

Lowry OH, Rosebrough NJ, Farr AL, Randall RJ. 1951. Protein measurement with the Folin phenol reagent. J Biol Chem 193:265–275.

Malik B, Fernandes C, KilliK R, Wroe R, Usardi A, Williamson R, Kellie S, Anderton BH, Reynolds CH. 2012. Oligomeric amyloid-beta peptide affects the expression of genes involved in steroid and lipid metabolism in primary neurons. Neurochem Int 61:321–333.

Marino M, Masella R, Bulzomi P, Campesi I, Malorni W, Franconi F. 2011. Nutrition and human health from a sex-gender perspective. Mol Aspects Med 32:1–70.

Ohvo-Rekila H, Ramstedt B, Leppimaki P, Slotte JP. 2002. Cholesterol interactions with phospholipids in membranes. Prog Lipid Res 41:66–97.

Pallottini V, Marino M, Cavallini G, Bergamini E, Trentalance A. 2003. Age-related changes of isoprenoid biosynthesis in rat liver and brain. Biogerontology 4:371–378.

Pallottini V, Martini C, Bassi AM, Romano P, Nanni G, Trentalance A. 2006. Rat HMGCoA reductase activation in thioacetamide-induced liver injury is related to an increased reactive oxygen species content. J Hepatol 44:368–374.

Pallottini V, Martini C, Cavallini G, Bergamini E, Mustard KJ, Hardie DG, Trentalance A. 2007. Age-related HMG-CoA reductase deregulation depends on ROS-induced p38 activation. Mech Ageing Dev 128:688–695.

Pallottini V, Montanari L, Cavallini G, Bergamini E, Gori Z, Trentalance A. 2004. Mechanisms underlying the impaired regulation of 3-hydroxy-3-methylglutaryl coenzyme A reductase in aged rat liver. Mech Ageing Dev 125:633–639.

Pepine CJ, Nichols WW, Pauly DF. 2006. Estrogen and different aspects of vascular disease in women and men. Circ Res 99:459–461.

Pfrieger FW. 2002. Role of glia in synapse development. Curr Opin Neurobiol 12:486–490.

Pfrieger FW. 2003. Role of cholesterol in synapse formation and function. Biochim Biophys Acta 1610:271–280.

Reddy P, Krieger M. 1989. Isolation and characterization of an extragenic suppressor of the low-density lipoprotein receptor-deficient phenotype of a Chinese hamster ovary cell mutant. Mol Cell Biol 9:4799–4806.

Refolo LM, Malester B, LaFrancois J, Bryant-Thomas T, Wang R, Tint GS, Sambamurti K, Duff K, Pappolla MA. 2000. Hypercholesterolemia accelerates the Alzheimer's amyloid pathology in a transgenic mouse model. Neurobiol Dis 7:321–331.

Repa JJ, Mangelsdorf DJ. 2000. The role of orphan nuclear receptors in the regulation of cholesterol homeostasis. Annu Rev Cell Dev Biol 16:459–481.

Segatto M, Trapani L, Lecis C, Pallottini V. 2012. Regulation of cholesterol biosynthetic pathway in different regions of the rat central nervous system. Acta Physiol (Oxf) 206:62–71.

Segatto M, Trapani L, Marino M, Pallottini V. 2011. Age- and sex-related differences in extra-hepatic low-density lipoprotein receptor. J Cell Physiol 226:2610–2616.

Shie FS, Jin LW, Cook DG, Leverenz JB, LeBoeuf RC. 2002. Diet-induced hypercholesterolemia enhances brain A beta accumulation in transgenic mice. Neuroreport 13:455–459.

Swaab DF, Hofman MA. 1995. Sexual differentiation of the human hypothalamus in relation to gender and sexual orientation. Trends Neurosci 18:264–270.

Tolleshaug H, Hobgood KK, Brown MS, Goldstein JL. 1983. The LDL receptor locus in familial hypercholesterolemia: Multiple mutations disrupt transport and processing of a membrane receptor. Cell 32:941–951.

Trapani L, Pallottini V. 2010. Age-related hypercholesterolemia and HMG-CoA reductase dysregulation: Sex does matter (A gender perspective). Curr Gerontol Geriatr Res 2010:1–7.

Trapani L, Segatto M, Simeoni V, Balducci V, Dhawan A, Parmar VS, Prasad AK, Saso L, Incerpi S, Pallottini V. 2011. Short- and long-term regulation of 3-hydroxy 3-methylglutaryl coenzyme A reductase by a 4-methylcoumarin. Biochimie 93:1165–1171.

Trapani L, Violo F, Pallottini V. 2010. Hypercholesterolemia and 3-hydroxy-3-methylglutaryl coenzyme A reductase regulation in aged female rats. Exp Gerontol 45:119–128.

Xiong H, Callaghan D, Jones A, Walker DG, Lue LF, Beach TG, Sue LI, Woulfe J, Xu H, Stanimirovic DB, Zhang W. 2008. Cholesterol retention in Alzheimer's brain is responsible for high beta- and gamma-secretase activities and Abeta production. Neurobiol Dis 29:422–437.

Zipp F, Waiczies S, Aktas O, Neuhaus O, Hemmer B, Schraven B, Nitsch R, Hartung HP. 2007. Impact of HMG-CoA reductase inhibition on brain pathology. Trends Pharmacol Sci 28:342–349.

Zlokovic BV, Deane R, Sagare AP, Bell RD, Winkler EA. 2010. Low density lipoprotein receptor-related protein-1: A serial clearance homeostatic mechanism controlling Alzheimer's amyloid beta peptide elimination from the brain. J Neurochem 115:1077–1089.

**Neuropsychopharmacology (2013),** 1–14

**www.neuropsychopharmacology.org**

# Simvastatin Treatment Highlights a New Role for the Isoprenoid/Cholesterol Biosynthetic Pathway in the Modulation of Emotional Reactivity and Cognitive Performance in Rats

**Marco Segatto[1], Antonia Manduca[1], Claudio Lecis[1], Pamela Rosso[1], Adam Jozwiak[2], Ewa Swiezewska[2], Sandra Moreno[1], Viviana Trezza[1] and Valentina Pallottini*[,1]**

*[1]Department of Science, University Roma Tre, Viale Marconi, Rome, Italy; [2]Institute of Biochemistry and Biophysics Polish Academy of Sciences, Warsaw, Poland*

The aim of the present work was to shed light on the role played by the isoprenoid/cholesterol biosynthetic pathway in the modulation of emotional reactivity and memory consolidation in rodents through the inhibition of the key and rate-limiting enzyme 3-hydroxy 3-methylglutaryl Coenzyme A reductase (HMGR) both *in vivo* and *in vitro* with simvastatin. Three-month-old male Wistar rats treated for 21 days with simvastatin or vehicle were tested in the social interaction, elevated plus-maze, and inhibitory avoidance tasks; after behavioral testing, the amygdala, hippocampus, prefrontal cortex, dorsal, and ventral striatum were dissected out for biochemical assays. In order to delve deeper into the molecular mechanisms underlying the observed effects, primary rat hippocampal neurons were used. Our results show that HMGR inhibition by simvastatin induces anxiogenic-like effects in the social interaction but not in the elevated plus-maze test, and improves memory consolidation in the inhibitory avoidance task. These effects are accompanied by imbalances in the activity of specific prenylated proteins, Rab3 and RhoA, involved in neurotransmitter release, and synaptic plasticity, respectively. Taken together, the present findings indicate that the isoprenoid/cholesterol biosynthetic pathway is critically involved in the physiological modulation of both emotional and cognitive processes in rodents.
*Neuropsychopharmacology* advance online publication, 30 October 2013; doi:10.1038/npp.2013.284

**Keywords:** simvastatin; memory; anxiety; RhoA; Rab3; CREB

## INTRODUCTION

The isoprenoid/cholesterol biosynthetic pathway, also known as the mevalonate (MVA) pathway, is one of the most notorious metabolic processes as it leads to the production of cholesterol and other non-sterol isoprenoids, which are essential in the induction and the maintenance of several cellular processes. The key enzyme of this pathway is the 3-hydroxy-3-methylglutaryl coenzyme A reductase (HMGR) (Brown and Goldstein, 1980; Segatto *et al*, 2013). The role of the MVA pathway is well-established in the liver, where a major part of lipid metabolism takes place (Horton, 2002; Pallottini *et al*, 2007; Segatto *et al*, 2013). However, this metabolic pathway is ubiquitously expressed in all eukaryotic cells, and recent studies sustain a pivotal role for MVA end-products in the brain. Although the CNS constitutes the 2% of the body weight, it contains about 25% of the total body cholesterol (Pfrieger, 2003; Segatto *et al*, 2013). The majority of cholesterol is present in myelin sheaths and in neuronal membranes, where this lipid fulfills structural and functional tasks. Given the crucial role of cholesterol in regulating different neuronal processes, eukaryotes have developed sophisticated homeostatic mechanisms to preserve cholesterol levels in an optimal range in each brain region (Segatto *et al*, 2013). Thus, alterations in this essential equilibrium could lead to pathological consequences in the CNS, such as the Smith-Lemli-Opitz syndrome, Alzheimer's, and Niemann-Pick type C diseases (Dietschy and Turley, 2004; Pfrieger, 2003; Segatto *et al*, 2011).

Besides cholesterol, isoprenoid compounds carry out important roles in the CNS. Prenylation, the covalent binding of farnesyl pyrophosphate (FPP) or geranylgeranyl pyrophosphate (GGPP) moieties to proteins, is a crucial post-translational modification for the regulation of protein localization on cell membranes and, in turn, for key cellular processes. Isoprenoids are not only required for protein prenylation but also constitute the side chain of Coenzyme Q (CoQ) (Matthews *et al*, 1998), whereas dolichols are involved in the N-linked glycosylation of proteins (Trapani *et al*, 2011b).

*Correspondence: Professor V Pallottini, Department of Science, University Roma Tre, Viale Marconi, Rome 446 00146, Italy, Tel: +39 06 57336320, Fax: +39 06 57336321,
E-mail: valentina.pallottini@uniroma3.it
Received 9 April 2013; revised 2 October 2013; accepted 3 October 2013; accepted article preview online 10 October 2013

The essential role of MVA end-products in the CNS physiology is also supported by growing preclinical and clinical studies on the pleiotropic effects of statins in the brain. Statins are strong HMGR inhibitors widely prescribed in therapies against hypercholesterolemia and their benefits in preventing atherosclerosis and other cardiovascular diseases are incontrovertible. Recently, it has been reported that high-dose statin treatment induces effects in emotional, learning, and memory processes (Kilic *et al*, 2012; Douma *et al*, 2011; Baytan *et al*, 2008; While and Keen, 2010). However, the role of the MVA biosynthetic pathway in the modulation of emotional behavior and cognitive performance is still unclear because of the lack of systematic studies on the causal link between the activation of this metabolic pathway and behavioral and cognitive outcomes. As a consequence, the effects exerted by statins in the CNS still remain confusing and unconvincing. Moreover, no data about a low-dose statin treatment are available. A better understanding of these processes could be of great interest toward new pharmacological interventions for CNS disorders. Thus, the aim of the present work was to shed light on the role played by the MVA pathway in the modulation of emotional reactivity and memory consolidation in rodents, through the inhibition by simvastatin of HMGR both *in vivo* and *in vitro*.

## MATERIALS AND METHODS

### Animals

Three-month-old male Wistar rats (Harlan Nossan, S Pietro al Natisone, Italy) were housed in groups of two and maintained under controlled temperature ($20 \pm 1\,^{\circ}C$), humidity ($55 \pm 10\%$), and illumination (12/12 h light cycle with lights on at 0700 hours). Food and water were provided *ad libitum*. All procedures involving animal care or treatments were approved by the Italian Ministry of Health and performed in compliance with the guidelines of the US National Institutes of Health (NIH) and the Italian Ministry of Health (n° 231/2012-B, according to DL 116/92), the Declaration of Helsinki, the Guide for the Care and Use of Mammals in Neuroscience and Behavioral Research (National Research Council 2004) and the Directive 2010/63/EU of the European Parliament and of the Council of 22 September 2010 on the protection of animals used for scientific purposes.

### Drug Treatment

Simvastatin (Sigma-Aldrich, Milan, Italy) was dissolved in a vehicle containing dimethyl sulfoxide—250 μl/kg body weight of 10% DMSO in sterile $H_2O$ (v/v)—and the dose of 1.5 mg/kg was daily administered by intraperitoneal injections for 3 weeks. Control animals were treated with vehicle only. Immediately after testing, rats were deeply anesthetized using Urethane (1.2 mg/kg) and plasma obtained from the blood collected into EDTA (1 mg/ml blood). Subsequently, rats were decapitated and their brains quickly removed. Brain regions of interest (amygdala, hippocampus, prefrontal cortex, dorsal, and ventral striatum) were collected and frozen in liquid nitrogen for subsequent biochemical analyses.

### Plasma Cholesterol Analysis

Plasma cholesterol content was estimated by the colorimetric CHOD-POD kit in accordance to the manufacturer's instructions (Assel, Rome, Italy).

### Plasma Triglycerides Analysis

The amount of plasma triglycerides was assessed by using the Triglyceride Quantification Kit in accordance to the manufacturer's instructions (BioVision, Mountain View, CA).

### Behavioral Tests

The behavioral experiments were performed the day following the last administration of either simvastatin or vehicle. Different groups of rats were used for each behavioral test.

*Social interaction test.* The social interaction test was performed under dim light conditions in a Plexiglas arena ($45 \times 45 \times 60$ cm) with $\sim 2$ cm of wood shavings covering the floor.

The test consisted in placing two similarly treated animals into the test cage for 10 min, with new sawdust as bedding. The animals in a pair did not differ more than 10 g in body weight; furthermore, they were housed in different cages and that therefore had no previous common social experience from the arrival in our Facility till the day of testing (File, 1980; Trezza *et al*, 2008).

The behavior of the animals was recorded on DVD for subsequent appropriate behavioral analysis carried out by the same observer, who was unaware of animal treatment, using the Observer 3.0 software (Noldus Information Technology BV, Wageningen, the Netherlands).

The total time spent in active social interaction was obtained as the sum of the time spent in the following behavioral elements scored per 10 min:

Play-related behaviors: (1) total time spent in pouncing (ie, when one animal attempts to nose or rub the nape of the neck of its play partner), which is an index of play solicitation; (2) total time spent in pinning (ie, the most common terminal component of a play bout, in which one animal stands over a supine partner), which is the consummatory measure of play (Panksepp *et al*, 1984; Trezza *et al*, 2010).

Social behaviors unrelated to play: total time spent in social exploration (sniffing any part of the body of the test partner, including the anogenital area; social grooming; following/chasing).

*Elevated plus-maze.* The elevated plus-maze test was performed as previously described (Pellow and File, 1986; Trezza *et al*, 2009). Briefly, the rats were individually placed on the central platform of the maze, facing a closed arm, and allowed to freely explore the maze for 5 min.

The 5 min test period was recorded on DVD for subsequent appropriate behavioral analysis carried out by the same observer, unaware of animal treatment, using the Observer 3.0 software (Noldus Information Technology BV, Wageningen, the Netherlands).

The following parameters were analyzed:

% time spent on the open arms (% TO): (seconds spent on the open arms of the maze/300) $\times$ 100;

% open arm entries (% OE): (the number of entries into the open arms of the maze/number of entries into open + center + closed arms) × 100;

Number of total arm entries (open + closed arm entries).

*Inhibitory avoidance.* The inhibitory-avoidance apparatus (Ugo Basile, Comerio, Italy) consisted of a Plexiglas cage with tilting floor, divided by a sliding door into two compartments (22 × 22 × 25 cm each). One of the compartments had white walls and was brightly illuminated by a 10-W bulb. The other compartment had black walls and was not illuminated. The tilting floor consisted of bars of stainless Steel connected to a source of scrambled shock. The procedure consisted of two sessions: acquisition and retention, that took place on 2 subsequent days (Mereu *et al*, 2003; Campolongo *et al*, 2007). For details see Supplementary Materials and Methods.

### Lipid Extraction

Lipid extraction from brain regions (amygdala, hippocampus, prefrontal cortex, dorsal striatum, and ventral striatum) was assessed by following the previously described protocol (Trapani *et al*, 2011a).

### HPLC-UV Analysis of Isoprenoids

Cholesterol, Coenzyme Q9 (CoQ9), Coenzyme Q10 (CoQ10), and dolichols were analyzed according to the previously described protocol (Tang *et al*, 2001) with modifications. For details see Supplementary Materials and Methods.

### Lysate, Cytosol, and Membrane Preparation from the Brain Tissue

Lysate and membrane from the brain tissue were prepared slightly modifying our previously used protocol (Segatto *et al*, 2011). For details, see Supplementary Materials and Methods.

### Synaptic Vesicle Preparation

Synaptic vesicles were prepared following the protocol described by Huttner *et al* (1983) with modifications. Rat brain regions (amygdala, hippocampus, prefrontal cortex, dorsal striatum, and ventral striatum) were homogenized in 10 vol of ice-cold HEPES-buffered sucrose (4 mM HEPES, 0.32 M sucrose, and 0.001 M PMSF, pH 7.4) with 10 strokes in a glass-Teflon homogenizer. Homogenates were centrifuged at 1000 *g* to remove nuclei, intact cells and cell debris (P1 fraction). The supernatant (S1) was spun at 10 000 *g* for 15 min to yield the crude synaptosomal pellet (P2). The supernatant (S2) was collected and subsequently centrifuged at 100 000 *g* for 15 min to produce the cytosolic fraction (S2′). The P2 fraction was then resuspended in 10 vol of HEPES-buffered sucrose and respun at 10 000 *g* for 15 min to obtain the washed crude synaptosomal fraction (P2′). The resulting pellet was lysed by hypoosmotic shock in 9 vol of ice-cold distilled water plus 0.001 M PMSF and three strokes of a glass-Teflon homogenizer. Four millimolars HEPES (pH 7.4) was rapidly added to the lysate which was mixed continuously in a cold room for 30 min to guarantee the total lysis of the sample. The lysate was subsequently centrifuged at 25 000 *g* for 20 min and the supernatant (S3) was collected and spun at 165 000 *g* for 2 h. The pellet of synaptic vesicles was finally solubilized in a sample buffer (0.125 M Tris-HCl, pH 6.8, containing 10% SDS, 0.001 M PMSF) and transferred into 1.5 ml Eppendorf tubes. Protein determination was assessed by the method of Lowry *et al* (1951). The synaptic vesicle samples were boiled for 3 min before loading for the western blotting method. In order to obtain an adequate amount of synaptic vesicles, each sample was made up from six brain regions pulled together from six different animals. The protein detection of synaptophysin (synaptic vesicle marker) and α-tubulin (cytosolic marker) verified and confirmed a high degree of purity of the synaptic vesicles (Supplementary Figure S1).

### Rab3 '*In Vitro*' Degradation Assay

Rab3 degradation assay was performed according to the protocol used by Pallottini *et al* (2004) with modifications. For details see Supplementary Materials and Methods.

### Hippocampal Neuron Primary Cultures and Drug Treatment

Primary hippocampal neurons were isolated and cultured according to the previously described protocol (Oh *et al*, 2006). For details see Supplementary Materials and Methods.

### Western Blotting Analysis

Western blot method was performed slightly modifying the protocol described by Trapani *et al* (2011a) by using the following antibodies: LDLr ab30532 (Abcam); SREBP-2 ab28482 (Abcam); NeuN A60 (Chemicon); GFAP 134B1 (Synaptic Systems); Rab3 G-1, CREB, p-CREB, H-Ras M90, RhoA 26C4, Akt1 B-1, RhoGDI A-20, RabGDI (V-20)-R, synaptophysin H-93, and caveolin N-20 (Santa Cruz Biotechnology); p-Akt 193H12 (Cell Signaling). For details see the Supplementary Materials and Methods.

### Immunohistochemistry

Immunohistochemical staining of p-CREB and PSD-95 was performed on sagittal brain sections of simvastatin- and vehicle-treated animals according to the previously used protocols (Moreno *et al*, 1995; Fanelli *et al*, 2013). For details see Supplementary Materials and Methods.

### Statistical Analysis

Data obtained from behavioral tests are expressed as means ± SEM (standard error of the mean); data derived from the analysis of biochemical results are expressed as means ± SD (standard deviation). Data were analyzed with unpaired Student's *t* test or with one-way analysis of variance (ANOVA) followed by the Dunnett post-test. Values of $P<0.05$ were considered to indicate a significant difference. Statistical analysis was performed using GRAPHPAD INSTAT3 (GraphPad, La Jolla, CA, USA) for Windows.

## RESULTS

### Systemic Effects of HMGR Inhibition on Lipid Metabolism

The inhibition of HMGR, and in turn the reduction in MVA end-products formation, leads to a homeostatic response that determines the increase of the low-density lipoprotein (LDL) receptor family members through the enhancement of their transcription and translocation onto cell membranes, subsequently reducing the amount of plasma lipids (Jones *et al*, 1998). Thus, the efficacy of the pharmacological treatment was checked by estimating the plasma cholesterol and triglycerides. As shown in Supplementary Table S1, both cholesterol ($t_{34} = 3.606$, $P = 0.001$) and triglycerides ($t_{34} = 4.562$, $P > 0.0001$) significantly decreased after simvastatin treatment (18% and 32%, respectively). Nevertheless, similar body weight of simvastatin- and vehicle-treated rats was observed, indicating that HMGR inhibition failed to induce changes in the basal metabolism of the animals (data not shown).

### Effects of HMGR Inhibition on Emotional Reactivity and Cognitive Performance

To evaluate the potential role of the MVA pathway inhibition by simvastatin in the modulation of emotional reactivity, rats were tested in the social interaction and elevated plus-maze tests, two validated animal methods to evaluate anxiety in rodents.

Chronic simvastatin treatment decreased the total time spent in active social interaction compared with vehicle-treated rats ($t_{18} = 4.123$, $P < 0.001$; Figure 1a), expressed as the sum of the time spent in play-related behaviors ($t_{18} = 3.386$, $P = 0.003$; figure not shown) and in social behaviors unrelated to play ($t_{18} = 2.390$, $P = 0.028$; figure not shown). In contrast, the percentage of time spent in the open arms ($t_{19} = -1.349$, $P = 0.193$; Figure 1b), the percentage of open entries ($t_{19} = -1.062$, $P = 0.302$; Figure 1c), and the total arm entries ($t_{19} = 1.768$, $P = 0.093$; Figure 1d) evaluated in the elevated plus-maze test were unaffected by the pharmacological inhibition of HMGR.

To investigate whether the MVA pathway has a role in the modulation of memory consolidation, rats were tested in the inhibitory avoidance task. Chronic simvastatin treatment had no effect on the approach latencies during the acquisition trial ($t_{17} = -0.620$, $P = 0.544$; Figure 1e); however, it caused a statistically significant improvement in 24-h retention performance ($t_{17} = -2.245$, $P = 0.038$; Figure 1f). This effects were not secondary to drug-induced hypersensivity to the electrical shock delivered during the acquisition trial, as simvastatin- and vehicle-treated rats did not differ in the response to the aversive stimulus during the acquisition trial ($t_{17} = -0.204$, $P = 0.841$; Figure 1g).

### Simvastatin Efficacy and Tolerance in the CNS

Evidence for the drug efficacy in the CNS were given by checking the levels of the active nuclear fraction of the transcription factor SREBP-2 (nSREBP-2) and the subsequent increase in LDL receptor (LDLr), which are induced by a compensative response due to intracellular cholesterol decrease (Brown and Goldstein, 1997; Trapani *et al*, 2011a). The biochemical analysis was mainly carried out on the amygdala, hippocampus, prefrontal cortex, dorsal striatum, and ventral striatum, whose interplay is deeply involved in the modulation of anxiety, memory, and learning (Mathew *et al*, 2001; LaBar and Cabeza, 2006). Our results showed that HMGR inhibition by chronic simvastatin treatment induced a classical feedback response, which led to a strong increase of the active nSREBP-2 in all the brain regions analyzed (amygdala: $t_{10} = 2.139$, $P = 0.0291$; hippocampus: $t_{10} = 2.434$, $P = 0.0176$; prefrontal cortex: $t_{10} = 2.590$, $P = 0.0135$; dorsal striatum: $t_{10} = 2.045$, $P = 0.034$; ventral striatum: $t_{10} = 2.637$, $P = 0.0124$; Figure 2a). HMGR inhibition was also supported by the subsequent and the contributory increase in LDLr expression (amygdala: $t_{10} = 2.263$, $P = 0.0236$; hippocampus: $t_{10} = 2.057$, $P = 0.0334$; prefrontal cortex: $t_{10} = 1.933$, $P = 0.0410$; dorsal striatum: $t_{10} = 1.909$, $P = 0.0427$; and ventral striatum: $t_{10} = 3.969$, $P = 0.0013$; Figure 2b). Moreover, the direct proof of the pharmacological inhibition was also given by assessing the HMGR activity (amygdala: $t_8 = 7.694$, $P < 0.0001$; hippocampus: $t_8 = 1.266$, $P < 0.0001$; prefrontal cortex: $t_8 = 7.259$, $P < 0.0001$; dorsal striatum: $t_8 = 4.934$, $P = 0.0011$; and ventral striatum: $t_8 = 5.092$, $P = 0.0009$; Supplementary Figure S2a), which was reduced in all the analyzed brain areas.

Once simvastatin efficacy was ascertained, we focused on the potential toxic effects exerted by HMGR inhibition on different brain areas. Protein levels of the neuronal marker NeuN (amygdala: $t_{10} = 1.627$, $P = 0.0674$; hippocampus: $t_{10} = 0.9974$, $P = 0.1710$; prefrontal cortex: $t_{10} = 1.271$, $P = 0.1162$; dorsal striatum: $t_{10} = 5.005$, $P = 0.3138$; and ventral striatum: $t_{10} = 0.8166$, $P = 0.2166$; Figure 2c) and of the astrocyte marker GFAP (amygdala: $t_{10} = 0.5949$, $P = 0.4769$; hippocampus: $t_{10} = 1.614$, $P = 0.0688$; prefrontal cortex: $t_{10} = 1.358$, $P = 0.1022$; dorsal striatum: $t_{10} = 0.8068$, $P = 0.2193$; and ventral striatum: $t_{10} = 0.7905$, $P = 0.2238$; Figure 2d) were unchanged in the examined brain areas. The analysis of cleaved caspase-3 also showed that the protein levels of this executive caspase were unaffected by simvastatin treatment (amygdala: $t_{10} = 0.5627$, $P = 0.2930$; hippocampus: $t_{10} = 0.06597$, $P = 0.4744$; prefrontal cortex: $t_{10} = 0.8944$, $P = 0.1961$; dorsal striatum: $t_{10} = 0.7460$, $P = 0.2364$; and ventral striatum: $t_{10} = 0.06921$, $P = 0.4731$; Supplementary Figure S2b).

### Effect of Simvastatin on Cholesterol, Dolichols, and CoQs

A prospective perturbation in the MVA pathway end-products induced by HMGR inhibition could be at the root of the behavioral and cognitive effects observed *in vivo*.

Thus, lipid estimation was performed in order to evaluate the effect of simvastatin on the main sterol and non-sterol compounds. As observable in Table 1, tissue cholesterol (amygdala: $t_7 = 0.2031$, $P = 0.8448$; hippocampus: $t_8 = 0.3502$, $P = 0.7352$; prefrontal cortex: $t_8 = 0.4874$, $P = 0.6391$; dorsal striatum: $t_7 = 1.556$, $P = 0.1636$; and ventral striatum: $t_6 = 0.5193$, $P = 0.6221$), CoQ9 (amygdala: $t_6 = 0.1524$, $P = 0.8838$; hippocampus: $t_8 = 0.04377$, $P = 0.9662$; prefrontal cortex: $t_8 = 1.211$, $P = 0.2605$; dorsal striatum: $t_8 = 1.623$, $P = 0.1433$; and ventral striatum: $t_5 = 0.2318$, $P = 0.8259$), CoQ10 (amygdala: $t_6 = 0.06480$,

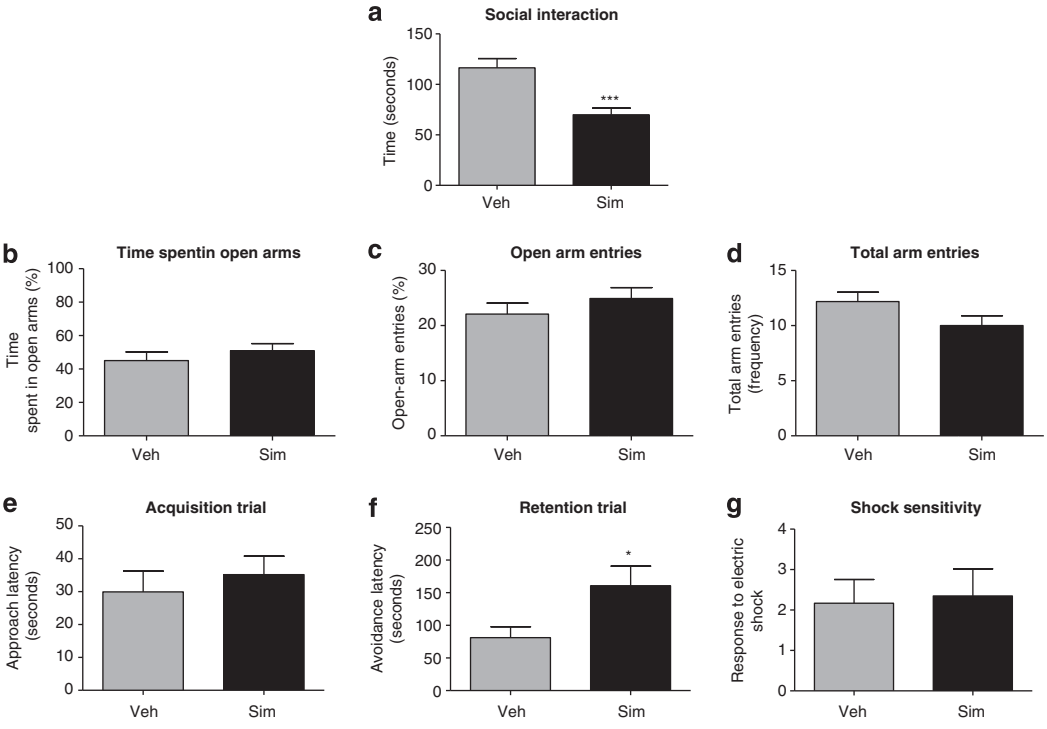


**Figure 1** Effects of chronic simvastatin treatment in the social interaction, elevated plus-maze, and inhibitory avoidance tests. Simvastatin treatment (1.5 mg/kg per day; i.p.) reduced the total time spent in active social interaction (a). No statistically significant difference was found in (b) the percentage of time spent in the open arms, (c) the percentage of open entries and in (d) the total arm entries evaluated in the elevated plus-maze test. Simvastatin treatment (e) had no effects on the approach latency in the acquisition trial of the inhibitory avoidance task, whereas (f) enhanced 24-h avoidance latencies in the retention trial. (g) No statistically significance difference was found between simvastatin-treated rats and their controls in response to shock delivered during the acquisition trial of the inhibitory avoidance test. Data represent mean values ± SEM. $^{*}P<0.05$, $^{***}P<0.001$ *vs* control ($n=10$–11 per treatment group). Veh, vehicle-treated rats. Sim, simvastatin-treated rats.

$P=0.9504$; hippocampus: $t_8=1.301$, $P=0.2294$; prefrontal cortex: $t_8=1.294$, $P=0.2319$; dorsal striatum: $t_8=1.440$, $P=0.1879$; and ventral striatum: $t_5=0.2467$, $P=0.8149$), and dolichol (amygdala: $t_8=1.805$, $P=0.1087$; hippocampus: $t_8=0.007556$, $P=0.9942$; prefrontal cortex: $t_8=0.9631$, $P=0.3637$; dorsal striatum: $t_8=0.2134$, $P=0.8363$; and ventral striatum: $t_6=0.8525$, $P=0.4266$) were not affected by HMGR inhibition among the brain regions analyzed.

## Prenylated Protein Involved in Synaptic Vesicle Release: Rab3 Determination

Simvastatin treatment could also induce a downregulation in the activity of small GTPases by affecting their prenylation. For the pivotal role in neurotransmitter release, Rab3 protein localization was analyzed. Rab3 fraction associated with the synaptic vesicle membranes was strongly reduced in the hippocampus ($t_2=3.675$, $P=0.0334$; Figure 3a) and the prefrontal cortex ($t_2=7.178$, $P=0.0094$; Figure 3a) after chronic simvastatin treatment, whereas no differences in the protein localization were observable in amygdala ($t_2=1.028$, $P=0.4120$; Figure 3a), dorsal striatum ($t_2=1.592$, $P=0.1262$; Figure 3a), and ventral striatum ($t_2=0.3310$, $P=0.3860$; Figure 3a). It is well accepted that membrane *vs* cytoplasm localization of Rab3, and other prenylated small GTPases in general, mirrors the prenylation status and, as a consequence, the activity of the protein of interest (Seasholtz *et al*, 1999; Homma *et al*, 2008). Thus, the amount of Rab3 active fraction was expressed as the membrane:cytosol ratio. To further assess Rab prenylation, coimmunoprecipitation experiments between RabGDI and Rab3 were performed on cytosolic fractions. The level of prenylated Rab3 is strongly reduced in the hippocampus ($t_4=1.315$, $P=0.0002$, Supplementary Figure S3a) and the prefrontal cortex ($t_4=6.759$, $P=0.0025$, Supplementary Figure S3b) of simvastatin-treated rats. Moreover, the total amount of RabGDI both in the hippocampus ($t_6=1.422$, $P=0.2048$, Supplementary Figure S3c) and the prefrontal cortex ($t_6=0.8552$, $P=0.4253$, Supplementary Figure S3d) did not change between the two experimental groups. The lack of the concurrent accumulation of unprenylated Rab3 in the cytosolic fraction (generally a typical phenomenon observed after statin administration) is in line with the results obtained by other research groups, who demonstrated that, under specific conditions, some prenylated proteins could have a shorter half-life compared with the membrane-bound forms (Haklai *et al*, 1998; Indolfi *et al*, 2002). To test this hypothesis, an '*in vitro*' degradation assay of Rab3 was performed. The results show that Rab3 was more susceptible to degradational events in the hippocampus and the prefrontal cortex, whereas no differences were detectable between the two experimental groups in the other brain regions (Figure 3b).

## Prenylated Proteins Involved in Long-Term Potentiation: Ras and RhoA Determinations

The enhanced memory consolidation in a 24 h inhibitory avoidance task could correlate with changes in long-term potentiation (LTP). Thus, prenylated proteins such as Ras

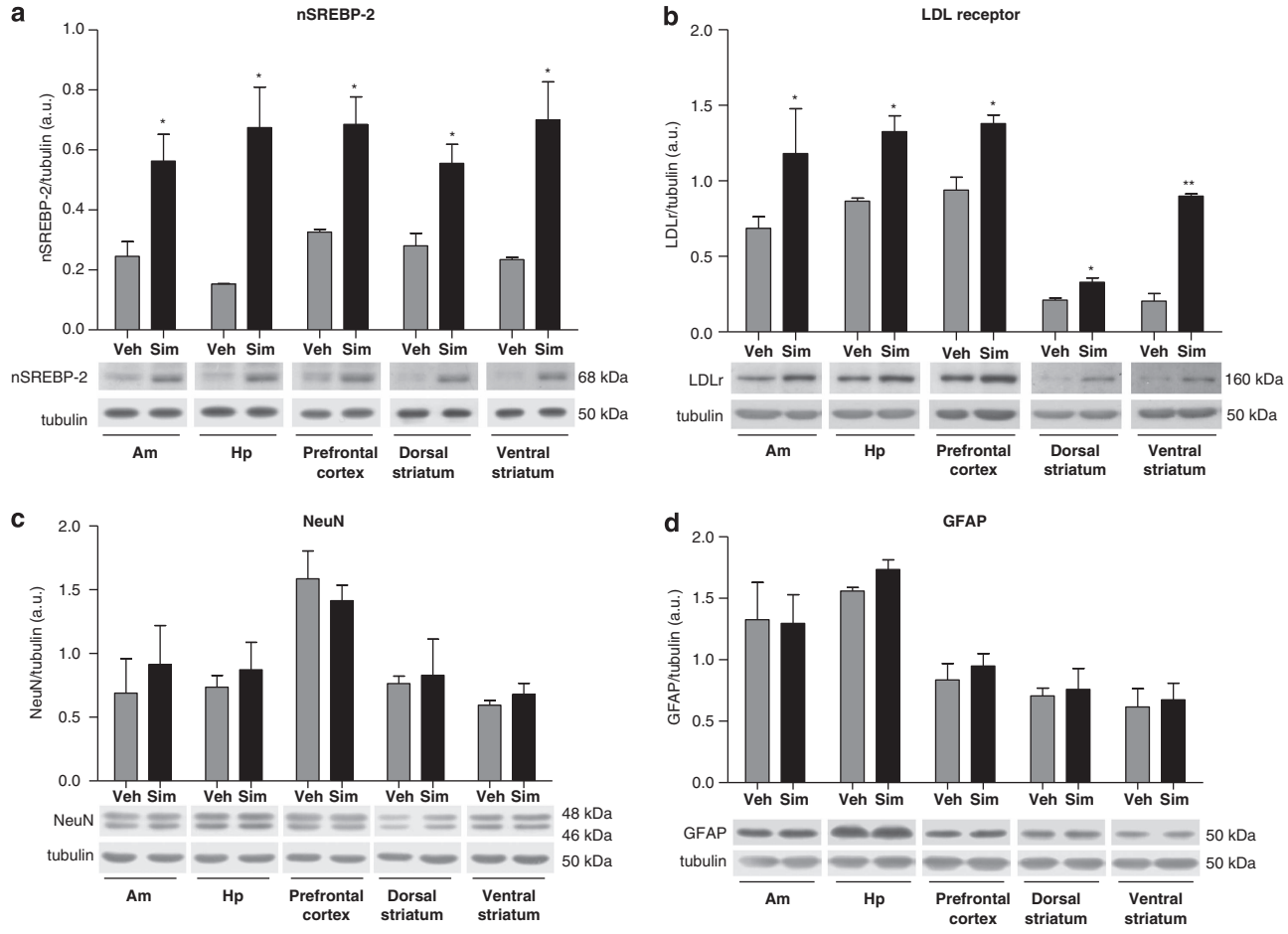


**Figure 2** Efficacy of 3-hydroxy 3-methylglutaryl Coenzyme A reductase (HMGR) inhibition by simvastatin and effects on neuronal and astrocytic content in different brain regions. (a) Representative western blot and densitometric analysis of nSREBP-2 in amygdala (Am), hippocampus (Hp), prefrontal cortex, dorsal striatum, and ventral striatum. (b) Representative western blot and densitometric analysis of low-density lipoprotein receptor (LDLr) in amygdala (Am), hippocampus (Hp), prefrontal cortex, dorsal striatum, and ventral striatum. (c) Representative western blot and densitometric analysis of the neuronal marker NeuN in amygdala (Am), hippocampus (Hp), prefrontal cortex, dorsal striatum, and ventral striatum. (d) Representative western blot and densitometric analysis of the astrocytic marker GFAP in amygdala (Am), hippocampus (Hp), prefrontal cortex, dorsal striatum, and ventral striatum. Protein levels were normalized with α-tubulin. The data are expressed as arbitrary units obtained by analyzing the protein bands with Image J software for Windows, for details see the main text. All the results obtained are presented as the mean ± SD $^{*}P<0.05$, $^{**}P<0.01$; Student's *t*-test with respect to the control group of the same brain region analyzed. $n=6$ animals/group. Veh, vehicle-treated rats. Sim, simvastatin-treated rats.

and RhoA, involved in the modulation of this form of synaptic plasticity (Mazzucchelli and Brambilla, 2000; Rex *et al*, 2009) were evaluated. HMGR inhibition did not induce any statistically significant modification in Ras translocation (amygdala: $t_{10}=0.2375$, $P=0.4085$; hippocampus: $t_{10}=0.2929$, $P=0.3881$; prefrontal cortex: $t_{10}=0.2798$, $P=0.3927$; dorsal striatum: $t_{10}=0.01021$, $P=0.4960$; and ventral striatum: $t_{10}=0.1791$, $P=0.4307$; Figure 4a), whereas it strongly reduced the active membrane-bound form of RhoA in the amygdala ($t_{10}=2.701$, $P=0.0111$; Figure 4b) and the hippocampus ($t_{10}=2.601$, $P=0.0132$; Figure 4b), with the contributory build-up of the protein in the cytosol. On the contrary, no differences were observable in the prefrontal cortex ($t_{10}=0.2867$, $P=0.3901$; Figure 4b), the dorsal striatum ($t_{10}=1.442$, $P=0.0899$; Figure 4b), and the ventral striatum ($t_{10}=0.2531$, $P=0.4026$; Figure 4b). As for Rab3, coimmunoprecipitation experiments highlighted a reduction in RhoA/RhoGDI complexes in both the amygdala ($t_4=6.188$, $P=0.0035$, Supplementary Figure S4a) and the hippocampus ($t_4=6.636$, $P=0.0027$, Supplementary Figure S4b), without showing any change in the RhoGDI protein content (amygdala: $t_6=1.493$, $P=0.1860$, Supplementary Figure S4c; hippocampus: $t_6=0.5134$, $P=0.6260$, Supplementary Figure S4d). In addition, the reduction in RhoA translocation to the membrane was accompanied by a marked and significant increase in Akt activation state in both the amygdala ($t_{10}=2.726$, $P=0.0107$; Figure 4c) and the hippocampus ($t_{10}=2.724$, $P=0.0107$; Figure 4c), whereas no differences are detectable in the prefrontal cortex ($t_{10}=1.365$, $P=0.1010$; Figure 4c), the dorsal striatum ($t_{10}=0.3652$, $P=0.3613$; Figure 4c), and the ventral striatum ($t_{10}=0.1979$, $P=0.4236$; Figure 4c). Similar results were also obtained from cell cultures. In primary rat hippocampal neurons, simvastatin treatment reproduced the reduction in RhoA active fraction observed *in vivo*, as demonstrated from the decrease in the membrane:cytosol ratio ($F(6, 21)=0.4016$, $P=0.0078$). The supplementation of the medium with either MVA (the direct product of HMGR) or geranylgeraniol (GG, one of the MVA pathway products and the substrate for RhoA

**Table 1** Effect of Simvastatin on Lipid Composition of Selected Brain Regions

| Cholesterol (mg/g tissue) | Dolichol (μg/g tissue) | CoQ9 (μg/g tissue) | CoQ10 (μg/g tissue) | |
|---|---|---|---|---|
| *Amygdala* | | | | |
| 31.77 ± 9.36 | 1.37 ± 0.16 | 3.13 ± 0.36 | 1.72 ± 0.16 | Veh (4) |
| 30.45 ± 9.81 | 1.55 ± 0.17 | 3.28 ± 0.70 | 1.75 ± 0.33 | Sim (4) |
| *Hippocampus* | | | | |
| 32.05 ± 6.47 | 1.47 ± 0.29 | 3.39 ± 0.07 | 1.77 ± 0.08 | Veh (5) |
| 34.15 ± 10.65 | 1.46 ± 0.13 | 3.40 ± 0.19 | 1.91 ± 0.07 | Sim (5) |
| *Prefrontal cortex* | | | | |
| 29.47 ± 9.82 | 1.35 ± 0.18 | 3.11 ± 0.29 | 1.56 ± 0.14 | Veh (5) |
| 31.76 ± 5.18 | 1.46 ± 0.17 | 3.48 ± 0.17 | 1.75 ± 0.08 | Sim (5) |
| *Dorsal striatum* | | | | |
| 34.49 ± 2.16 | 1.48 ± 0.05 | 3.58 ± 0.32 | 1.64 ± 0.17 | Veh (5) |
| 31.81 ± 2.83 | 1.46 ± 0.13 | 4.23 ± 0.24 | 1.85 ± 0.11 | Sim (5) |
| *Ventral striatum* | | | | |
| 27.42 ± 1.93 | 1.32 ± 0.06 | 2.80 ± 0.70 | 1.26 ± 0.32 | Veh (4) |
| 28.36 ± 5.06 | 1.46 ± 0.25 | 3.05 ± 0.76 | 1.38 ± 0.36 | Sim (4) |

Number of rats contributing to each value are shown in brackets.

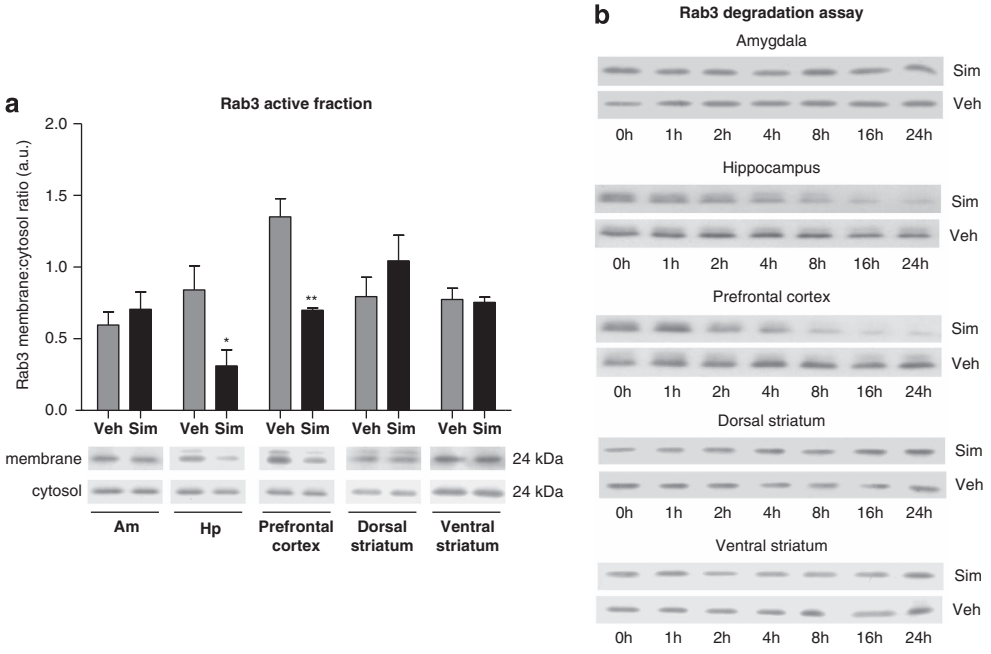


**Figure 3** Effect of 3-hydroxy 3-methylglutaryl Coenzyme A reductase (HMGR) inhibition on Rab3 membrane localization and degradation in different brain regions. (a) Representative Western blot and densitometric analysis of Rab3 in preparations of synaptic vesicle membranes from amygdala (Am), hippocampus (Hp), prefrontal cortex, dorsal striatum and ventral striatum. Rab3 active fraction was expressed as the membrane:cytosol ratio. Data are represented as arbitrary units obtained by analyzing the protein bands with Image J software for Windows, for details see the main text. All the results are expressed as the mean ± SD $^{*}P<0.05$ and $^{**}P<0.01$; Student's *t* test with respect to the control group of the same brain region analyzed. $n=6$ animals/group. Veh = vehicle-treated rats. Sim = simvastatin-treated rats. (b) Representative Western blot obtained by Rab3 degradation assay in cytosolic fractions from amygdala, hippocampus, prefrontal cortex, dorsal striatum and ventral striatum. The time course analysis was performed at 0, 1, 2, 4, 8, 16, and 24 h. The results are represented as arbitrary units obtained by evaluating the protein bands with Image J software for Windows, for details see the main text. $n=6$ animals/group. Veh = vehicle-treated rats. Sim = simvastatin-treated rats.

prenylation) completely reversed the effect of the pharmacological inhibition of HMGR. On the other hand, the administration of MVA, GG, and Rho kinase (ROCK) inhibitor hydroxyfasudil (HF) alone did not cause any effect in the protein translocation as expected (Figure 5a). The estimation of Akt protein levels in primary neuronal culture

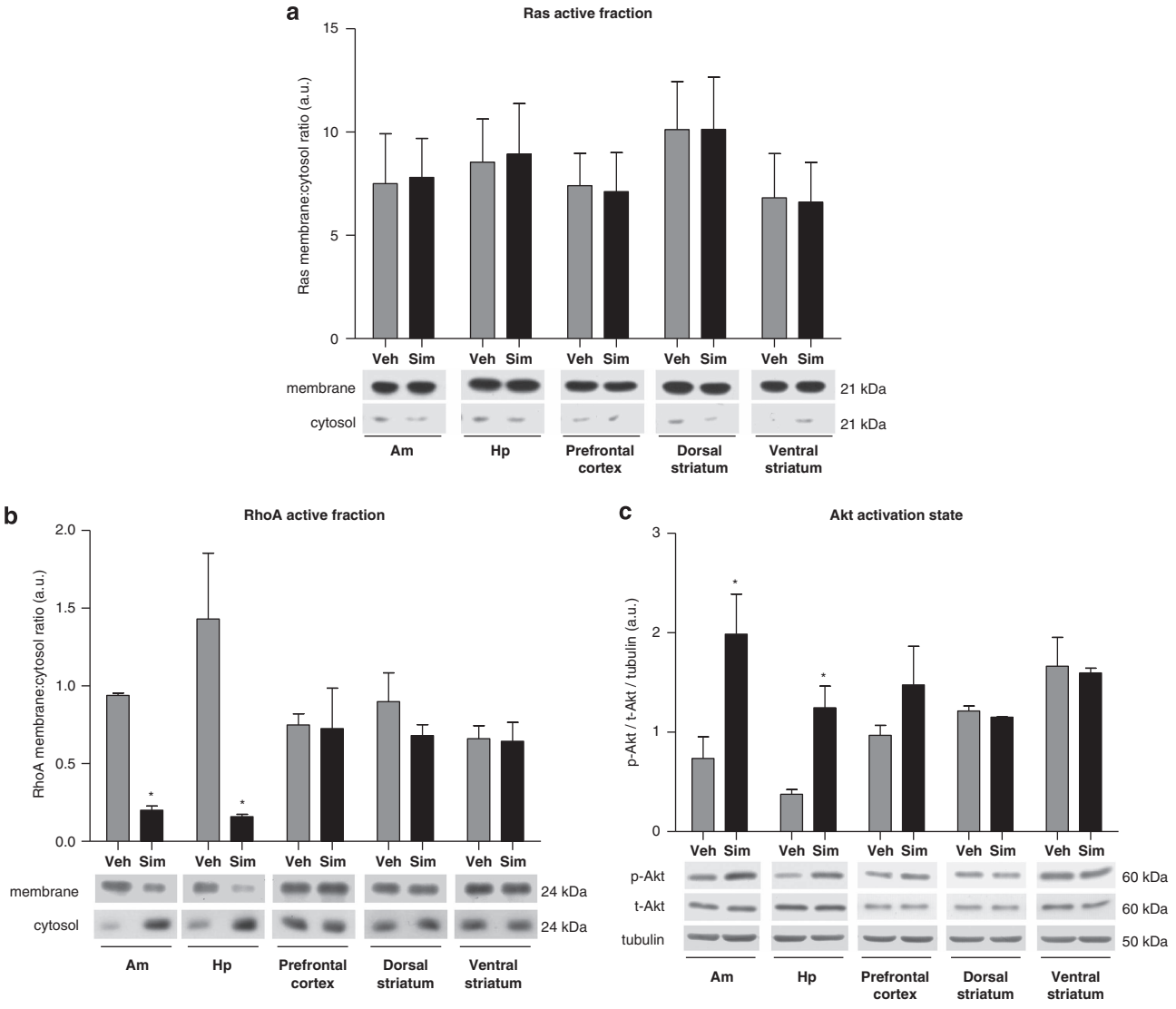


**Figure 4** Effect of 3-hydroxy 3-methylglutaryl Coenzyme A reductase (HMGR) inhibition by simvastatin on Ras, RhoA membrane localization and Akt activation in different brain regions. (a) Representative Western blot and densitometric analysis of Ras in amygdala (Am), hippocampus (Hp), prefrontal cortex, dorsal striatum, and ventral striatum. Ras active fraction was expressed as the membrane:cytosol ratio. (b) Representative western blot and densitometric analysis of RhoA in amygdala (Am), hippocampus (Hp), prefrontal cortex, dorsal striatum, and ventral striatum. RhoA active fraction was expressed as the membrane:cytosol ratio. (c) Representative western blot and densitometric analysis of Akt phosphorylation/activation in amygdala (Am), hippocampus (Hp), prefrontal cortex, dorsal striatum, and ventral striatum. Protein levels were normalized with α-tubulin. The results are represented as arbitrary units obtained by analyzing the protein bands with Image J software for Windows, for details see the main text. All the data are expressed as the mean ± SD $^{*}P<0.05$; Student's *t*-test with respect to the control group of the same brain region analyzed. $n=6$ animals/group. Veh, vehicle-treated rats. Sim, simvastatin-treated rats.

strongly suggests that Akt phosphorylation was dependent on RhoA inhibition by simvastatin, as the coadministration of MVA and GG completely restored the basal levels of Akt activation state ($F(6, 21)=37{,}02$, $P<0.0001$). HF-mediated inhibition of ROCK, the main downstream effector of RhoA, further supports this hypothesis by mimicking the effect of simvastatin through the induction of Akt phosphorylation (Figure 5b). Moreover, Akt activation induced a significant increase in the phosphorylation of the transcription factor CREB ($F(6, 21)=0.4849$, $P=0.003$; Figure 5c).

## Immunohistochemical Analyses

Morphological analysis of brains from either simvastatin- or vehicle-treated rats revealed good preservation of structures and overall normal cytoarchitecture. Immunohistochemical localization of p-CREB showed wide neuronal distribution in the hippocampal formation of both treated and control groups. Immunostaining was mainly seen in the nucleus of pyramidal cells in CA1–CA3 fields and of granule cells in DG. In addition, mossy cells in the hylus were especially immunoreactive. Consistent with western blot results obtained from primary hippocampal neuron cultures, remarkably higher immunostaining intensity throughout the hippocampus was detected in simvastatin-treated brains, as compared with their untreated counterparts (Figure 6a). PSD-95 also immunolocalized to the pyramidal cell layer of CA1–CA3, to granule neurons of DG, and to hylar mossy neurons. However, at difference with p-CREB immunohistochemistry, the staining intensity was

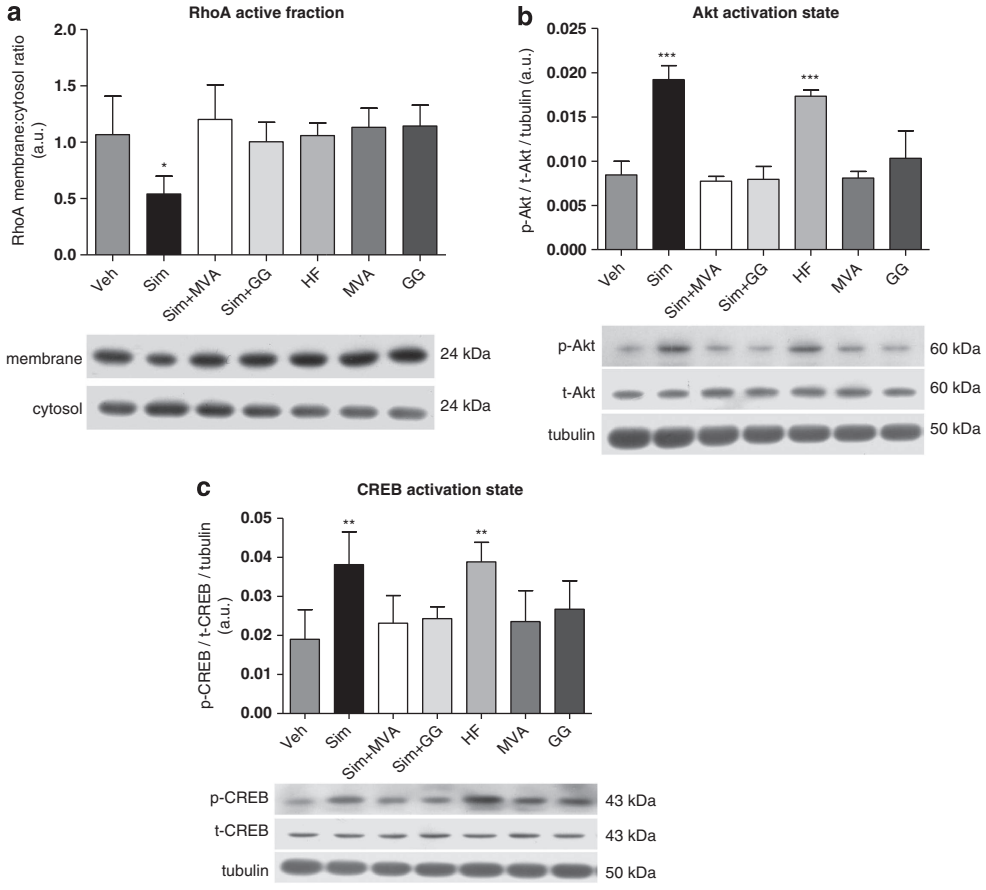


**Figure 5** Akt phosphorylation and the consequent CREB activation are dependent on the RhoA/ROCK pathway. (a) Representative western blot and densitometric analysis of RhoA in primary hippocampal neurons. RhoA active fraction was expressed as the membrane:cytosol ratio. All the data are expressed as arbitrary units obtained by analyzing the protein bands with Image J software for Windows, for details see the main text. (b) Representative western blot and densitometric analysis of Akt phosphorylation/activation in primary hippocampal neurons. p-Akt protein levels were normalized with total Akt levels and α-tubulin. (c) Representative western blot and densitometric analysis of CREB phosphorylation/activation in primary hippocampal neurons. p-CREB protein levels were normalized with total CREB levels and α-tubulin. All the data are expressed as arbitrary units obtained by evaluating the protein bands with Image J software for Windows, for details see the main text. All the results represent the mean ± SD of at least three different experiments. $^{*}P<0.05$, $^{**}P<0.01$, and $^{***}P<0.001$ determined using one-way one-way analysis of variance (ANOVA) followed by the Dunnett post-test. GG, geranylgeraniol; HF, hydroxyfasudil; MVA, mevalonate; Sim, simvastatin; Veh, vehicle.

comparable between the two experimental conditions, not being affected by simvastatin treatment (Figure 6b).

## DISCUSSION

The present study was performed to provide a deeper understanding of the CNS functional consequences following the pharmacological inhibition of the isoprenoid/cholesterol biosynthetic pathway in rodents. To this aim HMGR, the key and rate-limiting enzyme of this pathway, was inhibited in rats by chronic treatment with simvastatin, a powerful HMGR inhibitor, which is able to cross the blood–brain barrier because of its lipophilic properties (Saheki *et al*, 1994). To analyze the biological role of the MVA pathway on rat emotionality, we performed two of the most popular animal tests of anxiety currently used: the social interaction and the elevated plus-maze tests (File and Hyde, 1978; File, 1980; Pellow *et al*, 1985; Pellow and File, 1986). Chronic simvastatin treatment at a low dose induced a significant decrease in the total time spent in active social investigation in the social interaction test, whereas no significant differences were observed in the elevated plus-maze test. Although both the elevated plus-maze and the social interaction tests are two validated animal models to measure anxiety-like behaviors in rodents (File, 1980; File and Seth, 2003; Pinheiro *et al*, 2007; Pellow and File, 1986), it has been suggested that these tests evoke different states of anxiety in the laboratory animal (Gonzales *et al*, 1996; File, 1992) mediated by different neurobiological pathways (Cheeta *et al*, 2000; File *et al*, 2000; File *et al*, 2004), and thus they could have different sensitivity to simvastatin treatment. Specifically, it has been suggested that the elevated plus-maze test mimics a state of generalized anxiety, as it produces an approach/avoidance conflict because the animal is exposed to a novel situation that supposedly creates a conflict between the motivation to explore the environment and an unconditioned fear of novelty (File *et al*, 2004), and this may be the underlying mechanism rendering the elevated plus-maze test sensitive to anxiolytic-like drugs (Handley and McBlane, 1993; Pinheiro *et al*, 2007). On the other hand, in the social interaction test, the

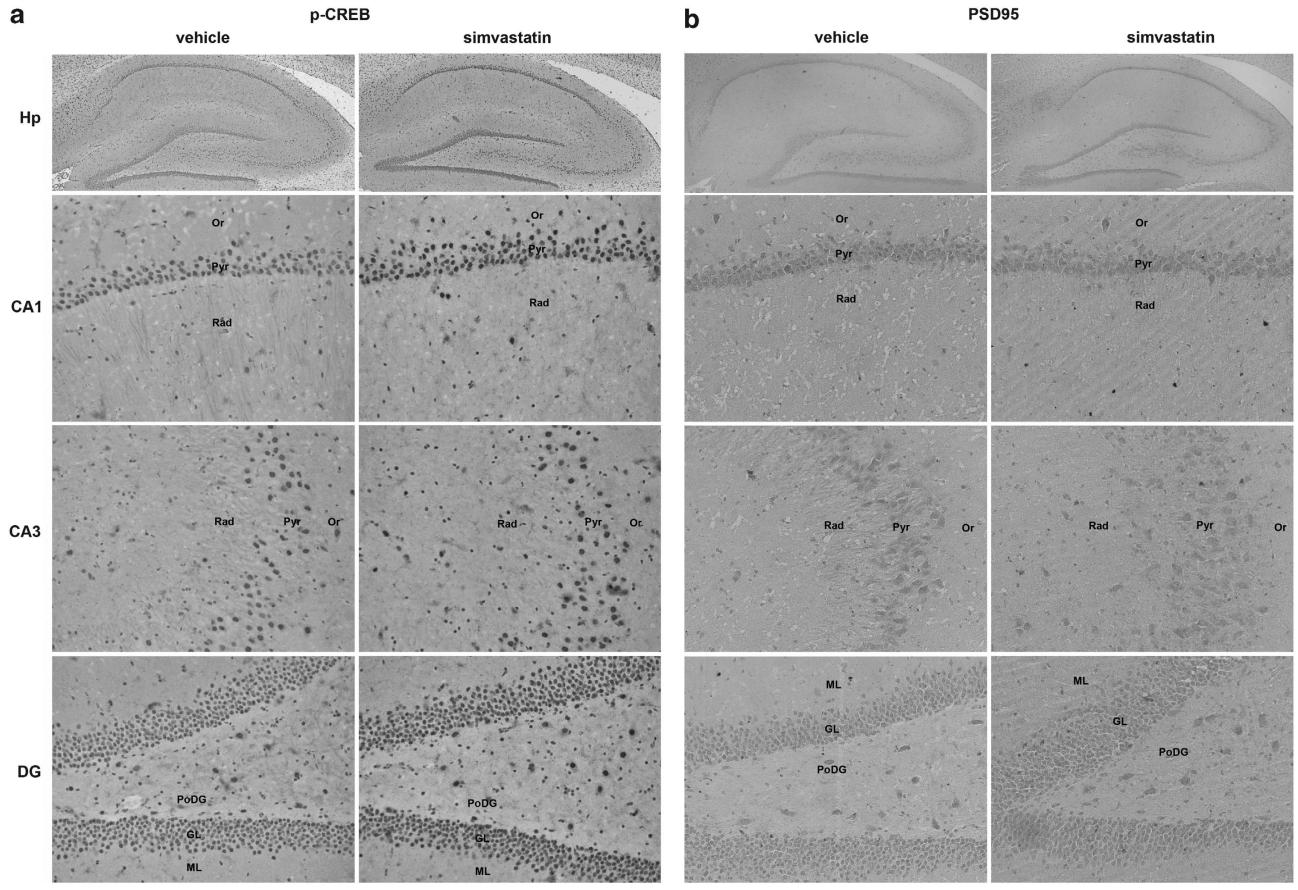


**Figure 6** p-CREB and PSD-95 distribution in hippocampus of simvastatin- and vehicle-treated rats. (a) Overview of p-CREB immunohistochemistry in a sagittal section of rat brain. Hippocampal formation showed higher positivity in the nucleus of pyramidal cells in CA1–CA3 fields and of granule cells in DG. Mossy cells in the hylus were especially immunoreactive. (b) Overview of PSD-95 immunohistochemistry in a sagittal section of rat brain showing immunopositivity localized to pyramidal cell layer of CA1–CA3, to granule neurons of DG, and to hylar mossy neurons. GL, granule cell layer; Hp, hippocampus; ML, molecular layer; Or, stratum oriens; PoDG, polymorphic layer; Pyr, stratum pyramidale; Rad, stratum radiatum.

variable is the time spent by pairs of male rats in active social interaction and one rat influences the behavior of the other; in fact, when pairs of male rats are placed in a situation in which neither one has established its territory, they engage in active social interaction (File and Hyde, 1978). Nevertheless, the social interaction test is also sensitive to a number of environmental and physiological factors such as test conditions (light level and familiarity to the test arena) that can affect anxiety mimicking a state of anxiety most similar to that experienced in generalized anxiety disorder (File, 1980; File and Seth, 2003). Furthermore, our results showed that the pharmacological modulation of the MVA pathway end-products is also involved in the modulation of memory consolidation of aversive experiences; in particular, HMGR inhibition by simvastatin treatment led to a specific enhancement of the consolidation phase of the memory process, as the approach latency, measured during the first day of the test, did not differ between the two experimental groups. Our results also corroborate with existing and recently published data, showing that a higher dose of simvastatin (10 mg/kg) resulted in improved memory performance in the passive avoidance test (Douma *et al*, 2011). Even though it was demonstrated that simvastatin induces apoptosis in neurons and astrocytes (Marz *et al*, 2007), the drug, at a dose of 1.5 mg/kg, did not cause any cell loss as observable by the unchanged levels of NeuN, GFAP, and of the executive caspase-3, excluding that potential neurotoxic effects exerted by simvastatin could be responsible for the behavioral outcomes observed in the current study. The lack of toxic effects could be explained by the low dose of simvastatin used in the present study. In addition, the safety in terms of necrosis and/or apoptosis of this chronic pharmacological treatment was also demonstrated in our previous work (Trapani *et al*, 2011a). The estimation of tissue cholesterol, dolichol, and CoQs through HPLC analyses also excluded the involvement of these end-products in the onset of the behavioral and cognitive changes. The lack of any variation in the amount of these isoprenoids following HMGR inhibition is not surprising if it is considered that they possess very long half-lives in the brain (Andersson *et al*, 1999). Thus, a 3-week chronic simvastatin treatment, at the dose used in our study, might not be able to impair the physiological levels of cholesterol, dolichol, CoQ9, and CoQ10 in the rat brain areas taken into consideration. On the opposite, membrane-bound Rab3 in the synaptic vesicle fraction, which corresponds to the active fraction of the protein, resulted to be strongly decreased in both the hippocampus and the prefrontal cortex after chronic HMGR inhibition. It is well-known that

Rab and Rho proteins require prenylation for membrane association and for binding to GDIs. GDIs hold prenylated proteins in the cytosol, acting not only as passive regulators of GTPase activity but also preventing their degradation (Boulter and Garcia-Mata, 2010; Mohamed *et al*, 2012). GDI capture of membrane-bound Rabs could be physically prevented by modifications in the cholesterol content within the membranes (Ganley and Pfeffer, 2006). Even though the amount of cholesterol into membranes was not evaluated in this work, GDI capture of prenylated Rab3 in cytosolic fractions excluded potential interferences of membrane cholesterol in RabGDI/Rab3 interaction, suggesting that the deregulation in Rab3 subcellular distribution is due, at least in part, to an impairment in Rab3 prenylation induced by HMGR inhibition. Moreover, Rab3 seem to be more susceptible to degradational events both in the hippocampus and the prefrontal cortex of simvastatin-treated rats. These findings lead us to hypothesize that the lack of prenylation could impair Rab3/RabGDI interaction in the cytosol, thus preventing the role of RabGDI in protecting Rab proteins from degradation. Although there is a conflicting evidence in literature about the modulation of the specific synaptic mechanisms, it is clear and well defined that Rab3 carries out important physiological roles in neurotransmitter release at a late step during the synaptic vesicle exocytosis (Geppert and Sudhof, 1998). Perturbations in Rab3 activity have already been established. For instance, deregulations in Mss4 (mammalian suppressor of Sec4), a regulator of Rab3 activity, are strongly linked to impairments in neurotransmitter release and to the appearance of neurodegenerative and psychological disorders in rodents such as depressive-like syndromes (Andriamampandry *et al*, 2002; Baskys *et al*, 2007; Blaveri *et al*, 2010). Given the important role of the hippocampus and the prefrontal cortex in the modulation of anxiety (Whitton and Curzon, 1990; Christianson *et al*, 2009), the decrease in Rab3 active fraction in both the brain regions as a molecular consequence of HMGR inhibition could be related to an impairment in the social behavior observed in the social interaction test and could represent a good explanation of the MVA pathway-related molecular mechanism underlying the social anxiety-related behavior observed in our study.

Besides the reduction in membrane-bound Rab3 protein levels, the role of the MVA pathway in emotional memory consolidation could be strongly dependent on the modulation of prenylated proteins that are crucial for the induction and the maintenance of LTP. In particular, a strong and statistically significant decrease in RhoA active fraction was observed in the amygdala and the hippocampus. As for Rab3, additional experiments based on RhoA/RhoGDI interaction further support the previous finding, indicating that the reduced amount of RhoA is the consequence of a defect in prenylation caused by HMGR pharmacological inhibition. Among Rho GTPases, RhoA has been implicated in key neurobiological processes, integrating extracellular and intracellular molecular signals to orchestrate refined and coordinated changes in gene expression and actin cytoskeleton, essential prerequisites for the neurite outgrowth and the modulation of synaptic connectivity (Gopalakrishnan *et al*, 2008; Lingor *et al*, 2007). For these reasons, it is not surprising that RhoA activity has been deeply related to the onset of developmental disabilities such as mental retardation (Ramakers and Storm, 2002). As RhoA is also considered a negative regulator of Akt, whose phosphorylation, and in turn activation, is a key and triggering event for LTP induction and consequent memory retention (Ming *et al*, 2002; Sui *et al*, 2008), Akt protein levels and phosphorylation state were analyzed. In the present work, the reduction in membrane-bound RhoA is accompanied by a sustained Akt activation. In order to fully confirm the causality between HMGR activity, RhoA activation, and Akt phosphorylation, an additional experiment was performed on cell culture. To this aim, primary hippocampal neurons were chosen as an experimental model in order to avoid the well-known incapability of some used compounds (eg, MVA) to cross the blood–brain barrier *in vivo* (Popjak *et al*, 1977). The rescue experiment performed on primary hippocampal neurons demonstrated that the modulation of Akt is strictly dependent on the RhoA/ROCK pathway, whose activation could be heavily affected by HMGR inhibition. A role of Akt in the modulation of cognitive performances in rodents has already been proposed, as it is able to induce LTP and other synaptic plasticity phenomena in both the amygdala and the hippocampus (Opazo *et al*, 2003; Sui *et al*, 2008; Lin *et al*, 2008). Akt could promote these processes, at least in part, by activating the nuclear factor CREB (Du and Montminy, 1998). Indeed, CREB-dependent gene transcription appears to be an essential component of long-term memory formation (Silva *et al*, 1998). Our data strengthen this possibility, as Akt activation is followed by an increased CREB phosphorylation in simvastatin- and HF-treated hippocampal neurons. The results obtained from hippocampal cell cultures are further sustained by p-CREB immunostaining, which is particularly positive in the hippocampus of simvastatin-treated rats if compared with vehicle ones. On the contrary no differences, in terms of immunoreactivity, were detectable in PSD-95. The obtained results are in agreement with other recent published data, which demonstrated that chronic simvastatin treatment restores the expression of the learning- and memory-related genes c-Fos and Egr-1 without inducing any modulation in the classical synaptic markers synaptophysin and PSD-95 (Tong *et al*, 2012). Moreover, considering that c-Fos and Egr-1 are downstream of CREB, our findings support the hypothetical model on cognition effects induced by simvastatin proposed by Tong *et al*, 2012. However, we cannot exclude that perturbations in cytoskeleton remodeling following HMGR inhibition, and in turn RhoA inactivation, could contribute, together with Akt induction, to the enhancement of the consolidation of aversive memories. Considering the divergences in the brain regional metabolism, it is possible to speculate that each brain area can be considered as a unique structure with a specific cellular context, able to react in a different manner to the same stimulus (Segatto *et al*, 2013). Moreover in this case, despite the generalized influence on the MVA pathway in the CNS, it is clear that simvastatin treatment selectively affected prenylated proteins in specific brain regions. Different effects of HMGR inhibition in dependence on the brain area taken into consideration have already been reported (Wang *et al*, 2006). Thus, the selective effects of simvastatin treatment in reducing the amount of Rab3 and

RhoA active fractions observed in this study could be influenced by differences in metabolism, function, turnover, or relative abundance of specific prenylated proteins in each brain region.

Despite the involvement of Rab3 and RhoA, other cellular mechanisms not evaluated in this work could contribute to the behavioral and cognitive outcomes induced by simvastatin. Growing evidence supports the hypothesis that statins could lead to brain effects, acting through pleiotropic mechanisms (Sierra *et al*, 2011). For instance, previous works identified changes in the plasma cholesterol with the onset of mood/anxiety disorders and the modulation of memory performance (Peter *et al*, 2002; Henderson *et al*, 2003; Granholm *et al*, 2008). Even though the biological significance of these connections is not widely accepted and remains to be clarified because of the presence of contradictory data (Papakostas *et al*, 2004; Taylor *et al*, 2011; Reitz *et al*, 2005), we cannot exclude that changes in plasma lipids, also observed in our work, could have a role in the functional effects exerted by simvastatin administration. Moreover, a very recent paper showed that the enhancement of the autophagic flux alleviates memory deficits in a transgenic mouse model of AD (Li *et al*, 2013). As statins induce autophagy in different cell types (Wei *et al*, 2013; Parikh *et al*, 2010), it is possible that a potential modulation of this process could participate, together with the alterations highlighted in this work, in the increased memory consolidation observed in simvastatin-treated rats.

In summary, these findings indicate that the modulation of the isoprenoid/cholesterol biosynthetic pathway is critically involved in the physiological modulation of both emotional and cognitive processes in rodents (Supplementary Figure S5). Even though our results provide some hints for the mechanisms of action of statins in the CNS, more efforts should be done in order to better understand their pleiotropic molecular effects in the CNS. Thus, the present work sets the stage for a future deeper understanding of the effects induced by simvastatin, which could be useful to better define the emerging and tight connection between MVA pathway and brain physiopathology.

## FUNDING AND DISCLOSURE

The authors declare no conflict of interest.

## ACKNOWLEDGEMENTS

The financial support from the University Roma Tre (CAL) to VP, from Marie Curie Career Reintegration Grant PCIG09-GA-2011-293589 to VT, from Polish National Cohesion Strategy Innovative Economy (UDA-POIG 01.03.01-14-036/09) and a support provided by the COST Action FA1006 (ES) to ES are gratefully acknowledged.

## REFERENCES

Andersson HC, Frentz J, Martinez JE, Tuck-Muller CM, Bellizaire J (1999). Adrenal insufficiency in Smith-Lemli-Opitz syndrome. *Am J Med Genet* **82**: 382–384.

Andriamampandry C, Muller C, Schmidt-Mutter C, Gobaille S, Spedding M, Aunis D *et al* (2002). Mss4 gene is up-regulated in rat brain after chronic treatment with antidepressant and down-regulated when rats are anhedonic. *Mol Pharmacol* **62**: 1332–1338.

Baskys A, Bayazitov I, Zhu E, Fang L, Wang R (2007). Rab-mediated endocytosis: linking neurodegeneration, neuroprotection, and synaptic plasticity? *Ann N Y Acad Sci* **1122**: 313–329.

Baytan SH, Alkanat M, Okuyan M, Ekinci M, Gedikli E, Ozeren M *et al* (2008). Simvastatin impairs spatial memory in rats at a specific dose level. *Tohoku J Exp Med* **214**: 341–349.

Blaveri E, Kelly F, Mallei A, Harris K, Taylor A, Reid J *et al* (2010). Expression profiling of a genetic animal model of depression reveals novel molecular pathways underlying depressive-like behaviours. *PLoS One* **5**: e12596.

Boulter E, Garcia-Mata R (2010). RhoGDI: a rheostat for the Rho switch. *Small GTPases* **1**: 65–68.

Brown MS, Goldstein JL (1980). Multivalent feedback regulation of HMG CoA reductase, a control mechanism coordinating isoprenoid synthesis and cell growth. *J Lipid Res* **21**: 505–517.

Brown MS, Goldstein JL (1997). The SREBP pathway: regulation of cholesterol metabolism by proteolysis of a membrane-bound transcription factor. *Cell* **89**: 331–340.

Campolongo P, Trezza V, Cassano T, Gaetani S, Morgese MG, Ubaldi M *et al* (2007). Perinatal exposure to delta-9-tetrahydrocannabinol causes enduring cognitive deficits associated with alteration of cortical gene expression and neurotransmission in rats. *Addict Biol* **12**: 485–495.

Cheeta S, Kenny PJ, File SE (2000). Hippocampal and septal injections of nicotine and 8-OH-DPAT distinguish among different animal tests of anxiety. *Prog Neuropsychopharmacol Biol Psychiatry* **24**: 1053–1067.

Christianson JP, Thompson BM, Watkins LR, Maier SF (2009). Medial prefrontal cortical activation modulates the impact of controllable and uncontrollable stressor exposure on a social exploration test of anxiety in the rat. *Stress* **12**: 445–450.

Dietschy JM, Turley SD (2004). Thematic review series: brain lipids. Cholesterol metabolism in the central nervous system during early development and in the mature animal. *J Lipid Res* **45**: 1375–1397.

Douma TN, Borre Y, Hendriksen H, Olivier B, Oosting RS (2011). Simvastatin improves learning and memory in control but not in olfactory bulbectomized rats. *Psychopharmacology (Berl)* **216**: 537–544.

Du K, Montminy M (1998). CREB is a regulatory target for the protein kinase Akt/PKB. *J Biol Chem* **273**: 32377–32379.

Fanelli F, Sepe S, D'Amelio M, Bernardi C, Cristiano L, Cimini A *et al* (2013). Age-dependent roles of peroxisomes in the hippocampus of a transgenic mouse model of Alzheimer's disease. *Mol Neurodegener* **8**: 8.

File SE (1980). The use of social interaction as a method for detecting anxiolytic activity of chlordiazepoxide-like drugs. *J Neurosci Methods* **2**: 219–238.

File SE (1992). Usefulness of animal models with newer anxiolytics. *Clin Neuropharmacol* **15**(Suppl 1): Pt A 525A–526A.

File SE, Cheeta S, Kenny PJ (2000). Neurobiological mechanisms by which nicotine mediates different types of anxiety. *Eur J Pharmacol* **393**: 231–236.

File SE, Hyde JR (1978). Can social interaction be used to measure anxiety? *Br J Pharmacol* **62**: 19–24.

File SE, Lippa AS, Beer B, Lippa MT (2004). Animal tests of anxiety. *Curr Protoc Neurosci* Chapter 8, Unit 8 3, 8.3.1–8.3.22.

File SE, Seth P (2003). A review of 25 years of the social interaction test. *Eur J Pharmacol* **463**: 35–53.

Ganley IG, Pfeffer SR (2006). Cholesterol accumulation sequesters Rab9 and disrupts late endosome function in NPC1-deficient cells. *J Biol Chem* **281**: 17890–17899.

Geppert M, Sudhof TC (1998). RAB3 and synaptotagmin: the yin and yang of synaptic membrane fusion. *Annu Rev Neurosci* **21**: 75–95.

Gonzales R, Bungay PM, Kilanmaa K, Samson HH, Rosselti ZL (1996). *In vivo* links between neurochemistry and behavioral effects of ethanol. *Alcohol Clin Exp Res* **20**(8 Suppl): 203A–209A.

Gopalakrishnan SM, Teusch N, Imhof C, Bakker MH, Schurdak M, Burns DJ *et al* (2008). Role of Rho kinase pathway in chondroitin sulfate proteoglycan-mediated inhibition of neurite outgrowth in PC12 cells. *J Neurosci Res* **86**: 2214–2226.

Granholm AC, Bimonte-Nelson HA, Moore AB, Nelson ME, Freeman LR, Sambamurti K (2008). Effects of a saturated fat and high cholesterol diet on memory and hippocampal morphology in the middle-aged rat. *J Alzheimers Dis* **14**: 133–145.

Haklai R, Weisz MG, Elad G, Paz A, Marciano D, Egozi Y *et al* (1998). Dislodgment and accelerated degradation of Ras. *Biochemistry* **37**: 1306–1314.

Handley SL, McBlane JW (1993). An assessment of the elevated X-maze for studying anxiety and anxiety-modulating drugs. *J Pharmacol Toxicol Methods* **29**: 129–138.

Henderson VW, Guthrie JR, Dennerstein L (2003). Serum lipids and memory in a population based cohort of middle age women. *J Neurol Neurosurg Psychiatry* **74**: 1530–1535.

Homma N, Nagaoka T, Karoor V, Imamura M, Taraseviciene-Stewart L, Walker LA *et al* (2008). Involvement of RhoA/Rho kinase signaling in protection against monocrotaline-induced pulmonary hypertension in pneumonectomized rats by dehydroepiandrosterone. *Am J Physiol Lung Cell Mol Physiol* **295**: L71–L78.

Horton JD (2002). Sterol regulatory element-binding proteins: transcriptional activators of lipid synthesis. *Biochem Soc Trans* **30**(Pt 6): 1091–1095.

Huttner WB, Schiebler W, Greengard P, De Camilli P (1983). Synapsin I (protein I), a nerve terminal-specific phosphoprotein. III. Its association with synaptic vesicles studied in a highly purified synaptic vesicle preparation. *J Cell Biol* **96**: 1374–1388.

Indolfi C, Di Lorenzo E, Perrino C, Stingone AM, Curcio A, Torella D *et al* (2002). Hydroxymethylglutaryl coenzyme A reductase inhibitor simvastatin prevents cardiac hypertrophy induced by pressure overload and inhibits p21ras activation. *Circulation* **106**: 2118–2124.

Jones P, Kafonek S, Laurora I, Hunninghake D (1998). Comparative dose efficacy study of atorvastatin versus simvastatin, pravastatin, lovastatin, and fluvastatin in patients with hypercholesterolemia (the CURVES study). *Am J Cardiol* **81**: 582–587.

Kilic FS, Ozatik Y, Kaygisiz B, Baydemir C, Erol K (2012). Acute antidepressant and anxiolytic effects of simvastatin and its mechanisms in rats. *Neurosciences (Riyadh)* **17**: 39–43.

LaBar KS, Cabeza R (2006). Cognitive neuroscience of emotional memory. *Nat Rev Neurosci* **7**: 54–64.

Li L, Zhang S, Zhang X, Li T, Tang Y, Liu H *et al* (2013). Autophagy enhancer carbamazepine alleviates memory deficits and cerebral amyloid-beta pathology in a mouse model of Alzheimer's disease. *Curr Alzheimer Res* **10**: 433–441.

Lin MT, Lujan R, Watanabe M, Adelman JP, Maylie J (2008). SK2 channel plasticity contributes to LTP at Schaffer collateral-CA1 synapses. *Nat Neurosci* **11**: 170–177.

Lingor P, Teusch N, Schwarz K, Mueller R, Mack H, Bahr M *et al* (2007). Inhibition of Rho kinase (ROCK) increases neurite outgrowth on chondroitin sulphate proteoglycan *in vitro* and axonal regeneration in the adult optic nerve *in vivo*. *J Neurochem* **103**: 181–189.

Lowry OH, Rosebrough NJ, Farr AL, Randall RJ (1951). Protein measurement with the Folin phenol reagent. *J Biol Chem* **193**: 265–275.

Marz P, Otten U, Miserez AR (2007). Statins induce differentiation and cell death in neurons and astroglia. *Glia* **55**: 1–12.

Mathew SJ, Coplan JD, Gorman JM (2001). Neurobiological mechanisms of social anxiety disorder. *Am J Psychiatry* **158**: 1558–1567.

Matthews RT, Yang L, Browne S, Baik M, Beal MF (1998). Coenzyme Q10 administration increases brain mitochondrial concentrations and exerts neuroprotective effects. *Proc Natl Acad Sci USA* **95**: 8892–8897.

Mazzucchelli C, Brambilla R (2000). Ras-related and MAPK signalling in neuronal plasticity and memory formation. *Cell Mol Life Sci* **57**: 604–611.

Mereu G, Fa M, Ferraro L, Cagiano R, Antonelli T, Tattoli M *et al* (2003). Prenatal exposure to a cannabinoid agonist produces memory deficits linked to dysfunction in hippocampal long-term potentiation and glutamate release. *Proc Natl Acad Sci USA* **100**: 4915–4920.

Ming XF, Viswambharan H, Barandier C, Ruffieux J, Kaibuchi K, Rusconi S *et al* (2002). Rho GTPase/Rho kinase negatively regulates endothelial nitric oxide synthase phosphorylation through the inhibition of protein kinase B/Akt in human endothelial cells. *Mol Cell Biol* **22**: 8467–8477.

Mohamed A, Saavedra L, Di Pardo A, Sipione S, Posse de Chaves E (2012). beta-amyloid inhibits protein prenylation and induces cholesterol sequestration by impairing SREBP-2 cleavage. *J Neurosci* **32**: 6490–6500.

Moreno S, Mugnaini E, Ceru MP (1995). Immunocytochemical localization of catalase in the central nervous system of the rat. *J Histochem Cytochem* **43**: 1253–1267.

Oh JE, Karlmark Raja K, Shin JH, Pollak A, Hengstschlager M, Lubec G (2006). Cytoskeleton changes following differentiation of N1E-115 neuroblastoma cell line. *Amino Acids* **31**: 289–298.

Opazo P, Watabe AM, Grant SG, O'Dell TJ (2003). Phosphatidylinositol 3-kinase regulates the induction of long-term potentiation through extracellular signal-related kinase-independent mechanisms. *J Neurosci* **23**: 3679–3688.

Pallottini V, Martini C, Cavallini G, Bergamini E, Mustard KJ, Hardie DG *et al* (2007). Age-related HMG-CoA reductase deregulation depends on ROS-induced p38 activation. *Mech Ageing Dev* **128**: 688–695.

Pallottini V, Montanari L, Cavallini G, Bergamini E, Gori Z, Trentalance A (2004). Mechanisms underlying the impaired regulation of 3-hydroxy-3-methylglutaryl coenzyme A reductase in aged rat liver. *Mech Ageing Dev* **125**: 633–639.

Panksepp J, Siviy S, Normansell L (1984). The psychobiology of play: theoretical and methodological perspectives. *Neurosci Biobehav Rev* **8**: 465–492.

Papakostas GI, Ongur D, Iosifescu DV, Mischoulon D, Fava M (2004). Cholesterol in mood and anxiety disorders: review of the literature and new hypotheses. *Eur Neuropsychopharmacol* **14**: 135–142.

Parikh A, Childress C, Deitrick K, Lin Q, Rukstalis D, Yang W (2010). Statin-induced autophagy by inhibition of geranylgeranyl biosynthesis in prostate cancer PC3 cells. *Prostate* **70**: 971–981.

Pellow S, Chopin P, File SE, Briley M (1985). Validation of open:closed arm entries in an elevated plus-maze as a measure of anxiety in the rat. *J Neurosci Methods* **14**: 149–167.

Pellow S, File SE (1986). Anxiolytic and anxiogenic drug effects on exploratory activity in an elevated plus-maze: a novel test of anxiety in the rat. *Pharmacol Biochem Behav* **24**: 525–529.

Peter H, Hand I, Hohagen F, Koenig A, Mindermann O, Oeder F *et al* (2002). Serum cholesterol level comparison: control subjects, anxiety disorder patients, and obsessive-compulsive disorder patients. *Can J Psychiatry* **47**: 557–561.

Pfrieger FW (2003). Role of cholesterol in synapse formation and function. *Biochim Biophys Acta* **1610**: 271–280.

Pinheiro SH, Zangrossi H Jr., Del-Ben CM, Graeff FG (2007). Elevated mazes as animal models of anxiety: effects of serotonergic agents. *An Acad Bras Cienc* **79**: 71–85.

Popjak G, Edmond J, Anet FA, Easton NR Jr. (1977). Carbon-13 NMR studies on cholesterol biosynthesized from [13C]mevalonates. *J Am Chem Soc* **99**: 931–935.

Ramakers GM, Storm JF (2002). A postsynaptic transient K(+) current modulated by arachidonic acid regulates synaptic integration and threshold for LTP induction in hippocampal pyramidal cells. *Proc Natl Acad Sci USA* **99**: 10144–10149.

Reitz C, Luchsinger J, Tang MX, Manly J, Mayeux R (2005). Impact of plasma lipids and time on memory performance in healthy elderly without dementia. *Neurology* **64**: 1378–1383.

Rex CS, Chen LY, Sharma A, Liu J, Babayan AH, Gall CM *et al* (2009). Different Rho GTPase-dependent signaling pathways initiate sequential steps in the consolidation of long-term potentiation. *J Cell Biol* **186**: 85–97.

Saheki A, Terasaki T, Tamai I, Tsuji A (1994). *In vivo* and *in vitro* blood-brain barrier transport of 3-hydroxy-3-methylglutaryl coenzyme A (HMG-CoA) reductase inhibitors. *Pharm Res* **11**: 305–311.

Seasholtz TM, Majumdar M, Brown JH (1999). Rho as a mediator of G protein-coupled receptor signaling. *Mol Pharmacol* **55**: 949–956.

Segatto M, Di Giovanni AL, Marino M, Pallottini V (2013). Analysis of the protein network of cholesterol homeostasis in different brain regions: an age and sex dependent perspective. *J Cell Physiol* **228**: 1561–1567.

Segatto M, Trapani L, Marino M, Pallottini V (2011). Age- and sex-related differences in extra-hepatic low-density lipoprotein receptor. *J Cell Physiol* **226**: 2610–2616.

Sierra S, Ramos MC, Molina P, Esteo C, Vazquez JA, Burgos JS (2011). Statins as neuroprotectants: a comparative in vitro study of lipophilicity, blood-brain-barrier penetration, lowering of brain cholesterol, and decrease of neuron cell death. *J Alzheimers Dis* **23**: 307–318.

Silva AJ, Kogan JH, Frankland PW, Kida S (1998). CREB and memory. *Annu Rev Neurosci* **21**: 127–148.

Sui L, Wang J, Li BM (2008). Role of the phosphoinositide 3-kinase-Akt-mammalian target of the rapamycin signaling pathway in long-term potentiation and trace fear conditioning memory in rat medial prefrontal cortex. *Learn Mem* **15**: 762–776.

Tang PH, Miles MV, DeGrauw A, Hershey A, Pesce A (2001). HPLC analysis of reduced and oxidized coenzyme Q(10) in human plasma. *Clin Chem* **47**: 256–265.

Taylor AE, Guthrie PA, Smith GD, Golding J, Sattar N, Hingorani AD *et al* (2011). IQ, educational attainment, memory and plasma lipids: associations with apolipoprotein E genotype in 5995 children. *Biol Psychiatry* **70**: 152–158.

Tong XK, Lecrux C, Rosa-Neto P, Hamel E (2012). Age-dependent rescue by simvastatin of Alzheimer's disease cerebrovascular and memory deficits. *J Neurosci* **32**: 4705–4715.

Trapani L, Melli L, Segatto M, Trezza V, Campolongo P, Jozwiak A *et al* (2011a). Effects of myosin heavy chain (MHC) plasticity induced by HMGCoA-reductase inhibition on skeletal muscle functions. *FASEB J* **25**: 4037–4047.

Trapani L, Segatto M, Ascenzi P, Pallottini V (2011b). Potential role of nonstatin cholesterol lowering agents. *IUBMB Life* **63**: 964–971.

Trezza V, Baarendse PJ, Vanderschuren LJ (2009). Prosocial effects of nicotine and ethanol in adolescent rats through partially dissociable neurobehavioral mechanisms. *Neuropsychopharmacology* **34**: 2560–2573.

Trezza V, Baarendse PJ, Vanderschuren LJ (2010). The pleasures of play: pharmacological insights into social reward mechanisms. *Trends Pharmacol Sci* **31**: 463–469.

Trezza V, Campolongo P, Cassano T, Macheda T, Dipasquale P, Carratu MR *et al* (2008). Effects of perinatal exposure to delta-9-tetrahydrocannabinol on the emotional reactivity of the offspring: a longitudinal behavioral study in Wistar rats. *Psychopharmacology (Berl)* **198**: 529–537.

Wang Q, Tang XN, Wang L, Yenari MA, Ying W, Goh BC *et al* (2006). Effects of high dose of simvastatin on levels of dopamine and its reuptake in prefrontal cortex and striatum among SD rats. *Neurosci Lett* **408**: 189–193.

Wei YM, Li X, Xu M, Abais JM, Chen Y, Riebling CR *et al* (2013). Enhancement of autophagy by simvastatin through inhibition of Rac1-mTOR signaling pathway in coronary arterial myocytes. *Cell Physiol Biochem* **31**: 925–937.

While A, Keen L (2010). The effects of statins on mood: a review of the literature. *Eur J Cardiovasc Nurs* **11**: 85–96.

Whitton P, Curzon G (1990). Anxiogenic-like effect of infusing 1-(3-chlorophenyl) piperazine (mCPP) into the hippocampus. *Psychopharmacology (Berl)* **100**: 138–140.

Supplementary Information accompanies the paper on the Neuropsychopharmacology website (http://www.nature.com/npp)

ARTICLE
Journal of Cellular Biochemistry 9999:1–9 (2016)

Journal of Cellular Biochemistry

# Modulation of the Isoprenoid/Cholesterol Biosynthetic Pathway During Neuronal Differentiation In Vitro

Veronica Cartocci,[1] Marco Segatto,[2] Ilenia Di Tunno,[1] Stefano Leone,[1] Frank W. Pfrieger,[3] and Valentina Pallottini[1]*

[1]*Department of Science, Biomedical and Technology Science Section, University Roma Tre, Viale Marconi, 446, 00146, Rome, Italy*

[2]*Department of Biosciences, University of Milan, Via Giovanni Celoria, 26, 20133, Milan, Italy*

[3]*Institute of Cellular and Integrative Neurosciences (INCI) CNRS UPR 3212, University of Strasbourg, 5 rue Blaise Pascal, 67084, Strasbourg, France*

## ABSTRACT

During differentiation, neurons acquire their typical shape and functional properties. At present, it is unclear, whether this important developmental step involves metabolic changes. Here, we studied the contribution of the mevalonate (MVA) pathway to neuronal differentiation using the mouse neuroblastoma cell line N1E-115 as experimental model. Our results show that during differentiation, the activity of 3-hydroxy 3-methylglutaryl Coenzyme A reductase (HMGR), a key enzyme of MVA pathway, and the level of Low Density Lipoprotein receptor (LDLr) decrease, whereas the level of LDLr-related protein-1 (LRP1) and the dimerization of Scavanger Receptor B1 (SRB-1) rise. Pharmacologic inhibition of HMGR by simvastatin accelerated neuronal differentiation by modulating geranylated proteins. Collectively, our data suggest that during neuronal differentiation, the activity of the MVA pathway decreases and we postulate that any interference with this process impacts neuronal morphology and function. Therefore, the MVA pathway appears as an attractive pharmacological target to modulate neurological and metabolic symptoms of developmental neuropathologies. J. Cell. Biochem. 9999: 1–9, 2016. 

**KEY WORDS:** 3-HYDROXY 3-METHYLGLUTARYL COENZYME A REDUCTASE; CHOLESTEROL; ISOPRENOID; LIPOPROTEIN RECEPTORS; N1E-115; NEURONAL DIFFERENTIATION

The differentiation of neurons is a decisive phase during brain development, which spans weeks in rodents and years in humans. Newly generated neurons acquire their cell-type specific shape and functional properties [da Silva and Dotti, 2002]. They grow axons and dendrites, they establish synaptic connections and they express transmitter receptors and ion channels that determine the cell-specific firing patterns [Hanson and Landmesser, 2004]. The function of the adult brain depends critically on the correct execution of these developmental events. Interference with neuronal differentiation due to genetic factors, drug treatment or environmental factor exposure can provoke late neurologic or psychiatric symptoms [Chaudhury et al., 2015; Hill et al., 2015; Nuttall, 2015]. For example, valproic acid treatment or bacterial infections during pregnancy can cause autism in offspring [Jensen, 1994]. Mutations in methyl-CpG-binding protein-2 (mecp2) cause Rett syndrome, a neurodevelopmental disorder [Amir et al., 1999].

A major goal is to identify the metabolic pathways that are decisive for neuronal differentiation and that are potentially implied in disease mechanisms. Here, we focused on the ubiquitously expressed mevalonate (MVA) pathway (Fig. 1). Its end products (e.g., coenzyme Q10, prenyls, and cholesterol) are essential for neuronal function [Lee et al., 2014; Segatto et al., 2014a; Villarroel-Campos et al., 2014]: cholesterol, for example, is a key component of the myelin sheath and of neuronal membranes in axons, dendrites, and synapses [Orth and Bellosta, 2012]. It must be synthesized within the brain as the blood-brain barrier prevents import of lipoproteins, but the cellular origin of the different pools in neurons are incompletely understood

Conflict of interest: Authors declare no conflict of interest.
Veronica Cartocci and Marco Segatto contributed equally to this work.
Grant sponsor: University of "Roma Tre"; Grant number: CLA 2013-2015.
*Correspondence to: Valentina Pallottini, Department of Science, Biomedical and Technology Science Section, University Roma Tre, Viale Marconi, 446, 00146, Rome, Italy. E-mail: valentina.pallottini@uniroma3.it
Manuscript Received: 22 January 2016; Manuscript Accepted: 25 January 2016
Accepted manuscript online in Wiley Online Library (wileyonlinelibrary.com): 00 Month 2016
DOI 10.1002/jcb.25500 • © 2016 Wiley Periodicals, Inc.

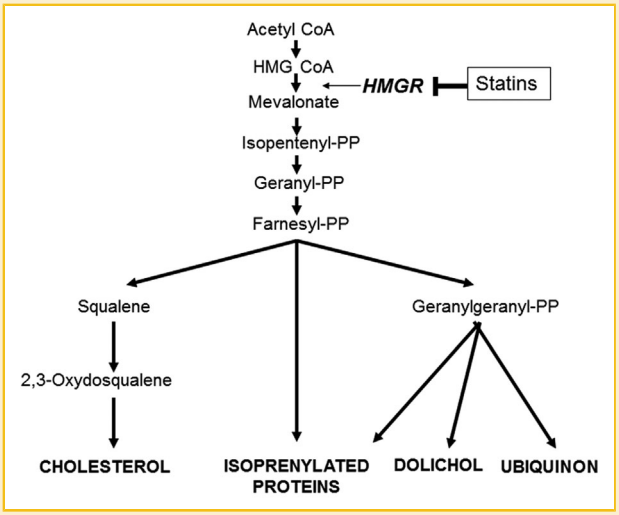


**Fig. 1.** Schematic representation of the mevalonate pathway.

[Pfrieger and Ungerer, 2011; Segatto et al., 2014a]. A perturbation of cholesterol homeostasis can cause neurologic and psychiatric symptoms and contribute to diseases like RETT syndrome [Buchovecky et al., 2013; Martin et al., 2014; Segatto et al., 2014c], Huntington disease [Valenza et al., 2015] or autism [Wang, 2014]. Besides cholesterol, isoprenoids play significant roles in the CNS. The post-translational binding of farnesyl pyrophosphate (FPP) or of geranylgeranyl pyrophosphate (GGPP) moieties to proteins is critical for protein localization and, in turn, for cell maturation and growth [Prendergast and Oliff, 2000; Sah et al., 2000].

A key enzyme of the MVA pathway is 3-hydroxy-3-methylglutaryl coenzyme A reductase (HMGR), which catalyses the production of MVA [Brown and Goldstein, 1980; Segatto et al., 2014b]. Its activity is regulated within minutes by phosphorylation and dephosphorylation through AMP activated enzyme (AMPK) and Protein Phosphatase 2A (PP2A), respectively [Pallottini et al., 2007], and within hours by transcriptional changes through the Sterol Regulatory Element Binding Proteins (SREBPs) [Espenshade and Hughes, 2007]. The enzyme is efficiently inhibited by statins, a group of drugs that are commonly used to treat hypercholesteremia [Trapani et al., 2011]. Statin treatment of humans and rodents impacts the adult brain and affects emotion, learning, and memory processes [Baytan et al., 2008; While and Keen, 2010; Douma et al., 2011; Kilic et al., 2012; Segatto et al., 2014b]. The effects of statins on the developing brain are less clear. Previous studies investigated how statins affect neuronal differentiation in vitro [Maltese and Sheridan, 1985; Fan et al., 2002; Schulz et al., 2004; Kim et al., 2009; Raina et al., 2013; Samuel et al., 2014], but the results vary depending on the experimental protocols and the statins used. Moreover, it is unclear, whether neuronal differentiation modulates the mevalonate pathway per se. We addressed these questions using a mouse neuroblastoma cell line as experimental model permitting DMSO-induced differentiation [Shim et al., 2006].

## MATERIALS AND METHODS

### CHEMICALS AND ANTIBODIES

Unless indicated otherwise, all materials were from Sigma–Aldrich (St. Louis, MO). Geranylgeraniol was a generous gift of Prof. Ewa Sviezewszka (Polish Academy of Science, Warsaw, Poland). For immunoblotting, antibodies against the following proteins were used: P-AMPKα and AMPKα (Cell Signalling Technology, Boston, MA), PP2A (catalytic sub-unit), RhoA, LRP1, and SREBP-1 (Santa Cruz Biotechnology, Santa Cruz, CA), LDLr (ab30532 and SREBP-2 (Abcam, Cambridge, United Kingdom), P-HMGR (Millipore, Temecula, CA), HMGR (Upstate, Lake Placid, NY), SRB-1 (Novus Biological, Littleton, CO). α-Tubulin (Sigma–Aldrich) or caveolin (Santa Cruz, CA) were used as loading controls . HRP-conjugated IgG produced in mouse or in rabbit used as secondary antibodies were obtained from Biorad Laboratories (Milan, Italy).

### CELL CULTURE

Mouse neuroblastoma clone N1E-115 was obtained from the European Collection of Cell Cultures (Cat. no. 88112303) (Salisbury, United Kingdom). Cells were grown in Dulbecco's modified Eagle's medium (DMEM) containing 4500 mg/L glucose, 2 mM L-glutamine, 10% fetal bovine serum (FBS), penicillin and streptomycin (Lonza, Milano, Italia) in a humidified incubator with 5% $CO_2$ at 37°C.

### NEURONAL DIFFERENTIATION

N1E-115 cells were plated for 5 h in DMEM medium (GIBCO) 10% serum to allow cell adhesion. Neuronal differentiation was induced by the addition of 2% dimethylsulfoxide (DMSO). The medium containing DMSO was changed on day 3 and neuronal differentiation was observed up to 120 h in the differentiation medium. For experimental treatments, cultures were incubated in the presence of differentiation medium supplemented with Ethanol (Et-OH) as control or with Simvastatin (Sim). In addition, culture dishes were treated with different products of the MVA pathway: Cholesterol (CHOL), Farnesol (Far), Geranylgeraniol (GG) in the presence or absence of Simvastatin. These pharmacological agents were used at a concentration of 1 μM dissolved in ET-OH.

### NEURITE EXTENSION ASSAY

The degree of differentiation was evaluated based on the length of neuritic processes in different directions and at different time intervals (16, 24, 48, 72, and 120 h) using an Olympus CKX 41 microscope equipped with a Leica DFC 420 camera. Electronic images were further processed using Adobe Photoshop CS2.

For each treatment, 10 randomly selected fields from three independent preparations were analyzed.

While small and spherical in their undifferentiated state, morphologically transformed N1E-115 cells are typically 40 μm or larger and extend processes which often span several hundred micrometer. The neurite length was evaluated with ImageJ software for Windows (NIH, Bethesda, MD) and was reported as arbitrary units. Only neuritic processes that were longer than two times the diameter of the cell were considered.

### XTT ASSAY

Cell viability was detected by the XTT assay following manufacturer instructions (Cell Signalling Technology; Boston, MA). This assay detects a formazan dye produced from XTT conversion by mitochondrial enzymes. $5 \times 10^3$ cells were plated in 96 well dishes. Cells were treated with 2% DMSO in presence and in absence of 1 μM simvastatin for 120 h using ET-OH as control.

### FLOW CYTOMETRY ANALYSIS

To evaluate cell viability, $1.5 \times 10^5$ N1E-115 cells were grown in 3.5 cm Petri dish in DMEM medium (GIBCO) with 10% FBS and treated with 2% DMSO in the presence of 1 μM simvastatin or of ET-OH alone (0.1% v/v) for 120 h. After trypsin detach, cells were treated with propidium iodide (PI) (2 μg/ml) and immediately analyzed by flow cytometry. For each experiment, 20,000 events on were acquired and the percentage of live cells was calculated by design an electronic gate on PI negative events. To stain SR-B1 on the live cell surface, $1.5 \times 10^5$ cells were seeded into 3, 5 cm Petri dish on DMEM supplemented with 10% FBS for each experimental point. After 5 h, medium was replaced by fresh complete medium containing 2 % DMSO or ET-OH. For each time point ($t_0$, $t_{72}$), cells were harvested with trypsin and washed twice with cold phosphate buffered saline (PBS) containing 5% BSA. For each sample, living cells were incubated with anti-SR-B1 (for 30 min at 4°C; 1:100 in PBS/5% BSA; Novus Biological). Samples were incubated with FITC-conjugated goat anti-rabbit secondary antibody (30 min at 4°C; 1:100 PBS/5% BSA; Cappel). Background controls with secondary antibody alone were included at each time point. Immunofluorescence intensity was measured by a Galaxy flow cytometer (DakoCytomation) and analyzed by Flowjo v.5.4.4 software (Tree Star Inc., Ashland, OR). For each sample, 20,000 events were recorded, data were obtained from three independent experiments. Dead cells were omitted from analysis by side scatter electronic gate exclusion.

### WESTERN BLOTTING ANALYSIS

To prepare total protein lysate, N1E-115 cells were washed at indicated times with 1 ml of phosphate buffered saline

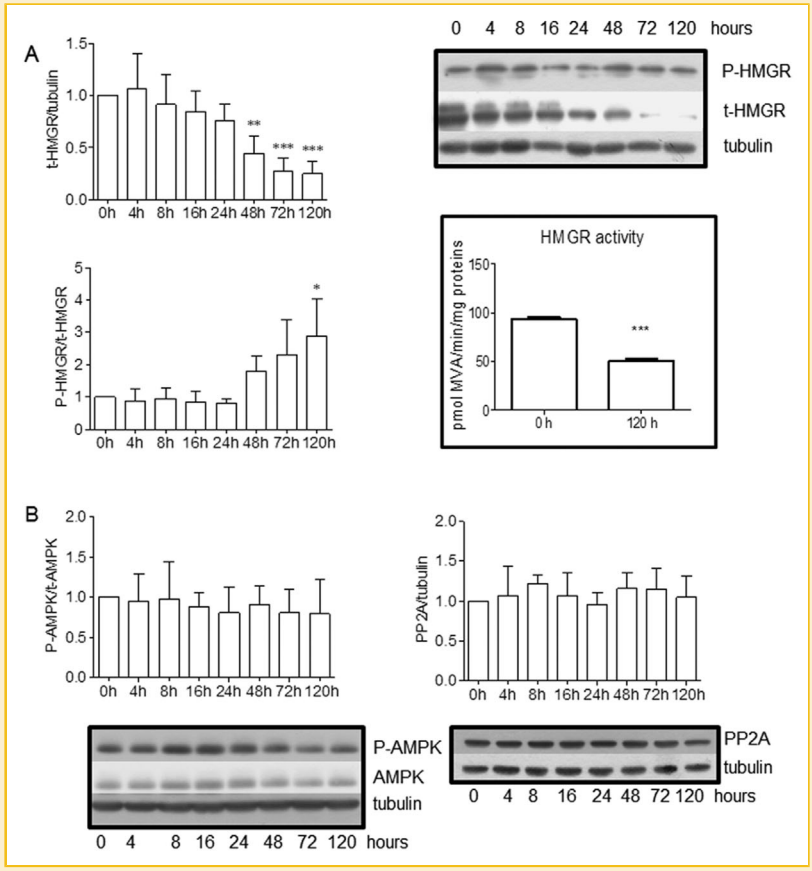


**Fig. 2.** HMGR, AMPK, and PP2A analysis in differentiating N1E-115 mouse neuroblastoma. Panel A illustrates HMGR analysis. On the left the densitometric analyses of total protein content (up) and the phosphorylation state of the enzyme (bottom), quantified as t-HMGR/tubulin and P-HMGR/t-HMGR, respectively. A representative Western blot is shown on the right (up). The size of HMGR is 90 kDa, the size of tubulin is 50 kDa. $^{**}P < 0.01$, $^{***}P < 0.001$ versus 0 h as from one-way analysis of variance (ANOVA) followed by Tukey post-test. Inset illustrates HMGR activity measured as pmol of [$^{14}$C]-MVA production/min/mg proteins at 0 h and 120 h after the induction of differentiation by using 2% DMSO. $^{***}P < 0.001$ versus 0 h as from a Student's *t*-test. Panel B illustrates AMPK (left) and PP2A catalytic sub-unit (right) analysis. On the bottom are represented the immunoblots from representative experiments. Average protein expression is quantified as P-AMPK/AMPK, and PP2A/tubulin (right graph). The size of AMPK is 68 kDa, The size of the catalytic subunit of PP2A is 35 kDa, the size of tubulin is 50 kDa. All the presented data derives from three independent experiments, for details see the main text.

(PBS; PH=7.4), trypsinized (2 min at 37°C), harvested, centrifuged (1 min at 13,000 rpm at room temperature), resuspended and sonicated (30 s) in 50 μl of sample buffer containing 0.125 M TrisHCL pH 6.8, 10% SDS, 0.062 M NaF and Protease Inhibitor Cocktail (Sigma).

To prepare the membrane fraction, cells were homogenized in a homogenization buffer (0.01 M Tris-HCl, 0.001 M $CaCl_2$, 0.15 M NaCl, 0.001 M PMSF, pH 7.5) and spun down (10,000 *g* for 10 min). The supernatant was centrifuged two times (100,000 g for 45 min), the pellet containing the membrane fraction was solubilized (0.125 M Tris-HCl -pH 6.8- containing 10% SDS, 0.001 M PMSF) and the protein concentration was measured [Lowry et al., 1951]. Membrane and total lysate samples were boiled for 3 min before SDS-PAGE and subsequent Western blotting. The presence of caveolin (membrane marker) and α-tubulin (cytosolic marker) confirmed the purity of the membrane fractions (data not shown). All experiments were carried out in triplicate.

Thirty micrograms of protein were separated by SDS–PAGE and blotted to nitrocellulose membranes (Trans-blott Turbo, BioRad). Immunoblots were incubated with primary antibodies (1:1,000) followed by secondary peroxidase-conjugated antibodies (1:10,000; Biorad). Immunoreactivity was detected by enhanced chemiluminescence (GE Healthcare, Little Chalfont, United Kingdom). All images derived from Western blotting were analyzed with ImageJ (National Institutes of Health, Bethesda, MD). Intensity values of

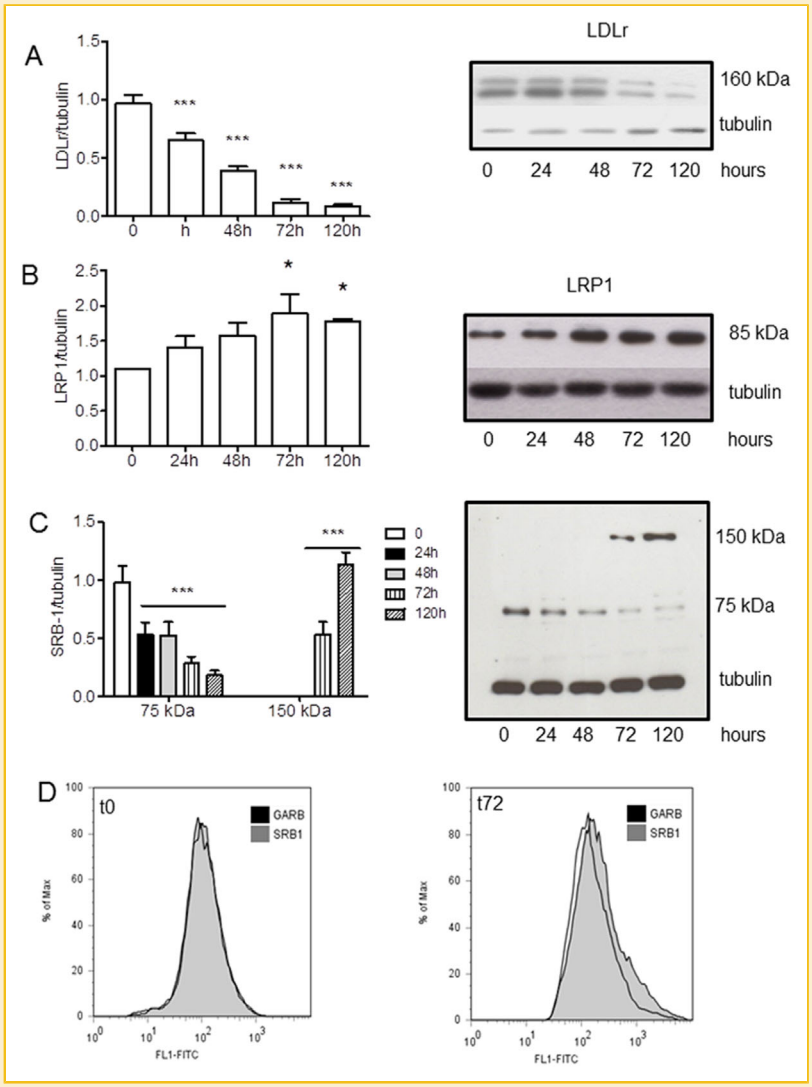


**Fig. 3.** LDLr, LRP1, and SR-B1 analysis in differentiating N1E-115 mouse neuroblastoma. Panel A illustrates LDLr analysis, Panel B illustrates LRP1 analysis, and Panel C illustrates SRB-1 analysis. On the right are represented the immunoblots from representative experiments. Average protein expression is represented on the left and quantified as ratio between protein and tubulin. $^{*}P < 0.05$, $^{***}P < 0.001$ versus 0 h as from one-way analysis of variance (ANOVA) followed by Tukey post-test. Panel D shows membrane expression of SRB-1 receptor on live cells before and after 72 hr of DMSO-induced differentiation. The results are presented as cytometric histograms distribution (goat anti-rabbit FITC conjugated control stain [black], versus surface anti-SRB-1 antibody [gray]). These results are representative of three similar experiments.

selected proteins were normalized to intensities of respective housekeeping proteins (tubulin or caveolin).

### HMGR ACTIVITY ASSAY

Activity was measured using a radioisotopic assay based on the production of $^{14}$C-MVA (mevalonate) from 3-[$^{14}$C]-HMGCoA (specific activity 57.0 mCi/mmol. Amersham-Pharmacia, Little Chalfont, UK). N1E-115 cells were differentiated with 2% DMSO for 120 h in the presence of 1 μM simvastatin or of ET-OH. Cells were homogenized in phosphate buffer (0.1 M sucrose, 0.05 M KCl, 0.04 M KH2PO4, 0.03 M EDTA, 50 mM NaF, pH 7.4) and incubated in the presence of co-factors (20 mM glucose-6-phosphate, 20 mM NADP sodium salt, 1 unit of glucose-6-phosphate dehydrogenase, and 5 mM dithiothreitol) in a final volume of 190 ml (for 100 μg protein). The assay was started by addition of 10 μl 3-[$^{14}$C]-HMG-CoA (0.088 mCi/11.7 nmol). The synthesized [$^{14}$C]-MVA was purified by chromatography (AG1-X8 ion exchange resin; BioRad, Italy) and the radioactivity measured (Liquid Scintillator Analyzer, Perkin Elmer). The recovery was calculated based on an internal standard (3-[$^{3}$H]-MVA, specific activity 24.0 Ci/mmol (Amersham-Pharmacia, Little Chalfont, United Kingdom).

### FILIPIN STAINING

$5 \times 10^3$ cells were seeded, into 96 wells plate (Falcon black/clear tissue culture treated plate flat bottom) and after adhesion (5 h) the medium was changed with complete medium in presence of 2% DMSO with or without 1 μM of Simvastatin. The medium was changed with fresh stimuli each 2 days and cells were cultured for 120 h. To visualize the intracellular cholesterol distribution, cultured cells were fixed (4% paraformaldehyde for 15 min) and incubated for 2 h with filipin (10μg/ml with 0.1% ethanol, Sigma). Filipin fluorescence was imaged on an inverted microscope (Axiovert 135TV; Zeiss) equipped with a metal halide lamp (10%; Lumen 200; Prior Scientific), an appropriate excitation/emission filter (XF02-2; Omega Optical Inc.), a 40× objective (N.A. 1.3; Zeiss) and an air-cooled monochrome CCD camera (Sensicam, PCO Computer Optics) controlled by custom-written Labview routines (National Instruments).

Data analysis was performed with ImageJ (National Institutes of Health, Bethesda, MD) software for Windows. The experiment was performed with four biological replicates. For each experimental group 10 randomly selected fields were analyzed.

### STATISTICAL ANALYSIS

Data were analyzed by Student's *t*-test in the case of two experimental conditions and by one-way analysis of variance (ANOVA) followed by Tukey post-test for multiple conditions (GraphPad Instat3; GraphPad, Inc., La Jolla, CA).

## RESULTS

We investigated the role of the MVA pathway during neuron differentiation using the N1E-115 cell line [Shim et al., 2006]. To avoid confounding effects of serum and thus cholesterol deprivation we induced neuronal differentiation by DMSO [Clejan et al., 1996; Rodrigues et al., 2005; Oh et al., 2006]. As a first step, we investigated whether DMSO affected HMGR, a key component of the MVA pathway. Indeed, as shown in Figure 2A, the amount of total HMGR protein in neurons decreased and the fraction of phosphorylated protein increased during differentiation. The levels of enzymes that regulate the phosphorylation status of HMGR, AMPK, and PP2A, were stable during 120 h of treatment (Fig. 2B). The observed changes in HMGR suggested that the level of the enzyme decreases during DMSO-induced differentiation. Indeed, metabolic labeling of mevalonate revealed that its activity was significantly reduced after

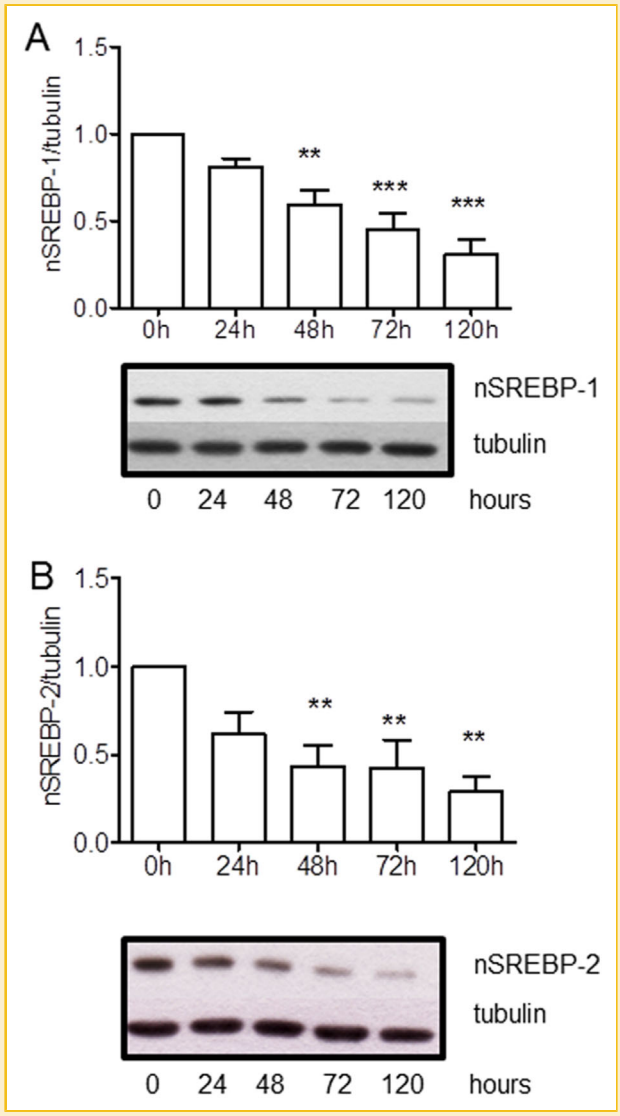


**Fig. 4.** SREBP-1 and SREBP-2 analysis, in differentiating N1E-115 mouse neuroblastoma. Panel A illustrates the transcriptionally active fragment of SREBP-1 (n-SREBP-1) analysis, Panel B illustrates transcriptionally active fragment of SREBP-2 (SERBP-2) analysis. On the bottom are represented the immunoblots from a representative experiment. Similar results were obtained from three independent experiments for each protein considered. Average protein expression quantified as ratio between protein and tubulin. $^{**}P < 0.01$, $^{***}P < 0.001$ versus 0 h as from one-way analysis of variance (ANOVA) followed by Tukey post-test.

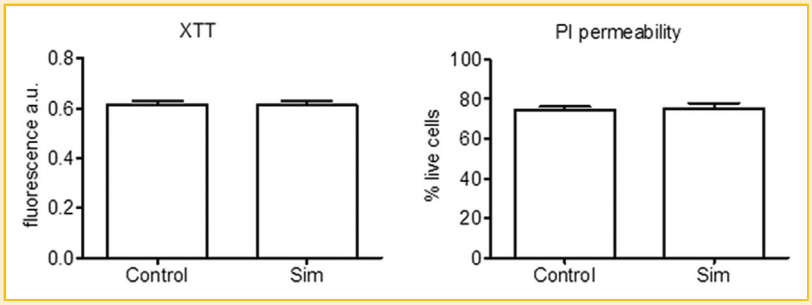


**Fig. 5.** Evaluation of cell viability in differentiating N1E-115 mouse neuroblastoma cells. Figure illustrates on the left XTT assay and on the right PI exclusion assay performed on N1E-115 cells induced to differentiate with 2% DMSO for 120 h in presence and in absence of 1 μM simvastatin. For details see the main text.

induction of differentiation (Fig. 2 inset), indicating that the metabolic flux through the MVA pathway decreases. The MVA pathway is an important component of lipid homeostasis in cells together with the machinery that mediates cholesterol uptake. We therefore tested next, whether lipoprotein receptors were affected by DMSO-induced neuronal differentiation. The level of LDLr decreased, whereas the level of LRP1 was increased (Fig. 3A and B). The latter change was not surprising, because LRP1 is a prominent component of neurites [Kanekiyo and Bu, 2014], whose growth is induced by DMSO. On the other hand, we also observed a decrease of SRB1 at 75 kDa (Fig. 3C), and interestingly, we observed at 72 h of treatment a band at 150 kDa which may signify the dimerization of SRB-1 and a possible translocation of the protein complex on plasma membrane . The appearance of SRB-1 on the cell surface after 72 h of treatment was confirmed by live labeling with the antibody and subsequent flow cytometric analyses (Fig. 3D).

The expression of MVA enzymes, lipoprotein receptors, and other components controlling lipid homeostasis is regulated by two transcription factors, the so called SREBP-1 and -2, which undergo cleavage and transfer to the nucleus upon declining lipid levels.

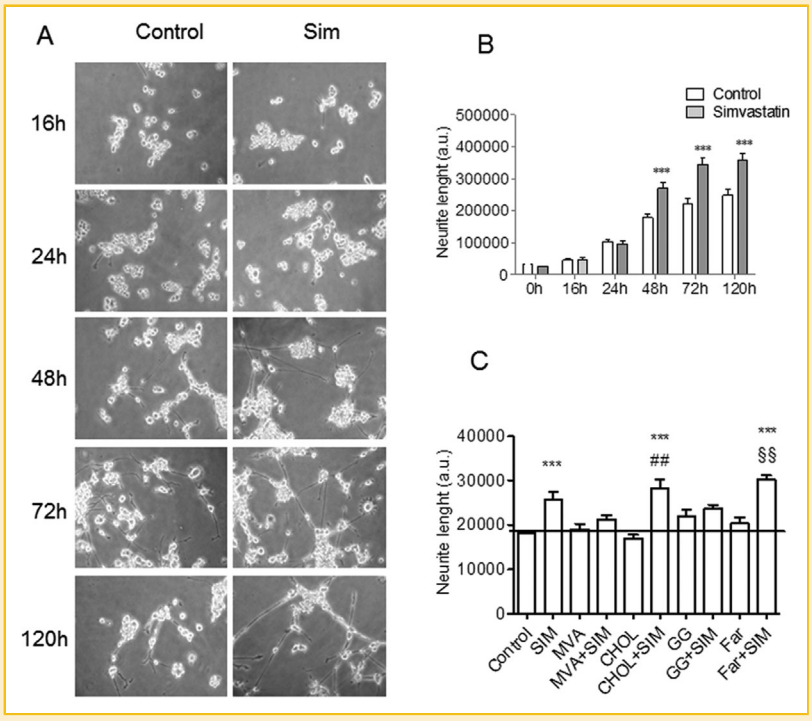


**Fig. 6.** Neurite elongation analysis of N1E-115 mouse neuroblastoma during DMSO-induced differentiation. Panel A shows representative pictures of "in vivo" cell detection under an Olympus CKX 41 microscope, equipped with a Leica DFC 420 camera. It represents the neurite elongation during DMSO-induced cell differentiation in presence and in absence of 1 μM simvastatin starting from 0 h to 120 h. Panel B shows the statistical analysis of neurite elongation performed on 10 randomly selected fields from three independent preparations. Panel C represents the neurite elongation analysis, at 120 h after the induction of the differentiation by DMSO, in presence and in absence of SIM or SIM + HMGR end products: MVA, cholesterol (CHOL), geranyl geraniol (GG), Farnesol (Far). All the compounds were administered at 1 μM. The analysis was performed on 10 randomly selected fields from three independent preparations. $^{***}P < 0.001$ versus Control, $^{\#\#}P < 0.01$ versus CHOL, $^{\S\S}P < 0.01$ versus Far; as from one-way analysis of variance (ANOVA) followed by Tukey post-test.

Immunoblotting revealed that the levels of transcriptionally active SREBP-1 and of SREBP-2 decreased during differentiation (Fig. 4).

Our results indicated that neuronal differentiation is accompanied by a decrease in MVA synthesis and predicted that a further decrease of MVA synthesis will accelerate neuronal differentiation. To test this hypothesis, we induced neuronal differentiation by DMSO in the presence or absence of simvastatin, a well-established HMGR inhibitor, at a concentration that was not toxic to neurons as indicated by XTT and Propidium Iodide exclusion test (Fig. 5). To determine the degree of neuronal differentiation, we measured neurite length. We observed that simvastatin treatment increased the length of neurites indicating that a decrease of MVA pathway promotes neuronal differentiation in our experimental model (Fig. 6A and B). We next tested, which end-product of MVA pathway mediated this effect. We induced neuronal differentiation in the presence of simvastatin and added MVA, cholesterol (CHOL), geranylgeranyiol (GG) or farnesol (Far) for 120 h. As shown in Figure 6C, only MVA and GG prevented the simvastatin-induced increase of neurite outgrowth. Filipin staining of neurons treated or not with simvastatin demonstrated that cellular cholesterol content did not change (Fig. 7).

GG is required for the prenylation of GTP binding proteins and prominent targets are the Rho family GTPases. A prominent member of this family is RhoA, which negatively controls neurite outgrowth [Govek et al., 2011] and whose prenylation allows its translocation to the plasma membrane and its subsequent activation [Segatto et al., 2014b]. We tested whether simvastatin affected the RhoA content of the membrane fraction. As shown in Figure 8 simvastatin decreased the RhoA level in membrane lysates, and this effect was reverted by MVA and GG indicating that the neurite growth promoting effect of simvastatin was mediated, at least in part, via reduced isoprenylation of RhoA.

## DISCUSSION

It is well known that neurons proliferate and then differentiate changing their morphology, outgrowing neurites and becoming functionally active. Here, we investigated the role of the MVA pathway during neuronal differentiation in mouse neuroblastoma N1E-115 cells, a valuable and widely used experimental model, which recapitulates key steps of neurite initiation and outgrowth [Shim et al., 2006].

We focused our attention on the protein network that controls the MVA pathway and in turn the cellular cholesterol homeostasis during neuronal differentiation. Intriguingly, HMGR activation decreased along the considered time points, suggesting a progressive reduction of cellular cholesterol synthesis during neuronal differentiation. This result is in good agreement with the hypothesis that during development, neurons decrease their cholesterol synthesis [Mauch et al., 2001; Pfrieger and Ungerer, 2011]. The decrease of HMGR activity is due to decline of the total protein levels and independent from phosphorylation/dephosphorylation mechanisms. The decrease of both the transcription factors (SREBP1 and -2) not only accounts for the reduced HMGR protein expression, but also for the significant fall in LDLr [Horton, 2002] and for the increased LRP1 levels [Llorente-Cortes et al., 2006; Llorente-Cortes et al., 2007]. Regarding SRB-1 we made interesting observations.

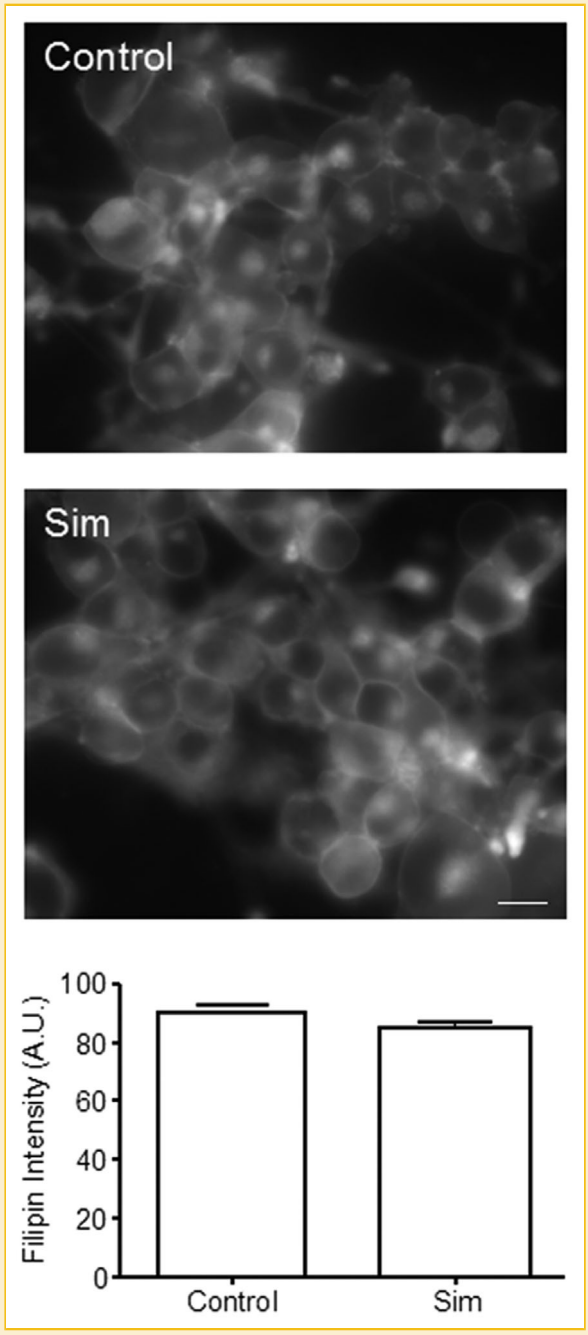


**Fig. 7.** Cholesterol content evaluation in differentiating N1E-115 mouse neuroblastoma. N1E-115 cells were treated or not with 1 μM Sim, for 120 h after DMSO administration. Cells were fixed with 4% paraformaldehyde and stained with filipin. Representative pictures of the filipin staining are shown on the top. On bottom, data analysis of filipin intensity measured as described in the main text is illustrated.

During differentiation the protein dimerizes leading to the appearance of a 150 kDa band. The dimerization represents a physiological event, since the protein is functional when expressed on the cell surface as a dimer [Gaidukov et al., 2011]. Indeed, our flow cytometric analysis, performed in live cells, does not show any SRB-1 signal on membrane surfaces of undifferentiated cells (0 h)

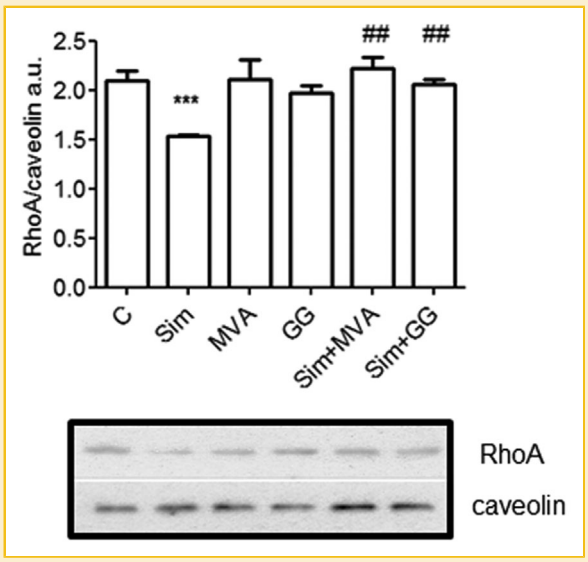


**Fig. 8.** RhoA analysis in undifferentiated and differentiated N1E-115 mouse neuroblastoma in presence of Sim and HMGR end-products. N1E-115 cells were treated with 1 μM Sim, or 1 μM MVA, or 1 μM GG, or Sim + MVA, or Sim + GG for 120 h after DMSO administration. Then cell membranes were prepared as illustrated in the main text. Bottom of the figure shows an immunoblot from a representative experiment. Similar results were obtained from three independent experiments. Average protein expression is represented on the top and quantified as ratio between RhoA and caveolin. The size of RhoA is 21 kDa, the size of caveolin is 22 kDa. $^{***}P < 0.001$ versus C, $^{\#\#}P < 0.01$ versus Sim as from one-way analysis of variance (ANOVA) followed by Tukey post-test.

whereas an increase of fluorescence intensity is detectable at 72 h in accordance with the appearance of the 150 kDa SRB-1 in Western blot analysis. Thus, since cholesterol synthesis decreases during neuronal differentiation, cells could supply their cholesterol needs through the increase of both LRP1 and the functional SRB-1. In our opinion SR-B1 dimerization may be considered a new marker of neuronal differentiation.

Our results show that the pharmacological inhibition of MVA pathway increases the rate of neurite outgrowth. These results are in good agreement with those obtained by other research groups [Maltese and Sheridan, 1985; Sato-Suzuki and Murota, 1996; Holmberg et al., 2006; Pooler et al., 2006; Raina et al., 2013]. These effects are completely prevented by MVA administration, indicating that simvastatin-induced neurite elongation depends on the specific HMGR inhibition and not by an effect exerted by simvastatin per se. Beside cholesterol, MVA is the precursor of isoprenoids such as GG or Far that are required for the prenylation and the subsequent activation of different proteins. Our finding that only GG prevented the simvastatin-induced neurite outgrowth, suggests that geranylgeranylated proteins, rather than farnesylated ones or cholesterol, promote neurite formation, and elongation. The intracellular cholesterol content as measured by filipin did not change in differentiating cells both in presence and in absence of simvastatin. Moreover, we found that simvastatin significantly reduced membrane-associated RhoA levels in N1E-115 cells. G Geranylgeranylation of RhoA is essential for membrane translocation and the activation of its signaling functions [Seasholtz et al., 1999]. This includes the actomyosin-based contractility of neurites and the disassembly of microtubules and intermediate filaments leading to neurite retraction [Hirose et al., 1998]. We therefore conclude that simvastatin promotes neurite elongation by preventing the activation of the negative regulator RhoA.

Taken together our presented data indicate that the decrease of the MVA pathway is fundamental for neurite outgrowth and in turn neuronal differentiation. The progressive decrease in the activation of isoprenoid/cholesterol metabolic pathways is a physiological feature in differentiating neurons, and assumes that any interference in the modulation of this metabolic pathway can alter neuronal function. In neuropathologies caused by disturbed neuronal development, statin treatment may help to improve the neurological and metabolic symptoms [Wang, 2014].

## ACKNOWLEDGMENTS

This work was supported by grants from the University of "Roma Tre" CLA 2013-2015 to V.P. We thank M. Perraut for help with cytochemical staining.

## REFERENCES

Amir RE, Van den Veyver IB, Wan M, Tran CQ, Francke U, Zoghbi HY. 1999. Rett syndrome is caused by mutations in X-linked MECP2, encoding methyl-CpG-binding protein 2. Nat Genet 23:185–188.

Baytan SH, Alkanat M, Okuyan M, Ekinci M, Gedikli E, Ozeren M, Akgun A. 2008. Simvastatin impairs spatial memory in rats at a specific dose level. Tohoku J Exp Med 214:341–349.

Brown MS, Goldstein JL. 1980. Multivalent feedback regulation of HMG CoA reductase, a control mechanism coordinating isoprenoid synthesis and cell growth. J Lipid Res 21:505–517.

Buchovecky CM, Turley SD, Brown HM, Kyle SM, McDonald JG, Liu B, Pieper AA, Huang W, Katz DM, Russell DW, Shendure J, Justice MJ. 2013. A suppressor screen in Mecp2 mutant mice implicates cholesterol metabolism in Rett syndrome. Nat Genet 45:1013–1020.

Chaudhury S, Sharma V, Kumar V, Nag TC, Wadhwa S. 2015. Activity-dependent synaptic plasticity modulates the critical phase of brain development. Brain Dev. In press.

Clejan S, Dotson RS, Wolf EW, Corb MP, Ide CF. 1996. Morphological differentiation of N1E-115 neuroblastoma cells by dimethyl sulfoxide activation of lipid second messengers. Exp Cell Res 224:16–27.

da Silva JS, Dotti CG. 2002. Breaking the neuronal sphere: Regulation of the actin cytoskeleton in neuritogenesis. Nat Rev Neurosci 3:694–704.

Douma TN, Borre Y, Hendriksen H, Olivier B, Oosting RS. 2011. Simvastatin improves learning and memory in control but not in olfactory bulbectomized rats. Psychopharmacology (Berl) 216:537–544.

Espenshade PJ, Hughes AL. 2007. Regulation of sterol synthesis in eukaryotes. Annu Rev Genet 41:401–427.

Fan QW, Yu W, Gong JS, Zou K, Sawamura N, Senda T, Yanagisawa K, Michikawa M. 2002. Cholesterol-dependent modulation of dendrite outgrowth and microtubule stability in cultured neurons. J Neurochem 80:178–190.

Gaidukov L, Nager AR, Xu S, Penman M, Krieger M. 2011. Glycine dimerization motif in the N-terminal transmembrane domain of the high density lipoprotein receptor SR-BI required for normal receptor oligomerization and lipid transport. J Biol Chem 286:18452–18464.

Govek EE, Hatten ME, Van Aelst L. 2011. The role of Rho GTPase proteins in CNS neuronal migration. Dev Neurobiol 71:528–553.

Hanson MG, Landmesser LT. 2004. Normal patterns of spontaneous activity are required for correct motor axon guidance and the expression of specific guidance molecules. Neuron 43:687–701.

Hill DS, Cabrera R, Wallis Schultz D, Zhu H, Lu W, Finnell RH, Wlodarczyk BJ. 2015. Autism-like behavior and epigenetic changes associated with autism as consequences of in utero exposure to environmental pollutants in a mouse model. Behav Neurol 2015:426263.

Hirose M, Ishizaki T, Watanabe N, Uehata M, Kranenburg O, Moolenaar WH, Matsumura F, Maekawa M, Bito H, Narumiya S. 1998. Molecular dissection of the Rho-associated protein kinase (p160ROCK)-regulated neurite remodeling in neuroblastoma N1E-115 cells. J Cell Biol 141:1625–1636.

Holmberg E, Nordstrom T, Gross M, Kluge B, Zhang SX, Doolen S. 2006. Simvastatin promotes neurite outgrowth in the presence of inhibitory molecules found in central nervous system injury. J Neurotrauma 23:1366–1378.

Horton JD. 2002. Sterol regulatory element-binding proteins: Transcriptional activators of lipid synthesis. Biochem Soc Trans 30:1091–1095.

Jensen RA. 1994. Autism and the chemical connection. J Autism Dev Disord 24:785–787.

Kanekiyo T, Bu G. 2014. The low-density lipoprotein receptor-related protein 1 and amyloid-beta clearance in Alzheimer′s disease. Front Aging Neurosci 6:93.

Kilic FS, Ozatik Y, Kaygisiz B, Baydemir C, Erol K. 2012. Acute antidepressant and anxiolytic effects of simvastatin and its mechanisms in rats. Neurosciences (Riyadh) 17:39–43.

Kim WY, Gonsiorek EA, Barnhart C, Davare MA, Engebose AJ, Lauridsen H, Bruun D, Lesiak A, Wayman G, Bucelli R, Higgins D, Lein PJ. 2009. Statins decrease dendritic arborization in rat sympathetic neurons by blocking RhoA activation. J Neurochem 108:1057–1071.

Lee D, Kim KY, Shim MS, Kim SY, Ellisman MH, Weinreb RN, Ju WK. 2014. Coenzyme Q10 ameliorates oxidative stress and prevents mitochondrial alteration in ischemic retinal injury. Apoptosis 19:603–614.

Llorente-Cortes V, Costales P, Bernues J, Camino-Lopez S, Badimon L. 2006. Sterol regulatory element-binding protein-2 negatively regulates low density lipoprotein receptor-related protein transcription. J Mol Biol 359:950–960.

Llorente-Cortes V, Royo T, Otero-Vinas M, Berrozpe M, Badimon L. 2007. Sterol regulatory element binding proteins downregulate LDL receptor-related protein (LRP1) expression and LRP1-mediated aggregated LDL uptake by human macrophages. Cardiovasc Res 74:526–536.

Lowry OH, Rosebrough NJ, Farr AL, Randall RJ. 1951. Protein measurement with the Folin phenol reagent. J Biol Chem 193:265–275.

Maltese WA, Sheridan KM. 1985. Differentiation of neuroblastoma cells induced by an inhibitor of mevalonate synthesis: Relation of neurite outgrowth and acetylcholinesterase activity to changes in cell proliferation and blocked isoprenoid synthesis. J Cell Physiol 125:540–558.

Martin MG, Pfrieger F, Dotti CG. 2014. Cholesterol in brain disease: Sometimes determinant and frequently implicated. EMBO Rep 15: 1036–1052.

Mauch DH, Nagler K, Schumacher S, Goritz C, Muller EC, Otto A, Pfrieger FW. 2001. CNS synaptogenesis promoted by glia-derived cholesterol. Science 294:1354–1357.

Nuttall JR. 2015. The plausibility of maternal toxicant exposure and nutritional status as contributing factors to the risk of autism spectrum disorders. Nutr Neurosci. [Epub ahead of print] in press.

Oh JE, Karlmark Raja K, Shin JH, Pollak A, Hengstschlager M, Lubec G. 2006. Cytoskeleton changes following differentiation of N1E-115 neuroblastoma cell line. Amino Acids 31:289–298.

Orth M, Bellosta S. 2012. Cholesterol: Its regulation and role in central nervous system disorders. Cholesterol 2012:292598.

Pallottini V, Martini C, Cavallini G, Bergamini E, Mustard KJ, Hardie DG, Trentalance A. 2007. Age-related HMG-CoA reductase deregulation depends on ROS-induced p38 activation. Mech Ageing Dev 128:688–695.

Pfrieger FW, Ungerer N. 2011. Cholesterol metabolism in neurons and astrocytes. Prog Lipid Res 50:357–371.

Pooler AM, Xi SC, Wurtman RJ. 2006. The 3-hydroxy-3-methylglutaryl coenzyme A reductase inhibitor pravastatin enhances neurite outgrowth in hippocampal neurons. J Neurochem 97:716–723.

Prendergast GC, Oliff A. 2000. Farnesyltransferase inhibitors: Antineoplastic properties, mechanisms of action, and clinical prospects. Semin Cancer Biol 10:443–452.

Raina V, Gupta S, Yadav S, Surolia A. 2013. Simvastatin induced neurite outgrowth unveils role of cell surface cholesterol and acetyl CoA carboxylase in SH-SY5Y cells. PLoS ONE 8:e74547.

Rodrigues JM, Luis AL, Lobato JV, Pinto MV, Faustino A, Hussain NS, Lopes MA, Veloso AP, Freitas M, Geuna S, Santos JD, Mauricio AC. 2005. Intracellular Ca2+ concentration in the N1E-115 neuronal cell line and its use for peripheric nerve regeneration. Acta Med Port 18:323–328.

Sah VP, Seasholtz TM, Sagi SA, Brown JH. 2000. The role of Rho in G protein-coupled receptor signal transduction. Annu Rev Pharmacol Toxicol 40:459–489.

Samuel F, Reddy J, Kaimal R, Segovia V, Mo H, Hynds DL. 2014. Inhibiting geranylgeranylation increases neurite branching and differentially activates cofilin in cell bodies and growth cones. Mol Neurobiol 50:49–59.

Sato-Suzuki I, Murota S. 1996. Simvastatin inhibits the division and induces neurite-like outgrowth in PC12 cells. Neurosci Lett 220:21–24.

Schulz JG, Bosel J, Stoeckel M, Megow D, Dirnagl U, Endres M. 2004. HMG-CoA reductase inhibition causes neurite loss by interfering with geranylgeranylpyrophosphate synthesis. J Neurochem 89:24–32.

Seasholtz TM, Majumdar M, Brown JH. 1999. Rho as a mediator of G protein-coupled receptor signaling. Mol Pharmacol 55:949–956.

Segatto M, Leboffe L, Trapani L, Pallottini V. 2014. Cholesterol homeostasis failure in the brain: Implications for synaptic dysfunction and cognitive decline. Curr Med Chem 21:2788–2802.

Segatto M, Manduca A, Lecis C, Rosso P, Jozwiak A, Swiezewska E, Moreno S, Trezza V, Pallottini V. 2014. Simvastatin treatment highlights a new role for the isoprenoid/cholesterol biosynthetic pathway in the modulation of emotional reactivity and cognitive performance in rats. Neuropsychopharmacology 39:841–854.

Segatto M, Trapani L, Di Tunno, I, Sticozzi C, Valacchi G, Hayek J, Pallottini V. 2014. Cholesterol metabolism is altered in Rett syndrome: A study on plasma and primary cultured fibroblasts derived from patients. PLoS ONE 9: e104834.

Shim KS, Rosner M, Freilinger A, Lubec G, Hengstschlager M. 2006. Bach2 is involved in neuronal differentiation of N1E-115 neuroblastoma cells. Exp Cell Res 312:2264–2278.

Trapani L, Segatto M, Ascenzi P, Pallottini V. 2011. Potential role of nonstatin cholesterol lowering agents. IUBMB Life 63:964–971.

Valenza M, Marullo M, Di Paolo E, Cesana E, Zuccato C, Biella G, Cattaneo E. 2015. Disruption of astrocyte-neuron cholesterol cross talk affects neuronal function in Huntington′s disease. Cell Death Differ 22:690–702.

Villarroel-Campos D, Gastaldi L, Conde C, Caceres A, Gonzalez-Billault C. 2014. Rab-mediated trafficking role in neurite formation. J Neurochem 129:240–248.

Wang H. 2014. Lipid rafts: A signaling platform linking cholesterol metabolism to synaptic deficits in autism spectrum disorders. Front Behav Neurosci 8:104.

While A, Keen L. 2010. The effects of statins on mood: A review of the literature. Eur J Cardiovasc Nurs 11:85–96.

**Altered brain cholesterol/isoprenoid metabolism in a rat model of autism spectrum disorders**

Veronica Cartocci[1], Martina Catallo[1], Massimo Tempestilli[2], Marco Segatto[3], Frank W. Pfrieger[4], Maria Rosanna Bronzuoli[5], Caterina Scuderi[5], Michela Servadio[1], Viviana Trezza[1], Valentina Pallottini[1]*

[1]Department of Science, Section of Biomedical Sciences and Technologies, University "Roma Tre", Viale Marconi 446, 00146, Rome, Italy.
[2]National Institute for Infectious Diseases, Via Portuense 292, 00149, Rome, Italy.
[3]Department of Biosciences, University of Milan, Via Giovanni Celoria, 26, 20133, Milan, Italy.
[4]Institute of Cellular and Integrative Neurosciences CNRS UPR 3212 University of Strasbourg; 5 rue Blaise Pascal; 67084 Strasbourg, France.
[5]Department of Physiology and Pharmacology "Vittorio Erspamer" SAPIENZA University of Rome, P.le A. Moro 5 00185 Rome, Italy.

**[*]Corresponding author:**
Valentina Pallottini
Department of Science, Section of Biomedical Sciences and Technologies
University "Roma Tre"
Viale G. Marconi 446
00146 Rome, Italy
tel: +39-0657336320
fax: +39-0657336321
email: valentina.pallottini@uniroma3.it

**ABSTRACT**

Autism spectrum disorders (ASDs) present a wide range of symptoms characterized by altered sociability, compromised communication and stereotyped/repetitive behaviors. These symptoms are probably caused by developmental changes, but the mechanisms remain largely unknown. Several lines of evidence suggest an impairment of the cholesterol/isoprenoid metabolism in the brain as possible cause, but systematic analyses in rodent models of ASDs are lacking. Prenatal exposure to the antiepileptic drug valproate (VPA) is a risk factor for ASDs in humans, and the basis of a well-established rodent model for the disease. Here, we studied cholesterol/isoprenoid metabolism in different brain areas of rats prenatally exposed to VPA. We show that VPA-treated rats presenting autistic-like symptoms display alterations in key elements of the cholesterol/isoprenoid metabolism and a decreased number of hippocampal oligodendrocytes. Our data suggest a relation between brain cholesterol homeostasis and ASDs that open new therapeutic possibilities for these disorders.

**Key words**: Autism; cholesterol; 3-hydroxy 3-methylglutaryl Coenzyme A reductase; isoprenoid.

**Highlights**:

- Brain cholesterol metabolism is altered in prenatally VPA-exposed rats.
- Prenylation is altered mainly in cerebellum of prenatally VPA-exposed rats.
- Hippocampal olygodendrocytes are reduced in prenatally VPA-exposed rats.

## INTRODUCTION

Autism spectrum disorders (ASDs) are neurodevelopmental syndromes that present altered social interactions, compromised communication, repetitive behaviors, and comorbid features such as anxiety (Lai et al., 2014; Gillott and Standen, 2007). Currently, genetic factors, maternal stressors, infectious agents and drug intake during pregnancy are discussed as causes of ASDs (Dietert et al., 2011). In particular, prenatal exposure to valproic acid (VPA), an antiepileptic drug, induces autistic symptoms in children (Williams et al., 2001) and rodents, which are used as preclinical models of ASDs (Servadio et al., 2015; Servadio et al., 2016).

At present, the molecular mechanisms provoking ASDs are largely unknown. Some lines of evidence point to an imbalanced cholesterol/isoprenoid metabolism in the brain (Wang, 2014); (Ling and Tejada-Simon, 2016). Characteristic elements of autistic behavior occur in developmental diseases including Smith-Lemli-Opitz syndrome (SLOS) (Thurm et al., 2016) or Rett Syndrome (Segatto et al., 2014b). SLOS is an autosomal recessive disorder caused by a deficiency of the 7-dehydrocholesterol (7-DHC) reductase, one of the main cholesterol synthesizing enzyme (DeBarber et al., 2011). RETT syndrome is a severe neurodevelopmental disorder that affects almost exclusively females where mutations in the gene Methyl-CpG-binding protein 2 were identified as the cause of this pathology (Amir and Zoghbi, 2000). Notably, cholesterol supplementation in SLOS patients can attenuate their autistic symptoms (Aneja and Tierney, 2008). Moreover, an imbalance of cholesterol homeostasis has been demonstrated *in vivo*, in an animal model of Rett syndrome (Buchovecky et al., 2013), and *in vitro* using human fibroblasts obtained from Rett patients (Segatto et al., 2014b).

Interestingly, several candidate proteins, such as ionotropic and metabotropic receptors and transporters, whose dysfunction has been attributed to ASDs, are associated also with cholesterol-rich lipid rafts (Wang, 2014).

Cells need cholesterol and isoprenoid compounds to develop and function correctly (Martini and Pallottini, 2007; Trapani et al., 2011; Segatto et al., 2014a; Cartocci et al., 2016). This applies particularly to neurons in the central nervous system (CNS) that require large amounts of these components to form and maintain axons, dendrites and spines and to sustain the function of different membrane proteins like neurotransmitter receptors, ion channels and transporters (Mauch et al., 2001; Pfrieger, 2003; Dufour et al., 2006; Pfrieger and Ungerer, 2011; Mathews et al., 2014; Cartocci et al., 2016; Moutinho et al., 2017). Cells in the brain must regulate their cholesterol and isoprenoid levels independently, because the blood brain barrier (BBB) prevents the entry of lipoproteins into the brain parenchyma (Dietschy and Turley, 2004). Consequently, alterations in

brain cholesterol/isoprenoid homeostasis can perturb CNS development and function (Linetti et al., 2010; Wang, 2014; Segatto et al., 2014a).

To further elucidate connections between ASDs and cholesterol/isoprenoid metabolism, we studied the protein network controlling cholesterol/isoprenoid homeostasis in different brain areas of male rats prenatally exposed to VPA. This protein network comprises a large array of sensors, enzymes and transporters enabling a feedback-controlled balance of biosynthesis, uptake and release (Brown and Goldstein, 1999; Espenshade and Hughes, 2007). For example, precursors of cholesterol and isoprenoids are synthesized by the mevalonate (MVA) pathway. The activity of its key enzyme, 3-hydroxy 3-methylglutaryl Coenzyme A reductase (HMGCR) (Brown and Goldstein, 1980; Pallottini, 2015), is rapidly inhibited by phosphorylation *via* AMP-activated kinase (AMPK) (Pallottini et al., 2007) depending on the energetic status of the cell (Hardie, 2008; Hardie et al., 2016).

To capture developmental changes, we analyzed three different postnatal ages (infancy, adolescence, and adulthood). Our study reveals that VPA-exposed rats presenting autistic symptoms display alterations in key elements of the cholesterol/isoprenoid metabolism and a reduced amount of oligodendrocytes in hippocampus of adolescent rats. These data suggest a role of cholesterol homeostasis in ASDs, and may open new therapeutic possibilities for these disorders.

## EXPERIMENTAL PROCEDURES

### Animals

Female Wistar rats (Charles River), weighing 250 ± 15 g, were mated overnight. The morning when spermatozoa were found was designated as gestational day 1 (GD1). Pregnant rats were singly housed in Macrolon cages (40l x 26w x 20h cm), under controlled conditions (temperature 20–21°C, 55–65% relative humidity and 12/12h light cycle with lights on at 07:00 a.m.). Food (standard laboratory diet, VRF1 (P) diet, Special Diets Services, Charles River) and water were available *ad libitum*. On gestational day 12.5, females received a single intraperitoneal injection of either sodium valproate (VPA) or saline (SAL). Newborn litters found up to 5 p.m. were considered to be born on that day designated postnatal day (PND) 0. On PND 1, the litters were culled to eight animals (six males and two females), in order to reduce the litter size-induced variability in the growth and development of pups during the postnatal period. On PND 21, the pups were weaned and housed in groups of three. Experiments were carried out on the male offspring during infancy (PNDs 9-13), adolescence (PND 35), and adulthood (PND 90). The experiments were approved by the Italian Ministry of Health (Rome, Italy) and performed in agreement with the guidelines

released by the Italian Ministry of Health (D.L. 26/14) and the European Community Directive 2010/63/EU.

**Drugs**

VPA (Cayman) was dissolved in saline at a concentration of 250 mg/ml and administered intraperitoneally to pregnant rats at a dose (500 mg/kg) and time (GD 12.5) that have been shown to induce autistic-like behavioral changes in the offspring (Markram et al., 2008); (Servadio et al., 2016).

**Isolation-induced ultrasonic vocalizations (USVs)**

On PND 9, 12 male pups (6 SAL- and 6 VPA-exposed) were removed from the nest and individually placed into a Plexiglas arena (30l × 30w × 30h cm), located inside a sound-attenuating and temperature-controlled chamber, with a camera positioned above the arena. The USVs emitted by the pup were detected for 3 min by an ultrasound microphone (Avisoft Bioacoustics, Version 5.1) sensitive to frequencies between 10 and 200 kHz. Pup axillary temperature was measured before and after the test by a digital thermometer.

**Three-chamber test**

The apparatus consisted of a rectangular three-chamber box with two lateral chambers (30l × 35w × 35h cm) connected to a central chamber (15l × 35w × 35h cm). Each lateral chamber contained a small Plexiglas cylindrical cage. The test was performed as previously described (Moy et al., 2007); (Servadio et al., 2016). At PND 35 or 90, 12 male rats (6 SAL- and 6 VPA-exposed) were individually allowed to explore the apparatus for 10 min, and then confined to the central compartment. An unfamiliar stimulus animal was placed into the Plexiglas cage in one chamber of the apparatus, while the cage in the other chamber was left empty. Both doors to the side chambers were then opened, allowing the experimental animal to freely explore the apparatus for 10 min. The percent of time spent in social approach (sniffing the stimulus and the cage confining it) was scored using the Observer 3.0 software (Noldus Information Technology, The Netherlands).

**Elevated plus-maze**

The apparatus comprised two open and two closed arms (50 Large × 10Wide × 40 High cm) that extended from a common central platform (10L × 10W cm). At PND 35, 12 male rats (6 SAL- and 6 VPA-exposed) were individually placed on the central platform of the maze for 5 min. Each session was recorded with a camera positioned above the apparatus for subsequent behavioral

analysis performed using the Observer 3.0 software (Noldus Information Technology, The Netherlands). The following parameters were analyzed (Manduca et al., 2015): 1) the percentage of time spent in the open arms (% TO): (seconds spent on the open arms of the maze/seconds spent on the open + closed arms) x 100; 2) the percentage of open arm entries (% OE): (the number of entries into the open arms of the maze/number of entries into open + closed arms) x 100 and 3) the number of closed arm entries (Number of CE).

**Sample collection**

Infant (n=12, 6 SAL and 6 VPA), adolescent (n=12, 6 SAL and 6 VPA), and adult (n=12, 6 SAL and 6 VPA) rats were rapidly decapitated. Plasma was obtained from blood collected into EDTA (Ethylenediaminetetraacetic acid; 1 mg/ml blood), and the livers and the brains were quickly removed. For biochemical evaluations, the brains were cut into coronal slices on a cold plate, and amygdala (Amy), cerebellum (Cereb) prefrontal cortex (Cortex), hippocampus (Hippo), nucleus accumbens (Nac), and dorsal striatum (Str) were dissected under the stereo-microscope within 2 min. Tissues were then stored to -80°C until use (Trezza et al., 2012). For immunohistochemical analysis whole brains were rapidly frozen in 2-methylbutane and stored at -80 °C.

**Sample preparation for western blot analysis**

Total lysate of the livers or the different brain regions (Amy, Cereb, Cortex, Hippo, Nac and Str) were obtained by tissue homogenization in 1:10 and 1:5 w/v buffer, respectively containing 0.001 M Tris-HCl, 0.0001 M $CaCl_{2,}$ 0.15 M NaCl, and 0.001 M phenylmethylsulfonyl fluoride (PMSF) (pH 7.5), and Phosphatase inhibitor 1:1000 v/v (SigmaAldrich, Milano). Livers and brain samples were sonicated (VCX 130 PB, Sonics, Newtown,06470 CT) on ice, for 1 min. Successively, for both the tissues, an aliquot of homogenate was diluted 1:1 in sample buffer 2X (0.25M Tris-HCl PH 6.8, 20% SDS and 1:1000 protease inhibitor cocktail and 1:1000 phosphatase inhibitor cocktail (Sigma-Aldrich)) (Pallottini et al., 2008). These samples were utilized to analyze the following proteins: Hydroxy methylglutaryl Coenzyme A reductase (HMGCR), Phospho-Hydroxy methylglutaryl Coenzyme A reductase (P-HMGCR), Low Density Lipoprotein receptor (LDLr), Scavenger Receptor B1 (SR-B1), LDL related protein 1 (LRP1), AMP-activated kinase (AMPK), Phospho-AMP activated kinase (P-AMPK), and Myelin Basic Protein (MBP).

To evaluate the active fraction of prenylated proteins, cellular membranes were prepared as following: homogenates were centrifuged for 45 min at 100,000 g and the pellets containing the membrane fractions were solubilized by sonication in sample buffer 1X (0.125M pH 6.8, 10% SDS, 1:1000 v/v protease inhibitor cocktail, and 1:1000 v/v phosphatase inhibitor cocktail). Protein

concentration was measured by the method of Lowry (Lowry et al., 1951). Membrane and total lysate samples were boiled for 5 min before loading to the SDS-PAGE.

**Immunoblotting**

Proteins (15 μg) from total and membrane lysates were resolved by 7% SDS-PAGE for P-HMGCR 09-356 (1:1000) (Millipore, Temecula, CA), total HMGCR 07457 (1:1000) (Upstate,Lake Placid, NY), LDLr sc 11824 (1:1000) (Santa Cruz Biotechnology, Santa Cruz, CA), LRP1 sc 25462 (1:1000) (Santa Cruz Biotechnology), SR-B1 NB400-104 (1:1000) (Novus Biologicals, Milano, Italy), total AMPKα #2532 (1:1000) (Cell Signalling Technology, Boston, MA,USA), P-AMPKα #2535 (1:1000) (Cell Signalling Technology, Boston, MA,USA); 12% SDS-PAGE for RhoA sc 418 (1:1000) (Santa Cruz Biotechnology); Ras sc 53959 (1:1000) (Santa Cruz Biotechnology) and MBP sc 808 (1:1000) (Santa Cruz Biotechnology). Proteins were separated at 30 mA (constant current) for 120 min and blotted to nitrocellulose membranes (Trans-Blott Turbo, BioRad, Milano, Italy). Immunoblots were incubated with primary antibodies overnight and hrp-conjugated IgG produced in mouse, in rabbit or goat were used as secondary antibodies (1:10000) (Biorad). Immunoreactivity was detected by enhanced chemiluminescence (GE Healthcare, Little Chalfont, United Kingdom).

**Immunohistochemistry**

The staining was performed as described (Scuderi et al., 2014). Briefly, rats were perfused intracardially and brains were cut using a cryostat to obtain coronal sections containing the hippocampal regions. Slices (12 μm thickness) were post-fixed for 7 min in 4% paraformaldehyde prepared in 0.1M phosphate buffer solution (PBS) at +4°C. Non-specific antibody binding was minimized by incubating slices (placed in a humid chamber) with a blocking solution composed of bovine serum albumin (BSA) 0.5% in PBS/triton x-100 0,25% for 1 hour at room temperature. Then, slices were incubated overnight at +4°C in a humid chamber, with a mouse anti-Olig2 primary antibody sc 293163 (1:500) (Santa Cruz Biotechnology) prepared in the same blocking solution. The day after, sections were incubated with the proper rhodamine (TRITC)-coupled goat anti-mouse IgG (H+L) secondary antibody 115-025-003 (1:200) (Jackson ImmunoResearch) and with the nuclear stain Hoechst 33258 (1:5000) (Sigma-Aldrich) in blocking solution at room temperature. Then, sections were rinsed in PBS and slices mounted in Fluoromount medium F4680 (Sigma-Aldrich). Signals were detected using an epifluorescent microscope Eclipse E600 (Nikon). Pictures were captured in the stratum radiatum of CA1, CA2 and CA3, and in the hilus of the

dentate gyrus (DG) in the hippocampus by a QImaging camera with NISelements BR 3.2 64-bit software.

Experiments were performed three times; at least four slices from each animal were analysed. In particular, we used slices corresponding to plates 55–64 in the rat brain atlas (Paxinos and Watson, VI ed, 2007).

**Tissue and plasma lipid analysis**

Total cholesterol and high-density lipoproteins (HDL) were evaluated in plasma samples. Lipid analyses were performed by a Roche Clinical Chemistry instrument with commercial reagents (Roche Diagnostics, GmbH). To evaluate the amount of tissue cholesterol, 50 mg and 25 mg of liver and brain areas, respectively, were homogenized in chloroform:methanol:$H_2O$ 4:2:1 v/v. The mixture was vortexed for 2 min, left for 15 min at room temperature and spun-down (10 min at 600 g). The chloroform fraction was transferred, dried under nitrogen, dissolved in 40 µl isopropanol and subjected separated by thin layer chromatography (Silica Gel 60 Å 5X20, Whatman, Maidston, England; pre-activated at 100 °C for 60 min). Samples were developed in petroleum ether/ethyl ether/acetic acid (75:25:1 v/v) and lipid bands were visualized with iodine vapor and compared with cholesterol standard.

**Data analysis**

Behavioral experiments were scored and analyzed by a trained observer unaware of treatment conditions (Noldus Information Technology, The Netherlands). Images derived from immunoblotting, immunofluorescence and TLC were analyzed by ImageJ (National Institutes of Health, Bethesda, MD). Data are expressed as mean ± SD for all the experiments except for behavioral and immunofluorescence analyses where data are expressed as mean ± SEM. To assess the effects of the prenatal treatment (VPA or SAL) on the behavior of the offspring, data were analyzed by Student's t-tests. (GraphPad Instat3; GraphPad, Inc., La Jolla, CA). Cholesterol, triglyceride, and HDL contents of plasma and the analysis within the ages were performed by ANOVA followed by Tukey-Kramer test (GraphPad Instat3; GraphPad, Inc., La Jolla, CA).

**RESULTS**

In this work, we aimed to uncover alterations of cholesterol/isoprenoid homeostasis in the brain of infant, adolescent and adult rats prenatally exposed to VPA.

**Confirmation of autistic-like behavior**

We first ensured that VPA-exposed animals displayed autistic-like symptoms compared to control rats (Fig. 1). At infancy (PND 9), pups prenatally exposed to VPA emitted less USVs than control pups when separated from the dam and the siblings (Fig. 1a) indicating communicative deficits induced by prenatal VPA exposure. The elevated plus maze test revealed increased anxiety in VPA-exposed adolescent rats (PND 35) as indicated by decreased spent time in the open arms of the maze (Fig. 1b) and a decreased number of open arm entries (Fig. 1c) compared to SAL-exposed rats. The three-chamber test revealed decreased sociability in adolescent (Fig. 1d) and adult (PND90) (Fig. 1e) rats as indicated by decreased time spent sniffing the stimulus animal during test compared to SAL-exposed animals (Fig. 1e). However, the two groups did not differ in locomotor activity as shown by similar closed arm entries (data not shown).

**Analyses of peripheral cholesterol/isoprenoid metabolism**

Next, we studied the impact of VPA on peripheral cholesterol homeostasis (Fig. 2). Our analysis revealed that VPA exposure *per se* did not affect both total cholesterol and HDL levels in plasma (Fig. 2a and 2b). Measurements in the liver, which is the metabolic power plant of lipid homeostasis (Trapani et al., 2012), showed a mild perturbation of proteins ensuring cholesterol homeostasis (Fig. 2 c-d-e-f) and of cholesterol content (Fig. 2g) only in the VPA-exposed infant rats (PND 13), but no changes at older ages. Thus, prenatal VPA exposure altered hepatic cholesterol metabolism only transiently and left plasma levels unaffected.

**Analyses of cholesterol/isoprenoid homeostasis in different brain areas**

We next studied the protein network ensuring cholesterol/isoprenoid homeostasis in several brain areas (Amy, Cereb, Cortex, Hippo, Nac, and Str) that are known to be involved in autism (Dichter et al., 2010; Donovan and Basson, 2017; Reim et al., 2017; Wu et al., 2017) (Fig. 2). Firstly, HMGCR and LDLr protein levels were measured in each brain region, since they are key components of cellular cholesterol homeostasis. Prenatal VPA exposure reduced HMGCR levels in the Cortex and the Nac of infant and adolescent rats, respectively, whereas all other brain areas were unaffected (Fig. 3a). LDLr (Fig 3b) was significantly reduced in Nac at all ages tested, decreased in the Str of infant rats and enhanced in the Cortex of adult animals. The fact that HMGCR content appeared largely unaffected by VPA does not exclude changes in enzyme activity, which is controlled at the posttranslational level by phosphorylation. Therefore, we investigated next the phosphorylation status of HMGCR. Our data revealed that prenatal VPA induced region- and age-dependent changes in the ratio of P-HMGCR to total enzyme levels (Fig. 3c). The Cortex, for example, showed an age-dependent reversal of the VPA effect: whereas in young mice, the P-

HMGCR/HMGCR ratio was reduced thereby increasing activity, adult mice showed the opposite effect. Interestingly, prenatal VPA exposure had the strongest impact on adolescent rats, where the ratio was altered in 5 out of 6 brain areas. To further explore these changes, we measured the activation state (phosphorylation) of AMPK, this kinase phosphorylates and thereby deactivates HMGCR. Our immunoblots revealed that VPA affected the phosphorylation state of AMPK in a manner that was highly correlated with the phosphorylation state of HMGCR (Fig 3d). These results suggested that VPA affected HMGCR activity via a signaling cascade involving AMPK rather than at the transcriptional level. This is further supported by the fact that changes in HMGCR and LDLr were not correlated, although the transcription of both components is controlled by a common transcription factor, the Sterol Regulatory Element Binding Protein 2 (SREBP2). To complete the picture, we also measured the levels of two lipoprotein receptors, LRP1 and SR-B1, which mediate the cellular trafficking of cholesterol which are not directly regulated by the SREBP2 pathway (Cartocci et al., 2016). Our data show that VPA affected LRP1 levels in each brain area tested, but with distinct age-dependent patterns. Whereas levels in Amy were enhanced in infant rats and decreased in adult mice, the levels in the cortex showed exactly the opposite changes (Fig. 4a). SR-B1 was altered in all areas in an age-dependent manner except for Cortex and the Nac (Fig. 4b). Together, these results indicated highly region- and age-specific effects of VPA on the different components of cholesterol/isoprenoid homeostasis. The good correlation between phosphorylation states of HMGCR and AMPK levels suggests that VPA induces AMPK-mediated changes in HMGCR activity in all regions of adolescent rats except for hippocampus. Among the lipoprotein receptors, LRP1 levels were particularly strongly affected by VPA in a region- and age-dependent manner.

**Analyses of HMGCR products in brain regions of adolescent rats**

To test whether the VPA-induced alterations of HMGCR activity impacted the levels of its products, we analyzed cholesterol content in brain regions of adolescent rats using quantitative thin-layer chromatography. As shown in Fig. 5a, we found that prenatal VPA exposure induced a significant reduction of cholesterol in the Hippo, but not in any other region tested. In parallel, we studied the impact of VPA on the levels of geranylgeranyl and farnesyl. As an indirect measure, we determined the levels of membrane-attached RhoA and Ras comparing them to the amount of the proteins in the total lysate. Post-translational attachment of geranylgeranyl and farnesyl residues to these proteins induces their transition to the plasma membrane. Prenatal VPA exposure strongly increased and decreased the level of membrane-attached RhoA (Fig. 5b) and Ras (Fig. 5c) in the Cereb and Nac, respectively. Moreover, the content of membrane-bound Ras was reduced in the

Str. Interestingly, the total protein content didn't change except for the Nac in which an increase of the total RhoA and Ras was observed, probably due to a compensatory action of the tissue.

**Analyses of oligodendrocyte-mediated myelination in the hippocampus**

Prenatal VPA exposure markedly reduced the level of cholesterol in the hippocampus of adolescent rats. Since most cholesterol in the brain is contained in myelin, we studied next whether VPA reduced the myelin content in the Hippo using myelin basic protein (MBP) as marker. As shown in Fig. 6a, VPA reduced MBP levels. The reduction of myelin content could have several causes. Based on published evidence that VPA inhibits differentiation of oligodendrocytes (Shen et al., 2008), we investigated the density of oligodendrocytes in the Hippo. Immunohistochemical staining for Olig2, an oligodendrocyte-specific transcription factor, revealed a VPA-induced reduction of Olig2 immunopositive ($Olig2^{+}$) cells in the CA1 and CA2 areas of the Hippo (Fig. 6b, c and d) indicating that reduction of myelin is caused by a VPA-induced inhibition of oligodendrocyte formation.

**Discussion**

Our results reveal that prenatal exposure to VPA provokes long-lasting region- and age-specific changes in brain cholesterol/isoprenoid homeostasis and thereby support the hypothesis that autistic-like symptoms could be caused by alterations in cholesterol/isoprenoid metabolism in the brain (Wang, 2014; Cartocci et al., 2017).

Our findings clearly underline that cholesterol homeostasis in the brain is vulnerable to pharmacologic manipulations. Whereas the hepatic cholesterol metabolism was only transiently perturbed by prenatal VPA exposure, the brain showed a wide array of changes that occurred immediately or with delays of several weeks, that differed among brain regions and that occasionally reverted within a given brain area. This complex reaction indicates, as previously suggested (Segatto et al., 2011; Segatto et al., 2013), that cholesterol/isoprenoid metabolism is differently regulated in brain areas and supports recent findings that prenatal VPA exposure provokes region-and gene-specific reactions (Lauber et al., 2016). These regional differences may be due to region-specific cellular composition namely the neuron/glia ratio, metabolic turnover and activity pattern. The levels of HMGCR and LDLr remained remarkably stable except for small changes that were surprisingly incongruent. Under normal conditions, both components are controlled by the SREBP2 pathway, which tightly regulates cholesterol levels in cells. In case of a deficit, HMGCR and LDLr are upregulated to increase synthesis and uptake. The divergent changes induced by VPA argue against a robust activation of the SREBP2 pathway and suggest that

different post-transcriptional regulation can be present, such as diverse mRNA stability as already demonstrated (Pallottini et al., 2006).

Our study reveals that VPA affects the activation state of HMGCR as implied by changing levels of the phosphorylated form. In particular, during adolescence, prenatal VPA altered HMGCR activity in five out of six brain areas. This includes an increase in Cereb, Cortex, and Strand a decrease in Amy and Nac. No changes were observed in the Hippo. The strong correlation between HMGCR activation state and the AMPK phosphorylation indicate that VPA acts via the AMPK-dependent pathway on cholesterol/isoprenoid metabolism. This is in line with previous evidence that VPA activates the kinase (Avery and Bumpus, 2014);(Ji et al., 2015). However, in our experimental model AMPK was differently modulated in each brain area. Possible reasons are the involvement of other factors or regional differences in cell composition. In line with this observation we previously demonstrated that each brain area responds differently to the same stimulus: as an example, rat Hippo and Cortex differently react to estradiol stimulation regarding HMGCR and LDLr expression (Segatto et al., 2011).

Our study revealed a strong impact of VPA on the membrane-associated fractions of Ras and RhoA and again, the direction of VPA-induced changes differed among brain regions. Their levels increased in the Cereb, but decreased in the Nac. In the case of the Cereb, it is likely that the change occurred in granule cells, as these cells represent the main cell type in this brain area. The functional impact of these changes remains unclear: small G proteins mediate a large number of cellular processes: an increase in prenylated Ras can impair long-term potentiation and has been associated with cognitive impairment (Hottman and Li, 2014; Mainberger et al., 2016). The increase in prenylated RhoA could alter proper neurite outgrowth and synaptic plasticity (Cartocci et al., 2016). Both proteins can be anchored at the membrane after posttranslational attachment of prenyl residues, whose availability is controlled by HMGCR activity. Moreover, prenylated proteins have important roles in neuronal development and plasticity (Homberg et al., 2016).Our analysis of adolescent rats revealed that prenatal VPA exposure decreased the cholesterol and myelin content in the Hippo, whereas HMGCR was not activated. This reduction was probably due to a reduced number of oligodendrocytes. This observation is in line with published evidence that VPA inhibits the differentiation of oligodendrocytes (Dehghan et al., 2016);(Pazhoohan et al., 2014);(Ye et al., 2009). VPA is an inhibitor of Histone Deacetylases (HDACs), and it has been demonstrated that inhibition of HDACs decreases myelination and Schwann cell differentiation in the peripheral nervous system (Jacob et al., 2011); (Brugger et al., 2017), it might induce epigenetic (long lasting) reprogramming, influencing cell types such as oligodendrocytes that are not even born at the time of injection (Bianchi et al., 2012). Our results reveal selective effects in the CA1

and CA2 regions of the hippocampus explaining the decrease of cholesterol in the same areas (Caporali et al., 2016);(Berghoff et al., 2017). At present, we cannot exclude, however, that the cholesterol content of neurons was reduced as well. This could impair their development and function, in particular at the level of synapses as well as could impact on neuronal survival (Mauch et al., 2001, Shrivastava et al., 2010);(Saxena and Chattopadhyay, 2012);(Jafurulla et al., 2014). In this regard, in a recent paper, Wu and colleagues demonstrated that FTY720, an immunosuppressor used for treatment of multiple sclerosis, rescues VPA-induced autistic behavior exerting a direct protection of neuron survival (Wu et al., 2017). Very interestingly, this drug is also able to reduce cholesterol content in human fibroblasts as recently demonstrated by Newton and colleague (Newton et al., 2017), so suggesting that cholesterol modulation could be really involved in ASDs, but further studies on specific cellular types in specific brain areas should necessarily be performed.

## CONCLUSIONS

Overall, our results demonstrate that brain cholesterol/isoprenoid metabolism is altered in a preclinical model of ASDs, and suggest that this alteration may impact the differentiation and function of neurons and oligodendrocytes. These findings set the basis for future studies to validate the implication of cholesterol/isoprenoid homeostasis in ASDs using different experimental models and to identify potential drug-based therapeutic approaches.

**Authors declare no conflict of interest**


## Acknowledgements

Supported by CAL Roma Tre University (V.P.) and by Netherlands Organization for Scientific Research (NWO) Veni grant 91611052 (V.T.), Marie Curie Career Reintegration Grant PCIG09-GA-2011-293589 (V.T.), FIRB Futuro in Ricerca grant RBFR10XKHS_001 (V.T.) and SAPIENZA University Grant C26A15X58E (C.S.).


## References


Amir RE, Zoghbi HY (Rett syndrome: methyl-CpG-binding protein 2 mutations and phenotype-genotype correlations. Am J Med Genet 97:147-152.2000).

Aneja A, Tierney E (Autism: the role of cholesterol in treatment. Int Rev Psychiatry 20:165-170.2008).

Avery LB, Bumpus NN (Valproic acid is a novel activator of AMP-activated protein kinase and decreases liver mass, hepatic fat accumulation, and serum glucose in obese mice. Mol Pharmacol 85:1-10.2014).

Berghoff SA, Gerndt N, Winchenbach J, Stumpf SK, Hosang L, Odoardi F, Ruhwedel T, Bohler C, Barrette B, Stassart R, Liebetanz D, Dibaj P, Mobius W, Edgar JM, Saher G (Dietary cholesterol promotes repair of demyelinated lesions in the adult brain. Nat Commun 8:14241.2017).

Bianchi MG, Franchi-Gazzola R, Reia L, Allegri M, Uggeri J, Chiu M, Sala R, Bussolati O (Valproic acid induces the glutamate transporter excitatory amino acid transporter-3 in human oligodendroglioma cells. Neuroscience 227:260-270.2012).

Brown MS, Goldstein JL (Multivalent feedback regulation of HMG CoA reductase, a control mechanism coordinating isoprenoid synthesis and cell growth. J Lipid Res 21:505-517.1980).

Brown MS, Goldstein JL (A proteolytic pathway that controls the cholesterol content of membranes, cells, and blood. Proc Natl Acad Sci U S A 96:11041-11048.1999).

Brugger V, Duman M, Bochud M, Munger E, Heller M, Ruff S, Jacob C (Delaying histone deacetylase response to injury accelerates conversion into repair Schwann cells and nerve regeneration. Nat Commun 8:14272.2017).

Buchovecky CM, Turley SD, Brown HM, Kyle SM, McDonald JG, Liu B, Pieper AA, Huang W, Katz DM, Russell DW, Shendure J, Justice MJ (A suppressor screen in Mecp2 mutant mice implicates cholesterol metabolism in Rett syndrome. Nat Genet 45:1013-1020.2013).

Caporali P, Bruno F, Palladino G, Dragotto J, Petrosini L, Mangia F, Erickson RP, Canterini S, Fiorenza MT (Developmental delay in motor skill acquisition in Niemann-Pick C1 mice reveals abnormal cerebellar morphogenesis. Acta Neuropathol Commun 4:94.2016).

Cartocci V, Segatto M, Di Tunno I, Leone S, Pfrieger FW, Pallottini V (Modulation of the Isoprenoid/Cholesterol Biosynthetic Pathway During Neuronal Differentiation In Vitro. J Cell Biochem 117:2036-2044.2016).

Cartocci V, Servadio M, Trezza V, Pallottini V (Can Cholesterol Metabolism Modulation Affect Brain Function and Behavior? J Cell Physiol.2017).

DeBarber AE, Eroglu Y, Merkens LS, Pappu AS, Steiner RD (Smith-Lemli-Opitz syndrome. Expert Rev Mol Med 13:e24.2011).

Dehghan S, Hesaraki M, Soleimani M, Mirnajafi-Zadeh J, Fathollahi Y, Javan M (Oct4 transcription factor in conjunction with valproic acid accelerates myelin repair in demyelinated optic chiasm in mice. Neuroscience 318:178-189.2016).

Dichter GS, Felder JN, Green SR, Rittenberg AM, Sasson NJ, Bodfish JW (Reward circuitry function in autism spectrum disorders. Soc Cogn Affect Neurosci 7:160-172.2010).

Dietert RR, Dietert JM, Dewitt JC (Environmental risk factors for autism. Emerg Health Threats J 4:7111.2011).

Dietschy JM, Turley SD (Thematic review series: brain Lipids. Cholesterol metabolism in the central nervous system during early development and in the mature animal. J Lipid Res 45:1375-1397.2004).

Donovan AP, Basson MA (The neuroanatomy of autism - a developmental perspective. J Anat 230:4-15.2017).

Dufour F, Liu QY, Gusev P, Alkon D, Atzori M (Cholesterol-enriched diet affects spatial learning and synaptic function in hippocampal synapses. Brain Res 1103:88-98.2006).

Espenshade PJ, Hughes AL (Regulation of sterol synthesis in eukaryotes. Annu Rev Genet 41:401-427.2007).

Gillott A, Standen PJ (Levels of anxiety and sources of stress in adults with autism. J Intellect Disabil 11:359-370.2007).

Hardie DG (AMPK: a key regulator of energy balance in the single cell and the whole organism. Int J Obes (Lond) 32 Suppl 4:S7-12.2008).

Hardie DG, Ross FA, Hawley SA (AMPK: a nutrient and energy sensor that maintains energy homeostasis. Nat Rev Mol Cell Biol 13:251-262.2016).

Homberg JR, Kyzar EJ, Nguyen M, Norton WH, Pittman J, Poudel MK, Gaikwad S, Nakamura S, Koshiba M, Yamanouchi H, Scattoni ML, Ullman JF, Diamond DM, Kaluyeva AA, Parker MO, Klimenko VM, Apryatin SA, Brown RE, Song C, Gainetdinov RR, Gottesman, II, Kalueff AV (Understanding autism and other neurodevelopmental disorders through experimental translational neurobehavioral models. Neurosci Biobehav Rev 65:292-312.2016).

Hottman DA, Li L (Protein prenylation and synaptic plasticity: implications for Alzheimer's disease. Mol Neurobiol 50:177-185.2014).

Jacob C, Christen CN, Pereira JA, Somandin C, Baggiolini A, Lotscher P, Ozcelik M, Tricaud N, Meijer D, Yamaguchi T, Matthias P, Suter U (HDAC1 and HDAC2 control the transcriptional program of myelination and the survival of Schwann cells. Nat Neurosci 14:429-436.2011).

Jafurulla M, Rao BD, Sreedevi S, Ruysschaert JM, Covey DF, Chattopadhyay A (Stereospecific requirement of cholesterol in the function of the serotonin1A receptor. Biochim Biophys Acta 1838:158-163.2014).

Ji MM, Wang L, Zhan Q, Xue W, Zhao Y, Zhao X, Xu PP, Shen Y, Liu H, Janin A, Cheng S, Zhao WL (Induction of autophagy by valproic acid enhanced lymphoma cell chemosensitivity through HDAC-independent and IP3-mediated PRKAA activation. Autophagy 11:2160-2171.2015).

Lai MC, Lombardo MV, Baron-Cohen S (Autism. Lancet 383:896-910.2014).

Lauber E, Filice F, Schwaller B (Prenatal Valproate Exposure Differentially Affects Parvalbumin-Expressing Neurons and Related Circuits in the Cortex and Striatum of Mice. Front Mol Neurosci 9:150.2016).

Linetti A, Fratangeli A, Taverna E, Valnegri P, Francolini M, Cappello V, Matteoli M, Passafaro M, Rosa P (Cholesterol reduction impairs exocytosis of synaptic vesicles. J Cell Sci 123:595-605.2010).

Ling Q, Tejada-Simon MV (Statins and the brain: New perspective for old drugs. Prog Neuropsychopharmacol Biol Psychiatry 66:80-86.2016).

Lowry OH, Rosebrough NJ, Farr AL, Randall RJ (Protein measurement with the Folin phenol reagent. J Biol Chem 193:265-275.1951).

Mainberger F, Langer S, Mall V, Jung NH (Impaired synaptic plasticity in RASopathies: a mini-review. J Neural Transm (Vienna) 123:1133-1138.2016).

Manduca A, Morena M, Campolongo P, Servadio M, Palmery M, Trabace L, Hill MN, Vanderschuren LJ, Cuomo V, Trezza V (Distinct roles of the endocannabinoids anandamide and 2-arachidonoylglycerol in social behavior and emotionality at different developmental ages in rats. Eur Neuropsychopharmacol 25:1362-1374.2015).

Markram K, Rinaldi T, La Mendola D, Sandi C, Markram H (Abnormal fear conditioning and amygdala processing in an animal model of autism. Neuropsychopharmacology 33:901-912.2008).

Martini C, Pallottini V (Cholesterol: from feeding to gene regulation. Genes Nutr 2:181-193.2007).

Mathews ES, Mawdsley DJ, Walker M, Hines JH, Pozzoli M, Appel B (Mutation of 3-hydroxy-3-methylglutaryl CoA synthase I reveals requirements for isoprenoid and cholesterol synthesis in oligodendrocyte migration arrest, axon wrapping, and myelin gene expression. J Neurosci 34:3402-3412.2014).

Mauch DH, Nagler K, Schumacher S, Goritz C, Muller EC, Otto A, Pfrieger FW (CNS synaptogenesis promoted by glia-derived cholesterol. Science 294:1354-1357.2001).

Moutinho M, Nunes MJ, Rodrigues E (The mevalonate pathway in neurons: It's not just about cholesterol. Exp Cell Res.2017).

Moy SS, Nadler JJ, Young NB, Perez A, Holloway LP, Barbaro RP, Barbaro JR, Wilson LM, Threadgill DW, Lauder JM, Magnuson TR, Crawley JN (Mouse behavioral tasks relevant to autism: phenotypes of 10 inbred strains. Behav Brain Res 176:4-20.2007).

Newton J, Hait NC, Maceyka M, Colaco A, Maczis M, Wassif CA, Cougnoux A, Porter FD, Milstien S, Platt N, Platt FM, Spiegel S (FTY720/fingolimod increases NPC1 and NPC2 expression and reduces cholesterol and sphingolipid accumulation in Niemann-Pick type C mutant fibroblasts. FASEB J 31:1719-1730.2017).

Pallottini V (3-Hydroxy-3-methylglutaryl-coenzyme A reductase modulator: toward age- and sex-personalized medicine. Expert Opin Ther Pat 1-5.2015).

Pallottini V, Guantario B, Martini C, Totta P, Filippi I, Carraro F, Trentalance A (Regulation of HMG-CoA reductase expression by hypoxia. J Cell Biochem 104:701-709.2008).

Pallottini V, Martini C, Cavallini G, Bergamini E, Mustard KJ, Hardie DG, Trentalance A (Age-related HMG-CoA reductase deregulation depends on ROS-induced p38 activation. Mech Ageing Dev 128:688-695.2007).

Pallottini V, Martini C, Cavallini G, Donati A, Bergamini E, Notarnicola M, Caruso MG, Trentalance A (Modified HMG-CoA reductase and LDLr regulation is deeply involved in age-related hypercholesterolemia. J Cell Biochem 98:1044-1053.2006).

Pazhoohan S, Satarian L, Asghari AA, Salimi M, Kiani S, Mani AR, Javan M (Valproic Acid attenuates disease symptoms and increases endogenous myelin repair by recruiting neural stem cells and oligodendrocyte progenitors in experimental autoimmune encephalomyelitis. Neurodegener Dis 13:45-52.2014).

Pfrieger FW (Role of cholesterol in synapse formation and function. Biochim Biophys Acta 1610:271-280.2003).

Pfrieger FW, Ungerer N (Cholesterol metabolism in neurons and astrocytes. Prog Lipid Res 50:357-371.2011).

Reim D, Distler U, Halbedl S, Verpelli C, Sala C, Bockmann J, Tenzer S, Boeckers TM, Schmeisser MJ (Proteomic Analysis of Post-synaptic Density Fractions from Shank3 Mutant Mice Reveals Brain Region Specific Changes Relevant to Autism Spectrum Disorder. Front Mol Neurosci 10:26.2017).

Saxena R, Chattopadhyay A (Membrane cholesterol stabilizes the human serotonin(1A) receptor. Biochim Biophys Acta 1818:2936-2942.2012).

Scuderi C, Stecca C, Valenza M, Ratano P, Bronzuoli MR, Bartoli S, Steardo L, Pompili E, Fumagalli L, Campolongo P (Palmitoylethanolamide controls reactive gliosis and exerts neuroprotective functions in a rat model of Alzheimer's disease. Cell Death Dis 5:e1419.2014).

Segatto M, Di Giovanni A, Marino M, Pallottini V (Analysis of the protein network of cholesterol homeostasis in different brain regions: an age and sex dependent perspective. J Cell Physiol 228:1561-1567.2013).

Segatto M, Leboffe L, Trapani L, Pallottini V (Cholesterol homeostasis failure in the brain: implications for synaptic dysfunction and cognitive decline. Curr Med Chem 21:2788-2802.2014a).

Segatto M, Trapani L, Di Tunno I, Sticozzi C, Valacchi G, Hayek J, Pallottini V (Cholesterol metabolism is altered in Rett syndrome: a study on plasma and primary cultured fibroblasts derived from patients. PLoS One 9:e104834.2014b).

Segatto M, Trapani L, Marino M, Pallottini V (Age- and sex-related differences in extra-hepatic low-density lipoprotein receptor. J Cell Physiol 226:2610-2616.2011).

Servadio M, Melancia F, Manduca A, di Masi A, Schiavi S, Cartocci V, Pallottini V, Campolongo P, Ascenzi P, Trezza V (Targeting anandamide metabolism rescues core and associated

autistic-like symptoms in rats prenatally exposed to valproic acid. . Translational Psychiatry.2016).

Servadio M, Vanderschuren LJ, Trezza V (Modeling autism-relevant behavioral phenotypes in rats and mice: Do 'autistic' rodents exist? Behav Pharmacol 26:522-540.2015).

Shen S, Sandoval J, Swiss VA, Li J, Dupree J, Franklin RJ, Casaccia-Bonnefil P (Age-dependent epigenetic control of differentiation inhibitors is critical for remyelination efficiency. Nat Neurosci 11:1024-1034.2008).

Shrivastava S, Pucadyil TJ, Paila YD, Ganguly S, Chattopadhyay A (Chronic cholesterol depletion using statin impairs the function and dynamics of human serotonin(1A) receptors. Biochemistry 49:5426-5435.2010).

Thurm A, Tierney E, Farmer C, Albert P, Joseph L, Swedo S, Bianconi S, Bukelis I, Wheeler C, Sarphare G, Lanham D, Wassif CA, Porter FD (Development, behavior, and biomarker characterization of Smith-Lemli-Opitz syndrome: an update. J Neurodev Disord 8:12.2016).

Trapani L, Segatto M, Ascenzi P, Pallottini V (Potential role of nonstatin cholesterol lowering agents. IUBMB Life 63:964-971.2011).

Trapani L, Segatto M, Pallottini V (Regulation and deregulation of cholesterol homeostasis: The liver as a metabolic "power station". World J Hepatol 4:184-190.2012).

Trezza V, Damsteegt R, Manduca A, Petrosino S, Van Kerkhof LW, Pasterkamp RJ, Zhou Y, Campolongo P, Cuomo V, Di Marzo V, Vanderschuren LJ (Endocannabinoids in amygdala and nucleus accumbens mediate social play reward in adolescent rats. J Neurosci 32:14899-14908.2012).

Wang H (Lipid rafts: a signaling platform linking cholesterol metabolism to synaptic deficits in autism spectrum disorders. Front Behav Neurosci 8:104.2014).

Williams G, King J, Cunningham M, Stephan M, Kerr B, Hersh JH (Fetal valproate syndrome and autism: additional evidence of an association. Dev Med Child Neurol 43:202-206.2001).

Wu H, Wang X, Gao J, Liang S, Hao Y, Sun C, Xia W, Cao Y, Wu L (Fingolimod (FTY720) attenuates social deficits, learning and memory impairments, neuronal loss and neuroinflammation in the rat model of autism. Life Sci 173:43-54.2017).

Ye F, Chen Y, Hoang T, Montgomery RL, Zhao XH, Bu H, Hu T, Taketo MM, van Es JH, Clevers H, Hsieh J, Bassel-Duby R, Olson EN, Lu QR (HDAC1 and HDAC2 regulate oligodendrocyte differentiation by disrupting the beta-catenin-TCF interaction. Nat Neurosci 12:829-838.2009).

**Figure 1. Behavioral tests in infant, adolescent, and adult rats prenatally exposed to VPA.** Behavioral results obtained in infant rats (PND 9) tested in the isolation-induced USV test (**a)**, in adolescent rats (PND 35) tested in the elevated plus-maze test (**b**-**c**), and in adolescent and adult (PND 90) rats tested in the three-chamber test (**d-e**).

**Figure 2. Peripheral cholesterol metabolism in infant, adolescent, and adult rats prenatally exposed to VPA.** Levels of both plasma cholesterol and plasma HDL in infant, adolescent and adult rats respectively (**a**-**b**). The following four panels show the densitometric analysis (left) and a typical Western blots (right) of HMGCR phosphorylation state (**c**), and the protein levels of LDLr (**d**), LRP1 (**e**), and SR-B1 (**f**). The densitometric analysis of Western blot is expressed as fold of change of VPA treated versus SAL treated (1 value) rats. Panel **g** illustrates the densitometric analysis and a typical TLC of cholesterol contents in livers of infant (PND 13) rats. The data are expressed as means ± SD of the arbitrary units obtained analyzing bands (from Western blots or TLC, for details see the main text) using the software ImageJ. The densitometric analysis are the mean of the results obtained from 6 different animals performed in duplicate. b $P<0.01$ vs SAL, c $P<0.001$ vs SAL as from a Student's t test. ***$P<0.001$ as from ANOVA followed by Tukey-Kramer test (GraphPad Instat3; GraphPad, Inc., La Jolla, CA).

**Figure 3. Proteins involved in cholesterol/isoprenoid homeostasis in the brain of infant, adolescent, and adult rats prenatally exposed to VPA or SAL.** Densitometric analysis (left) and typical Western blot (right) of total HMGCR (**a**), LDLr (**b**), HMGCR phosphorylation state (**c)** and AMPK phospholylation state (**d**) in indicated brain regions of infant (PND 13), adolescent (PND 35) and adult (PND 90) rats prenatally exposed to VPA or SAL. Western blot analysis shows proteins levels in SAL and VPA rats,. The densitometric analysis of Western blot is expressed as fold of change of VPA treated versus SAL treated (1 value) rats. The data are expressed as means ± SD of the arbitrary units obtained analyzing bands (from Western blots, for details see the main text) using the software ImageJ. The densitometric analysis are the mean of the results obtained from 6 different animals performed in duplicate. a=$P<0.05$ vs SAL; b=$P<0.01$ vs SAL; c=$P<0.001$ vs SAL as from a Student's t test; *$P<0.05$ **$P<0.01$ ***$P<0.001$ as from ANOVA followed by Tukey-Kramer test (GraphPad Instat3; GraphPad, Inc., La Jolla, CA).

**Figure 4. Receptors involved in cholesterol/isoprenoid homeostasis in the brain of infant, adolescent and adult rats prenatally exposed to VPA or SAL.** LRP1 (**a**) and SR-B1 (**b**) expression in indicated brain regions of infant (PND 13), adolescent (PND 35) and adult (PND 90)

rats prenatally exposed to VPA or SAL. Western blot analysis shows proteins levels in SAL and VPA rats. The densitometric analysis of Western blot is expressed as fold of change of VPA treated versus SAL treated (1 value) rats. The data are expressed as means ± SD of the arbitrary units obtained analyzing bands (from Western blots, for details see the main text) using the software ImageJ. The densitometric analysis are the mean of the results obtained from 6 different animals performed in duplicate. a=P<0.05 vs SAL; b=P<0.01 vs SAL; c=P<0.001 vs SAL as from a Student's t test; ***P<0.001 as from ANOVA followed by Tukey-Kramer test (GraphPad Instat3; GraphPad, Inc., La Jolla, CA).

**Figure 5. Cholesterol and expression levels of membrane-bound Ras and RhoA in different brain areas of VPA- or SAL-exposed adolescent (PND 35) rats.** Densitometric analysis (left) and a typical TLC (right) of cholesterol content (**a**) in different brain areas of VPA- or SAL-exposed adolescent (PND 35) rats. The following panels show the densitometric analysis (left) and a typical Western blot (right) of RhoA total lysate and membrane content (**b**) and the Ras total lysate and membrane content (**c**) in indicated brain region of SAL and VPA exposed adolescent rats (PND 35). The densitometric analysis of Western blot is expressed as fold of change of VPA treated versus SAL treated (1 value) rats. For details see the main text. The data are expressed as means ± SD of the arbitrary units obtained analyzing the bands using the software ImageJ. The densitometric analysis are the mean of the results obtained from 6 different animals performed in duplicate. **P<0.01 and ***P<0.001 as from a Student's t test vs SAL (1 value).

**Figure 6. MBP protein content and oligodendrocytes immunofluorescence in hippocampi of VPA- or SAL-exposed adolescent (PND 35) rats.** Densitometric analysis (left) and a typical Western blot (right) of MBP content (**a)** in the hippocampus of VPA- or SAL-exposed adolescent rats (PND 35). For details see the main text. (b) Exemplifying photomicrograph of the entire hippocampus which shows the sub-regions analyzed (magnification 4X). (c) Representative fluorescent photomicrographs of Olig2 (red) staining performed in the stratum radiatum of CA1, CA2, CA3, and in the hilus of the DG regions of hippocampi of SAL- and VPA-exposed PND35 rats (magnification 20X). (d) Cell count analysis expressed as $Olig2^+$ cells/$4\times10^4$ $\mu m^2$. Nuclei were stained with Hoechst (blue). The data are expressed as means ± SD for Western blot experiments, and means ± SEM for immunofluorescence experiments. Images were analyzed using the software ImageJ. The densitometric analyses are the mean of the results obtained from 6 different animals performed in duplicate. The cell count analysis is representative of three different experiments performed in quadruplicate. *P<0.05 vs SAL; **P<0.01 vs SAL as from a Student's t test.

Figure 1

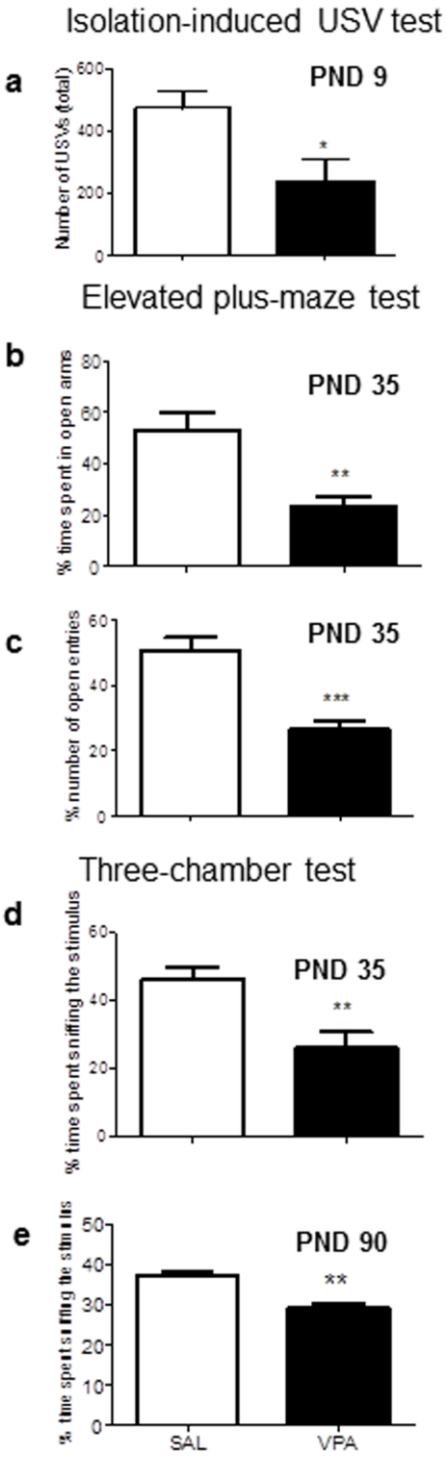
Isolation-induced USV test
a
PND 9
Number of USVs (total)
600
400
200
0
*
Elevated plus-maze test
b
PND 35
% time spent in open arms
80
60
40
20
0
**
c
PND 35
% number of open entries
60
40
20
0
***
Three-chamber test
d
PND 35
% time spent sniffing the stimulus
60
40
20
0
**
e
PND 90
% time spent sniffing the stimulus
50
40
30
20
10
0
**
SAL
VPA

Figure 2

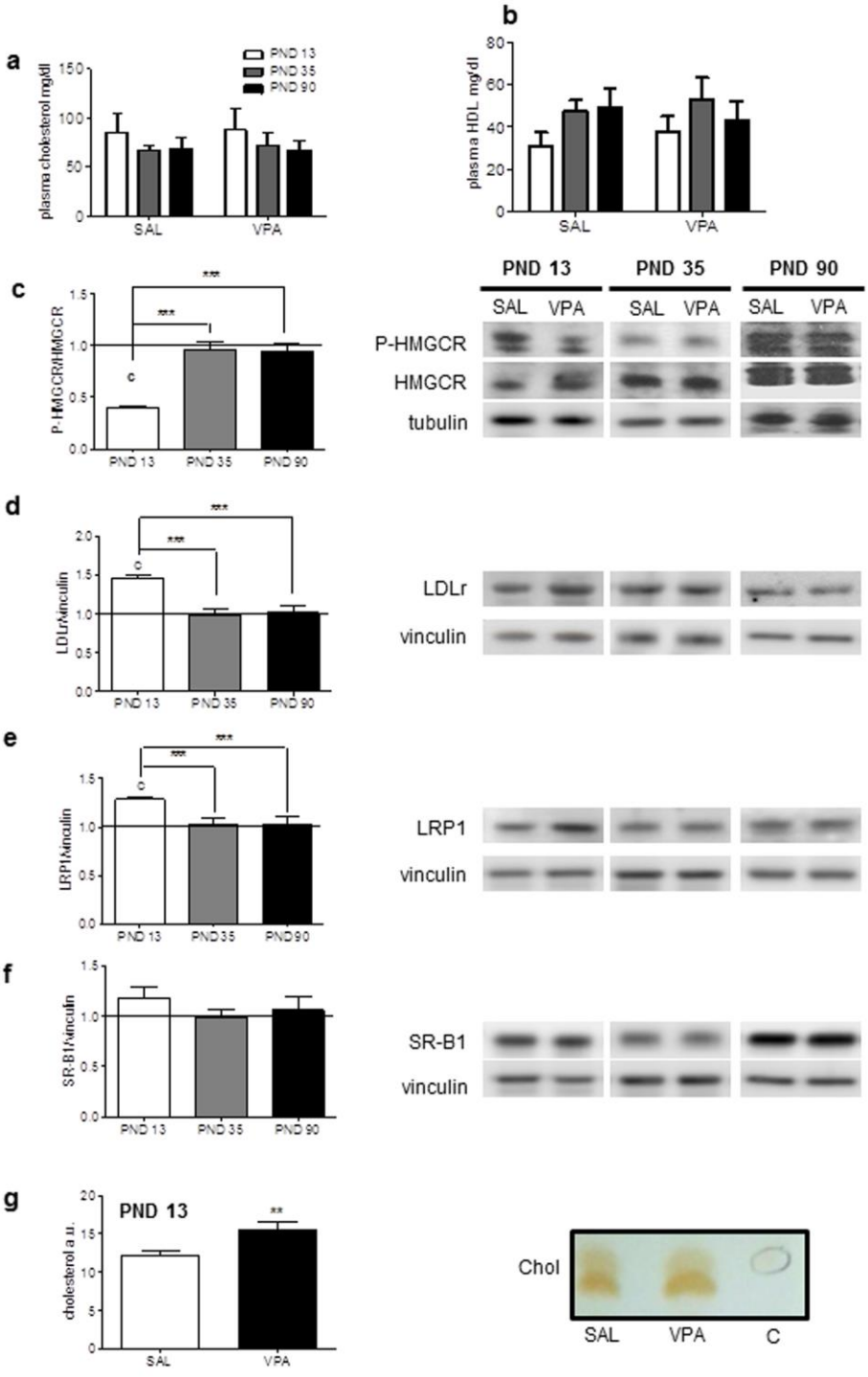
a
plasma cholesterol mg/dl
PND 13
PND 35
PND 90
SAL
VPA
b
plasma HDL mg/dl
SAL
VPA
c
P-HMGCR/HMGCR
PND 13
PND 35
PND 90
PND 13
PND 35
PND 90
SAL
VPA
P-HMGCR
HMGCR
tubulin
d
LDLr/vinculin
LDLr
vinculin
e
LRP1/vinculin
LRP1
vinculin
f
SR-B1/vinculin
SR-B1
vinculin
g
PND 13
cholesterol a.u.
Chol
SAL
VPA
C

Figure 3

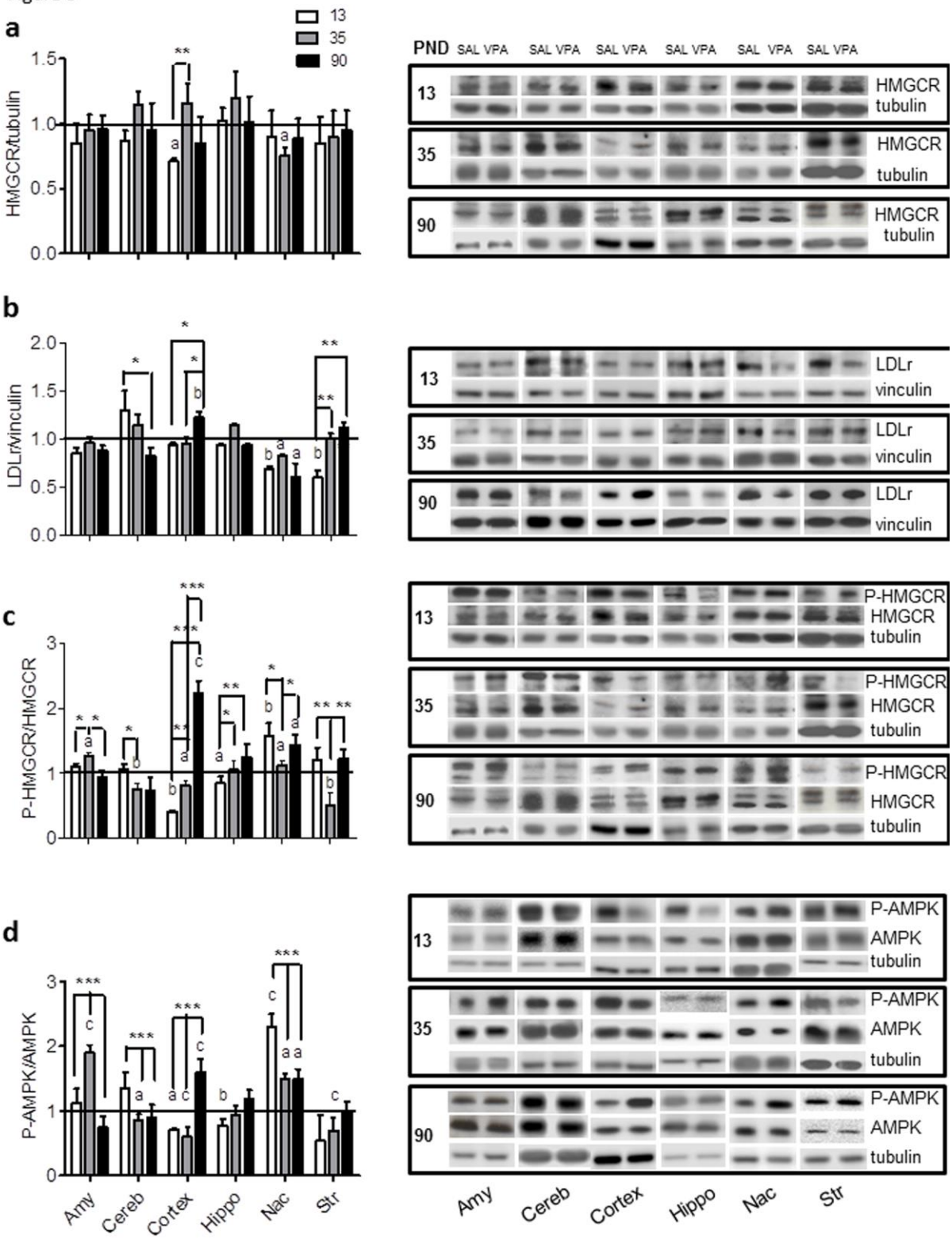
a
13
35
90
HMGCR/tubulin
1.5
1.0
0.5
0.0
PND SAL VPA SAL VPA SAL VPA SAL VPA SAL VPA SAL VPA
13
HMGCR
tubulin
35
HMGCR
tubulin
90
HMGCR
tubulin
b
LDLr/vinculin
2.0
1.5
1.0
0.5
0.0
13
LDLr
vinculin
35
LDLr
vinculin
90
LDLr
vinculin
c
P-HMGCR/HMGCR
3
2
1
0
13
P-HMGCR
HMGCR
tubulin
35
P-HMGCR
HMGCR
tubulin
90
P-HMGCR
HMGCR
tubulin
d
P-AMPK/AMPK
3
2
1
0
13
P-AMPK
AMPK
tubulin
35
P-AMPK
AMPK
tubulin
90
P-AMPK
AMPK
tubulin
Amy
Cereb
Cortex
Hippo
Nac
Str
Amy
Cereb
Cortex
Hippo
Nac
Str

Figure 4

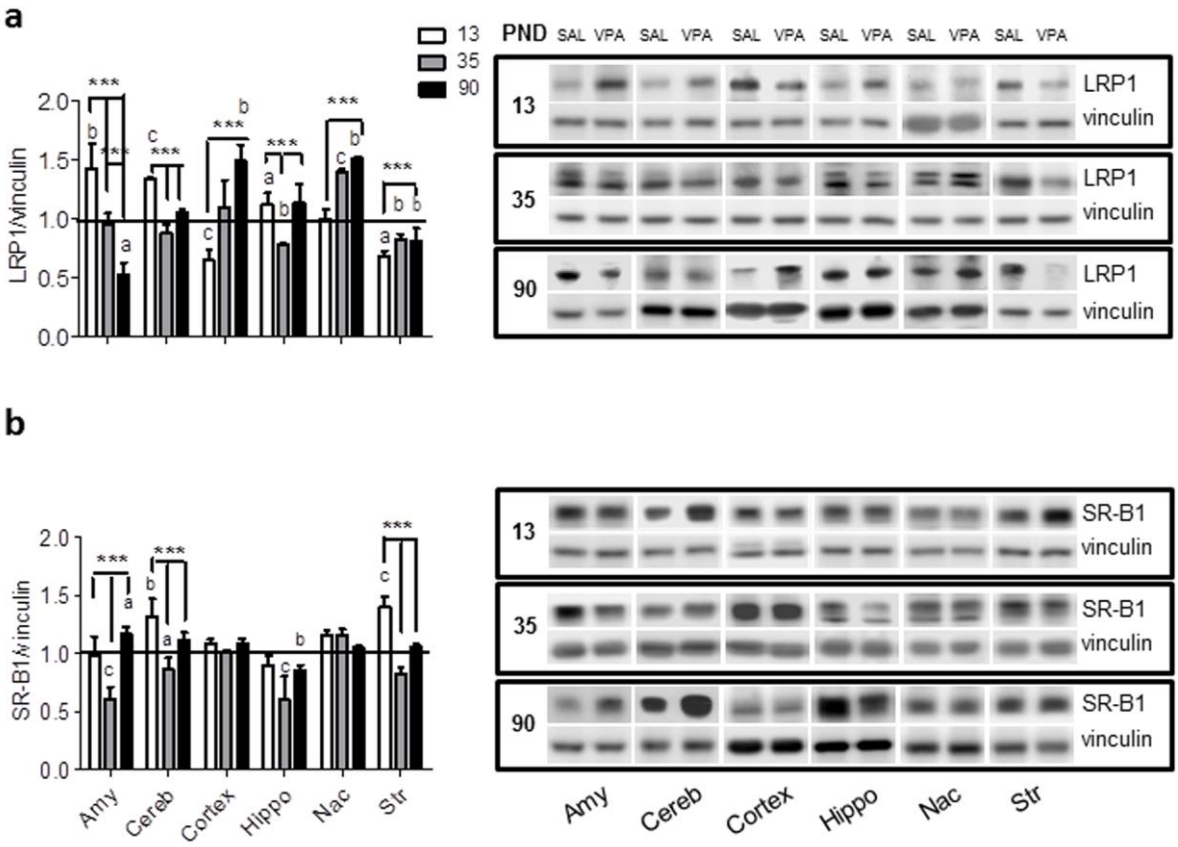
a
13
35
90
PND SAL VPA SAL VPA SAL VPA SAL VPA SAL VPA SAL VPA
LRP1/Vinculin
2.0
1.5
1.0
0.5
0.0
13
35
90
LRP1
vinculin
b
SR-B1/Vinculin
SR-B1
Amy
Cereb
Cortex
Hippo
Nac
Str

Figure 5

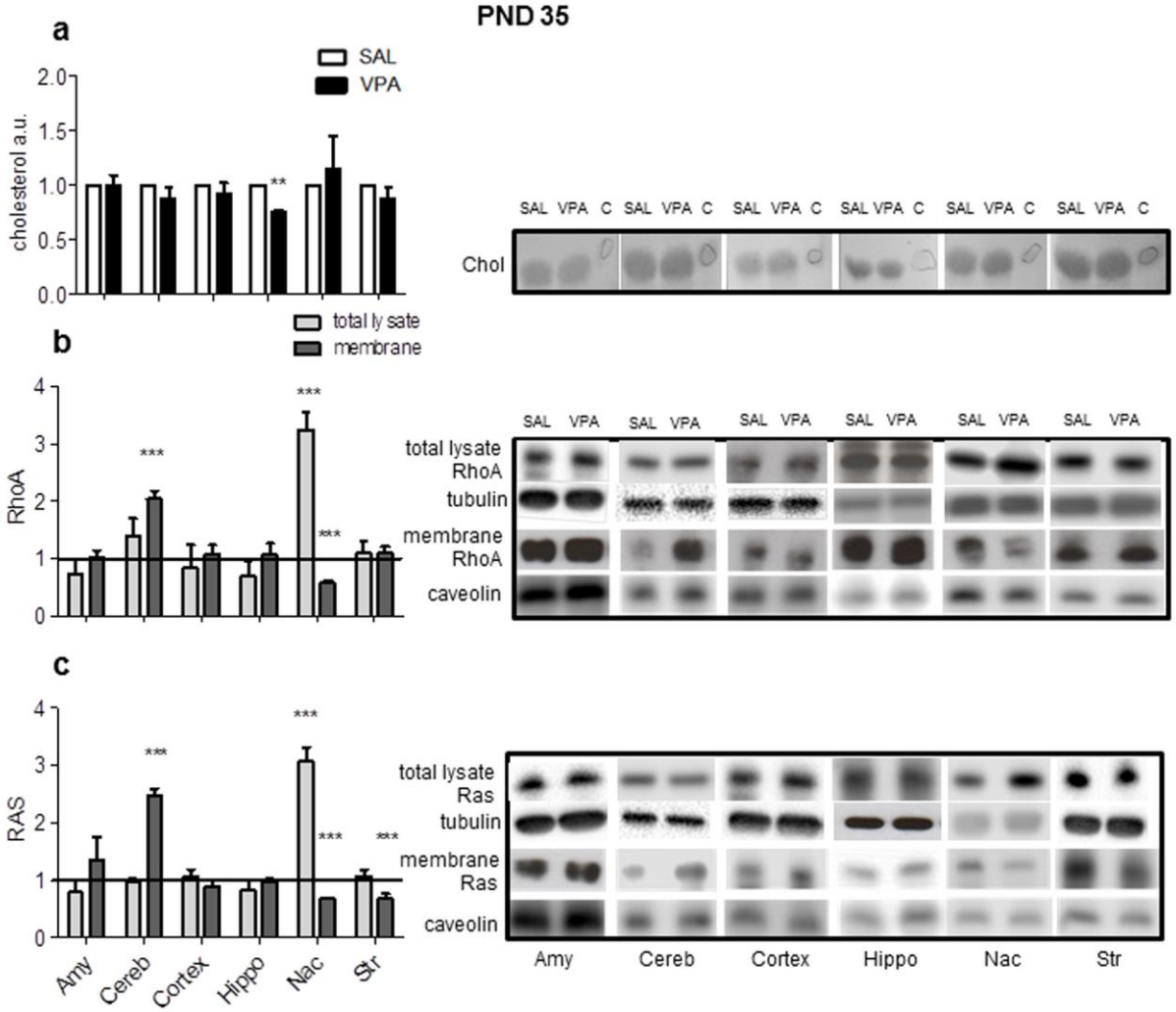
PND 35
a
SAL
VPA
cholesterol a.u.
2.0
1.5
1.0
0.5
0.0
**
SAL VPA C SAL VPA C SAL VPA C SAL VPA C SAL VPA C SAL VPA C
Chol
b
total lysate
membrane
RhoA
4
3
2
1
0
***
***
***
SAL VPA SAL VPA SAL VPA SAL VPA SAL VPA SAL VPA
total lysate RhoA
tubulin
membrane RhoA
caveolin
c
RAS
4
3
2
1
0
***
***
***
***
total lysate Ras
tubulin
membrane Ras
caveolin
Amy
Cereb
Cortex
Hippo
Nac
Str

Figure 6

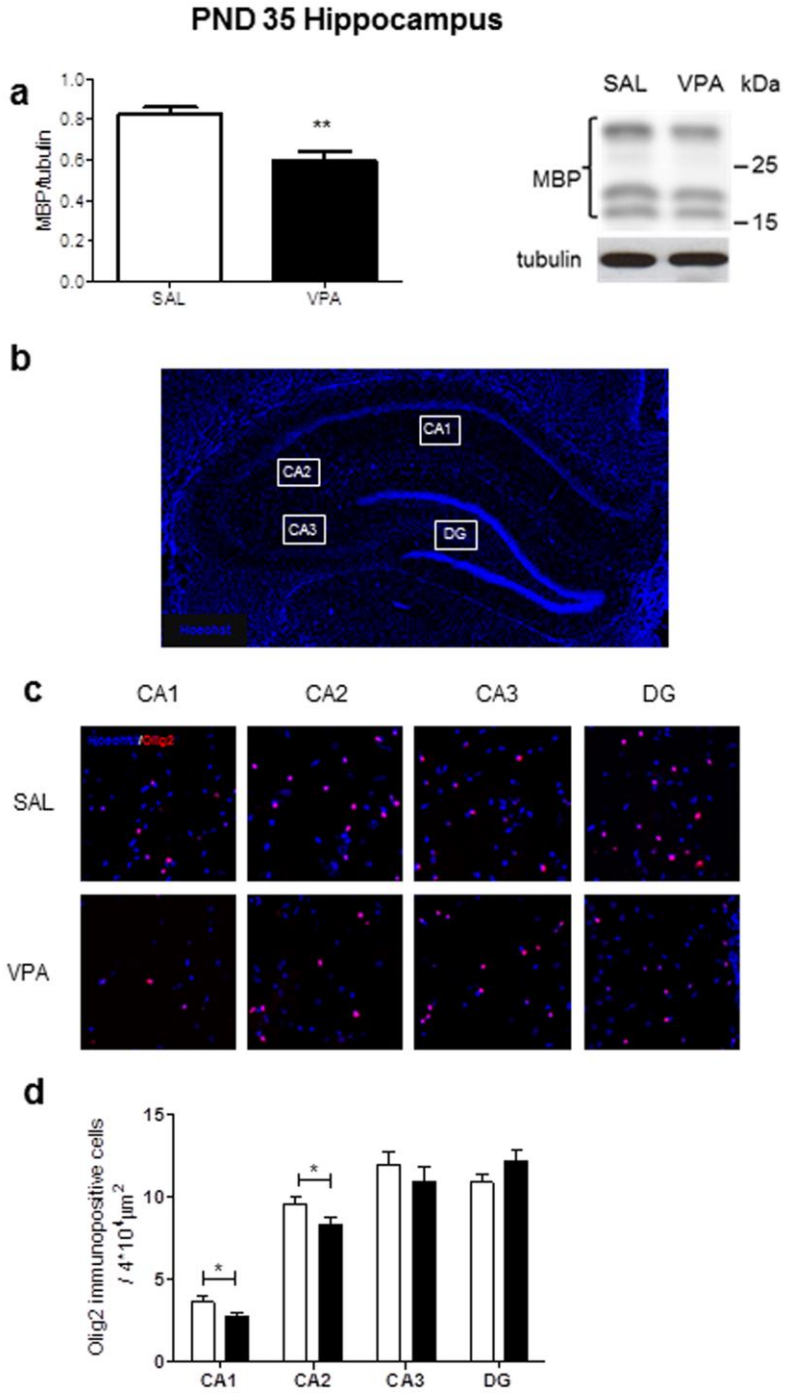
PND 35 Hippocampus
a
MBP/tubulin
1.0
0.8
0.6
0.4
0.2
0.0
**
SAL
VPA
SAL
VPA
kDa
MBP
25
15
tubulin
b
CA1
CA2
CA3
DG
c
CA1
CA2
CA3
DG
SAL
VPA
d
Olig2 immunopositive cells
/ 4*10⁴µm²
15
10
5
0
*
*
CA1
CA2
CA3
DG

## General conclusions and outlook

My experimental work demonstrated that the MVA pathway is differently active in each brain region in adult male rats, and emphasizes marked regional differences in the regulation of HMGCR and LDLR. In particular, the hippocampus followed by the brain cortex, exhibited vigorous isoprenoid metabolism, as indicated by the highest levels of HMGCR and LDLR protein expression. On the contrary, the MVA pathway seems to be nearly suppressed in the brain stem, because of the low HMGCR activation/protein levels and the very low LDLR expression (Segatto et al., 2012). The observed differences may be caused by the rate of cholesterol turnover, regional myelin content and the modulation of synaptic plasticity of each brain region.

My studies reveal that the MVA pathway is subject to age- and sex-dependent modulation in each brain area. LDLR expression in the brain cortex is strongly decreased in aged female rats. The hormonal replacement with exogenous 17-β-estradiol highlighted that this alteration is related to the circulating levels of the sex hormone (Segatto et al., 2011). On the contrary, in the hippocampus, the age- and sex-dependent modulation of HMGCR and LDLR are completely independent from plasma estrogen levels (Segatto et al., 2013). The differences between adult male and female rats support the evidence of physiological sex-related dissimilarities among the brain areas (Lebron-Milad and Milad, 2012). They appear to achieve cholesterol homeostasis by different mechanisms as reported in other systems like the cardiovascular system (Pepine et al., 2006; Marino et al., 2011). Considering the strong divergences in the regional modulation of MVA metabolism shown by my work, it is clear that each brain area can be considered as a unique and independent structure with a specific cellular context responding in a specific way to the same stimuli (i.e., estrogens). Some of the observed differences should be taken into consideration in therapeutic practice, as they may have clinical relevance in terms of disease incidence, manifestation, prognosis and treatment, such as in Alzheimer disease (AD). For this disorder, the incidence is higher in female and seems to be related, at least in part, to cholesterol dysmetabolism (Snyder et al., 2016; Peng et al., 2016; Cartocci et al., 2017; Pike, 2017).

My results also highlight a critical role of the MVA pathway in the modulation of behavior and cognition. Inhibition of HMGCR by simvastatin induces social anxiety-related behaviors and improves memory retention in rodents. The outcomes induced by the reduced HMGCR activity could be mediated, at least in part, by the specific prenylated proteins. It is well known that Rab3 carries out important physiological roles in neurotransmitter release at a late

step during the synaptic vesicle exocytosis (Geppert and Sudhof, 1998), and pathologic consequences of alterations in Rab3 activity have already been established. For instance, deregulation in Mss4 (mammalian suppressor of Sec4), a regulator of Rab3 activity, has been linked to impaired neurotransmitter release and to the appearance of neurodegenerative and psychological disorders in rodents such as depressive-like syndromes (Andriamampandry et al., 2002). Given the important role of the hippocampus and the prefrontal cortex in anxiety (Whitton and Curzon, 1990; Christianson et al., 2009), the observed decrease in the prenylated fraction of Rab3 in these brain regions may explain how modulation of the MVA pathway contributes to social anxiety-related behavior emerged in our study (Segatto et al., 2014b). Besides the reduction in protein levels, MVA pathway may contribute to the consolidation of emotional memory by the modulation of prenylated proteins that are crucial for the induction and the maintenance of LTP. In particular, a strong and statistically significant decrease in the active fraction of RhoA occurs in the amygdala and the hippocampus of simvastatin-treated rats. Experiments performed on acutely isolated hippocampal neuron highlighted that perturbations in the fraction of active RhoA are accompanied by enhanced phosphorylation of Akt and by the subsequent rise in the CREB activation state: modulation of the RhoA signal transduction pathway could play a crucial role in cognitive performance, as CREB-dependent gene transcription appears to be an essential component of long-term memory (Silva et al., 1998). The biological relevance of my results is further supported by other studies showing a crucial role for prenylated proteins in the pathophysiology of cognitive dysfunction. Notably, it was observed that prenyl production is elevated in AD brains, suggesting that protein prenylation may be altered and may contribute to AD neuropathophysiology (Eckert et al., 2009).

My finding that simvastatin promotes neurite elongation by preventing the activation of the negative regulator RhoA indicates that inhibition of the MVA pathway is fundamental for neurite outgrowth and for neuronal differentiation (Cartocci et al., 2016). The decreasing activity isoprenoid/cholesterol metabolic pathway during development is a physiological feature in differentiating neurons, and predicts that any interference with this metabolic pathway will alter neuronal function. In pathologic conditions caused by disturbed neuronal development, a deliberate modulation of the MVA pathway may help to improve the neurological and metabolic symptoms. I addressed this topic in a neurodevelopmental pathology characterized by altered emotional reactivity and memory, the Autism Spectrum Disorders (ASDs) using a well established VPA-exposed animal model (Servadio et al., 2015; Servadio et al., 2016). My studies revealed that the MVA pathway in the brain of male

exposed rats is altered indeed suggesting that modulation of the MVA pathway in these areas could contribute to this psychiatric disorder. The link between cholesterol homeostasis and psychiatric symptoms is further indicated by my observations that pharmacologic inhibition of HMGCR in the brain of adult rats altered their emotional reactivity and cognitive performance (Segatto et al., 2014b). Intriguingly, preliminary data from my laboratory reveal that the VPA-induced modulation of the studied proteins is stronger in males than in females confirming the sex-dependent modulation of MVA pathway (Cartocci et al., in preparation). This observation could correlate to the sex-dependent incidence of ASDs since they are four times more common in boys than girls with a ratio of 4:1 (Vijayakumar and Judy, 2016; Halladay et al., 2016).

Taken together, my studies provide new insights in the physiology and pathophysiology of the MVA pathway in the brain. They demonstrate that this metabolic process is expressed and modulated in a highly region-dependent manner and that age and sex induce physiological differences. Notably, the impact of the MVA pathway on behavior and neuronal development together with its modulation in the experimental model of autism suggest that different proteins and enzymatic products of the MVA pathway may be considered as potential molecular targets when designing novel therapeutic approaches for the treatment of neurodevelopmental disorders.

A major question rises by my results: which kind of cell does contribute to the observed changes in the MVA pathway? Therefore, a next goal should be to evaluate cell-specific changes in MVA pathway homeostasis. This will reveal which cell types (neurons and non-neuronal glial cells) contribute to the observed physiological modulation and reveal their respective role in the studied phenomena. Furthermore, the putative therapeutic interventions in neurological disease should be tailored to specific cells. A main obstacle to address this topic is the lack of *in vivo* experimental approaches to monitor the activity of the MVA pathway in a cell-specific manner. Knockout mice cannot provide answers because they die embryonically (Tozawa et al., 1999). A solution could be based on immunohistochemical analyses revealing cell-specific levels of enzymes, although this will not reveal their activity. Another possibility could be to acutely isolate cells from the different brain areas in all the experimental models I used, and although the amounts of the cells are limited, the analyses could reveal the cell-specific impact on brain physiopathology. These considerations demonstrate that further preclinical studies on animal experimental models should be performed to better understand whether modulation of MVA pathway in the brain could be a potential pharmacological target to treat CNS diseases. So, I strongly feel that advances on

cholesterol/isoprenoid metabolism in the brain and its implications in neurologic diseases require radically new and innovative approaches that allow to follow the pathway activities in a more detailed and specific manner.

## References


Anderson TJ, Meredith IT, Yeung AC, Frei B, Selwyn AP, Ganz P (The effect of cholesterol-lowering and antioxidant therapy on endothelium-dependent coronary vasomotion. N Engl J Med 332:488-493.1995).

Andriamampandry C, Muller C, Schmidt-Mutter C, Gobaille S, Spedding M, Aunis D, Maitre M (Mss4 gene is up-regulated in rat brain after chronic treatment with antidepressant and down-regulated when rats are anhedonic. Mol Pharmacol 62:1332-1338.2002).

Baytan SH, Alkanat M, Okuyan M, Ekinci M, Gedikli E, Ozeren M, Akgun A (Simvastatin impairs spatial memory in rats at a specific dose level. Tohoku J Exp Med 214:341-349.2008).

Beg ZH, Stonik JA, Brewer HB, Jr. (Phosphorylation of hepatic 3-hydroxy-3-methylglutaryl coenzyme A reductase and modulation of its enzymic activity by calcium-activated and phospholipid-dependent protein kinase. J Biol Chem 260:1682-1687.1985).

Belo RS, Jamieson JC, Wright JA (Studies on the effect of mevinolin (lovastatin) and mevastatin (compactin) on the fusion of L6 myoblasts. Mol Cell Biochem 126:159-167.1993).

Bentinger M, Tekle M, Brismar K, Chojnacki T, Swiezewska E, Dallner G (Stimulation of coenzyme Q synthesis. Biofactors 32:99-111.2008).

Bjorkhem I, Lutjohann D, Breuer O, Sakinis A, Wennmalm A (Importance of a novel oxidative mechanism for elimination of brain cholesterol. Turnover of cholesterol and 24(S)-hydroxycholesterol in rat brain as measured with 18O2 techniques in vivo and in vitro. J Biol Chem 272:30178-30184.1997).

Bjorkhem I, Meaney S (Brain cholesterol: long secret life behind a barrier. Arterioscler Thromb Vasc Biol 24:806-815.2004).

Bos JL, Rehmann H, Wittinghofer A (GEFs and GAPs: critical elements in the control of small G proteins. Cell 129:865-877.2007).

Brown MS, Goldstein JL (The SREBP pathway: regulation of cholesterol metabolism by proteolysis of a membrane-bound transcription factor. Cell 89:331-340.1997).

Brown MS, Goldstein JL (A proteolytic pathway that controls the cholesterol content of membranes, cells, and blood. Proc Natl Acad Sci U S A 96:11041-11048.1999).

Buczkowska A, Swiezewska E, Lefeber DJ (Genetic defects in dolichol metabolism. J Inherit Metab Dis 38:157-169.2015).

Burg JS, Espenshade PJ (Regulation of HMG-CoA reductase in mammals and yeast. Prog Lipid Res 50:403-410.2011).

Cartocci V, Segatto M, Di Tunno I, Leone S, Pfrieger FW, Pallottini V (Modulation of the Isoprenoid/Cholesterol Biosynthetic Pathway During Neuronal Differentiation In Vitro. J Cell Biochem 117:2036-2044.2016).

Cartocci V, Servadio M, Trezza V, Pallottini V (Can Cholesterol Metabolism Modulation Affect Brain Function and Behavior? J Cell Physiol.2017).

Cherfils J, Zeghouf M (Regulation of small GTPases by GEFs, GAPs, and GDIs. Physiol Rev 93:269-309.2013).

Christianson JP, Thompson BM, Watkins LR, Maier SF (Medial prefrontal cortical activation modulates the impact of controllable and uncontrollable stressor exposure on a social exploration test of anxiety in the rat. Stress 12:445-450.2009).

Dietschy JM, Turley SD (Thematic review series: brain Lipids. Cholesterol metabolism in the central nervous system during early development and in the mature animal. J Lipid Res 45:1375-1397.2004).

Eckert GP, Hooff GP, Strandjord DM, Igbavboa U, Volmer DA, Muller WE, Wood WG (Regulation of the brain isoprenoids farnesyl- and geranylgeranylpyrophosphate is altered in male Alzheimer patients. Neurobiol Dis 35:251-257.2009).

Friesen JA, Rodwell VW (The 3-hydroxy-3-methylglutaryl coenzyme-A (HMG-CoA) reductases. Genome Biol 5:248.2004).

Geppert M, Sudhof TC (RAB3 and synaptotagmin: the yin and yang of synaptic membrane fusion. Annu Rev Neurosci 21:75-95.1998).

Goldstein JL, Brown MS, Anderson RG, Russell DW, Schneider WJ (Receptor-mediated endocytosis: concepts emerging from the LDL receptor system. Annu Rev Cell Biol 1:1-39.1985).

Gomez-Diaz C, Rodriguez-Aguilera JC, Barroso MP, Villalba JM, Navarro F, Crane FL, Navas P (Antioxidant ascorbate is stabilized by NADH-coenzyme Q10 reductase in the plasma membrane. J Bioenerg Biomembr 29:251-257.1997).

Haines TH (Do sterols reduce proton and sodium leaks through lipid bilayers? Prog Lipid Res 40:299-324.2001).

Halladay AK, Bishop S, Constantino JN, Daniels AM, Koenig K, Palmer K, Messinger D, Pelphrey K, Sanders SJ, Singer AT, Taylor JL, Szatmari P (Sex and gender differences in autism spectrum disorder: summarizing evidence gaps and identifying emerging areas of priority. Mol Autism 6:36.2016).

Hamilton SJ, Chew GT, Watts GF (Therapeutic regulation of endothelial dysfunction in type 2 diabetes mellitus. Diab Vasc Dis Res 4:89-102.2007).

Hardie DG, Ross FA, Hawley SA (AMPK: a nutrient and energy sensor that maintains energy homeostasis. Nat Rev Mol Cell Biol 13:251-262.2016).

Holstein SA, Hohl RJ (Isoprenoids: remarkable diversity of form and function. Lipids 39:293-309.2004).

Istvan ES, Deisenhofer J (The structure of the catalytic portion of human HMG-CoA reductase. Biochim Biophys Acta 1529:9-18.2000).

Janssens V, Goris J (Protein phosphatase 2A: a highly regulated family of serine/threonine phosphatases implicated in cell growth and signalling. Biochem J 353:417-439.2001).

Karasinska JM, Hayden MR (Cholesterol metabolism in Huntington disease. Nat Rev Neurol 7:561-572.2011).

Krakowski M, Czobor P (Cholesterol and cognition in schizophrenia: a double-blind study of patients randomized to clozapine, olanzapine and haloperidol. Schizophr Res 130:27-33.2011).

Lebron-Milad K, Milad MR (Sex differences, gonadal hormones and the fear extinction network: implications for anxiety disorders. Biol Mood Anxiety Disord 2:3.2012).

Leoni V, Caccia C (24S-hydroxycholesterol in plasma: a marker of cholesterol turnover in neurodegenerative diseases. Biochimie 95:595-612.2013).

Lingor P, Teusch N, Schwarz K, Mueller R, Mack H, Bahr M, Mueller BK (Inhibition of Rho kinase (ROCK) increases neurite outgrowth on chondroitin sulphate proteoglycan in vitro and axonal regeneration in the adult optic nerve in vivo. J Neurochem 103:181-189.2007).

Lutjohann D, Breuer O, Ahlborg G, Nennesmo I, Siden A, Diczfalusy U, Bjorkhem I (Cholesterol homeostasis in human brain: evidence for an age-dependent flux of 24S-hydroxycholesterol from the brain into the circulation. Proc Natl Acad Sci U S A 93:9799-9804.1996).

Maes M, Mihaylova I, Kubera M, Uytterhoeven M, Vrydags N, Bosmans E (Lower plasma Coenzyme Q10 in depression: a marker for treatment resistance and chronic fatigue in depression and a risk factor to cardiovascular disorder in that illness. Neuro Endocrinol Lett 30:462-469.2009).

Marino M, Masella R, Bulzomi P, Campesi I, Malorni W, Franconi F (Nutrition and human health from a sex-gender perspective. Mol Aspects Med 32:1-70.2011).

Martin MG, Pfrieger F, Dotti CG (Cholesterol in brain disease: sometimes determinant and frequently implicated. EMBO Rep 15:1036-1052.2014).

Martini C, Pallottini V (Cholesterol: from feeding to gene regulation. Genes Nutr 2:181-193.2007).

Mauch DH, Nagler K, Schumacher S, Goritz C, Muller EC, Otto A, Pfrieger FW (CNS synaptogenesis promoted by glia-derived cholesterol. Science 294:1354-1357.2001).

Mazzucchelli C, Brambilla R (Ras-related and MAPK signalling in neuronal plasticity and memory formation. Cell Mol Life Sci 57:604-611.2000).

Messa C, Notarnicola M, Russo F, Cavallini A, Pallottini V, Trentalance A, Bifulco M, Laezza C, Gabriella Caruso M (Estrogenic regulation of cholesterol biosynthesis and cell growth in DLD-1 human colon cancer cells. Scand J Gastroenterol 40:1454-1461.2005).

Mitchell P (The protonmotive Q cycle: a general formulation. FEBS Lett 59:137-139.1975).

Morava E, Kuhnisch J, Drijvers JM, Robben JH, Cremers C, van Setten P, Branten A, Stumpp S, de Jong A, Voesenek K, Vermeer S, Heister A, Claahsen-van der Grinten HL, O'Neill CW, Willemsen MA, Lefeber D, Deen PM, Kornak U, Kremer H, Wevers RA (Autosomal recessive mental retardation, deafness, ankylosis, and mild hypophosphatemia associated with a novel ANKH mutation in a consanguineous family. J Clin Endocrinol Metab 96:E189-198.2011).

Nakagami H, Jensen KS, Liao JK (A novel pleiotropic effect of statins: prevention of cardiac hypertrophy by cholesterol-independent mechanisms. Ann Med 35:398-403.2003).

Nervi FO, Weis HJ, Dietschy JM (The kinetic characteristics of inhibition of hepatic cholesterogenesis by lipoproteins of intestinal origin. J Biol Chem 250:4145-4151.1975).

Ness GC, Chambers CM (Feedback and hormonal regulation of hepatic 3-hydroxy-3-methylglutaryl coenzyme A reductase: the concept of cholesterol buffering capacity. Proc Soc Exp Biol Med 224:8-19.2000).

Nieweg K, Schaller H, Pfrieger FW (Marked differences in cholesterol synthesis between neurons and glial cells from postnatal rats. J Neurochem 109:125-134.2009).

Nilsson A, Duan RD (Absorption and lipoprotein transport of sphingomyelin. J Lipid Res 47:154-171.2006).

Ohvo-Rekila H, Ramstedt B, Leppimaki P, Slotte JP (Cholesterol interactions with phospholipids in membranes. Prog Lipid Res 41:66-97.2002).

Oram JF, Heinecke JW (ATP-binding cassette transporter A1: a cell cholesterol exporter that protects against cardiovascular disease. Physiol Rev 85:1343-1372.2005).

Pallottini V, Martini C, Cavallini G, Bergamini E, Mustard KJ, Hardie DG, Trentalance A (Age-related HMG-CoA reductase deregulation depends on ROS-induced p38 activation. Mech Ageing Dev 128:688-695.2007).

Pallottini V, Martini C, Cavallini G, Donati A, Bergamini E, Notarnicola M, Caruso MG, Trentalance A (Modified HMG-CoA reductase and LDLr regulation is deeply involved in age-related hypercholesterolemia. J Cell Biochem 98:1044-1053.2006).

Papucci L, Schiavone N, Witort E, Donnini M, Lapucci A, Tempestini A, Formigli L, Zecchi-Orlandini S, Orlandini G, Carella G, Brancato R, Capaccioli S (Coenzyme q10 prevents apoptosis by inhibiting mitochondrial depolarization independently of its free radical scavenging property. J Biol Chem 278:28220-28228.2003).

Parentini I, Cavallini G, Donati A, Gori Z, Bergamini E (Accumulation of dolichol in older tissues satisfies the proposed criteria to be qualified a biomarker of aging. J Gerontol A Biol Sci Med Sci 60:39-43.2005).

Peng X, Xing P, Li X, Qian Y, Song F, Bai Z, Han G, Lei H (Towards Personalized Intervention for Alzheimer's Disease. Genomics Proteomics Bioinformatics 14:289-297.2016).

Pepine CJ, Kerensky RA, Lambert CR, Smith KM, von Mering GO, Sopko G, Bairey Merz CN (Some thoughts on the vasculopathy of women with ischemic heart disease. J Am Coll Cardiol 47:S30-35.2006).

Pfrieger FW (Outsourcing in the brain: do neurons depend on cholesterol delivery by astrocytes? Bioessays 25:72-78.2003a).

Pfrieger FW (Role of cholesterol in synapse formation and function. Biochim Biophys Acta 1610:271-280.2003b).

Pfrieger FW, Ungerer N (Cholesterol metabolism in neurons and astrocytes. Prog Lipid Res 50:357-371.2011).

Pike CJ (Sex and the development of Alzheimer's disease. J Neurosci Res 95:671-680.2017).

Ramakers GM, Storm JF (A postsynaptic transient K(+) current modulated by arachidonic acid regulates synaptic integration and threshold for LTP induction in hippocampal pyramidal cells. Proc Natl Acad Sci U S A 99:10144-10149.2002).

Ridker PM, Rifai N, Clearfield M, Downs JR, Weis SE, Miles JS, Gotto AM, Jr. (Measurement of C-reactive protein for the targeting of statin therapy in the primary prevention of acute coronary events. N Engl J Med 344:1959-1965.2001).

Rip JW, Rupar CA, Ravi K, Carroll KK (Distribution, metabolism and function of dolichol and polyprenols. Prog Lipid Res 24:269-309.1985).

Rozman D, Monostory K (Perspectives of the non-statin hypolipidemic agents. Pharmacol Ther 127:19-40.2010).

Saher G, Stumpf SK (Cholesterol in myelin biogenesis and hypomyelinating disorders. Biochim Biophys Acta 1851:1083-1094.2015).

Segatto M, Di Giovanni A, Marino M, Pallottini V (Analysis of the protein network of cholesterol homeostasis in different brain regions: an age and sex dependent perspective. J Cell Physiol 228:1561-1567.2013).

Segatto M, Leboffe L, Trapani L, Pallottini V (Cholesterol homeostasis failure in the brain: implications for synaptic dysfunction and cognitive decline. Curr Med Chem 21:2788-2802.2014a).

Segatto M, Manduca A, Lecis C, Rosso P, Jozwiak A, Swiezewska E, Moreno S, Trezza V, Pallottini V (Simvastatin treatment highlights a new role for the isoprenoid/cholesterol biosynthetic pathway in the modulation of emotional reactivity and cognitive performance in rats. Neuropsychopharmacology 39:841-854.2014b).

Segatto M, Trapani L, Lecis C, Pallottini V (Regulation of cholesterol biosynthetic pathway in different regions of the rat central nervous system. Acta Physiol (Oxf) 206:62-71.2012).

Segatto M, Trapani L, Marino M, Pallottini V (Age- and sex-related differences in extra-hepatic low-density lipoprotein receptor. J Cell Physiol 226:2610-2616.2011).

Servadio M, Melancia F, Manduca A, di Masi A, Schiavi S, Cartocci V, Pallottini V, Campolongo P, Ascenzi P, Trezza V (Targeting anandamide metabolism rescues core and associated autistic-like symptoms in rats prenatally exposed to valproic acid. . Translational Psychiatry.2016).

Servadio M, Vanderschuren LJ, Trezza V (Modeling autism-relevant behavioral phenotypes in rats and mice: Do 'autistic' rodents exist? Behav Pharmacol 26:522-540.2015).

Sever N, Yang T, Brown MS, Goldstein JL, DeBose-Boyd RA (Accelerated degradation of HMG CoA reductase mediated by binding of insig-1 to its sterol-sensing domain. Mol Cell 11:25-33.2003).

Shanmugaratnam J, Berg E, Kimerer L, Johnson RJ, Amaratunga A, Schreiber BM, Fine RE (Retinal Muller glia secrete apolipoproteins E and J which are efficiently assembled into lipoprotein particles. Brain Res Mol Brain Res 50:113-120.1997).

Shepherd J, Cobbe SM, Ford I, Isles CG, Lorimer AR, MacFarlane PW, McKillop JH, Packard CJ (Prevention of coronary heart disease with pravastatin in men with hypercholesterolemia. West of Scotland Coronary Prevention Study Group. N Engl J Med 333:1301-1307.1995).

Silva AJ, Kogan JH, Frankland PW, Kida S (CREB and memory. Annu Rev Neurosci 21:127-148.1998).

Snipes GJ, Orfali W (Common themes in peripheral neuropathy disease genes. Cell Biol Int 22:815-835.1998).

Snyder HM, Asthana S, Bain L, Brinton R, Craft S, Dubal DB, Espeland MA, Gatz M, Mielke MM, Raber J, Rapp PR, Yaffe K, Carrillo MC (Sex biology contributions to vulnerability to Alzheimer's disease: A think tank convened by the Women's Alzheimer's Research Initiative. Alzheimers Dement 12:1186-1196.2016).

Surmacz L, Swiezewska E (Polyisoprenoids - Secondary metabolites or physiologically important superlipids? Biochem Biophys Res Commun 407:627-632.2011).

Tabas I (Cholesterol in health and disease. J Clin Invest 110:583-590.2002).

Takai Y, Sasaki T, Matozaki T (Small GTP-binding proteins. Physiol Rev 81:153-208.2001).

Thomas SR, Neuzil J, Stocker R (Cosupplementation with coenzyme Q prevents the prooxidant effect of alpha-tocopherol and increases the resistance of LDL to transition metal-dependent oxidation initiation. Arterioscler Thromb Vasc Biol 16:687-696.1996).

Tozawa R, Ishibashi S, Osuga J, Yagyu H, Oka T, Chen Z, Ohashi K, Perrey S, Shionoiri F, Yahagi N, Harada K, Gotoda T, Yazaki Y, Yamada N (Embryonic lethality and defective neural tube closure in mice lacking squalene synthase. J Biol Chem 274:30843-30848.1999).

Trapani L, Segatto M, Ascenzi P, Pallottini V (Potential role of nonstatin cholesterol lowering agents. IUBMB Life 63:964-971.2011).

Valenza M, Cattaneo E (Emerging roles for cholesterol in Huntington's disease. Trends Neurosci 34:474-486.2011).

van Deijk AF, Camargo N, Timmerman J, Heistek T, Brouwers JF, Mogavero F, Mansvelder HD, Smit AB, Verheijen MH (Astrocyte lipid metabolism is critical for synapse development and function in vivo. Glia 65:670-682.2017).

Vetter IR, Wittinghofer A (The guanine nucleotide-binding switch in three dimensions. Science 294:1299-1304.2001).

Vigo C, Grossman SH, Drost-Hansen W (Interaction of dolichol and dolichyl phosphate with phospholipid bilayers. Biochim Biophys Acta 774:221-226.1984).

Vijayakumar NT, Judy MV (Autism spectrum disorders: Integration of the genome, transcriptome and the environment. J Neurol Sci 364:167-176.2016).

Wang H (Lipid rafts: a signaling platform linking cholesterol metabolism to synaptic deficits in autism spectrum disorders. Front Behav Neurosci 8:104.2014).

Welti M, Hulsmeier AJ (Ethanol-induced impairment in the biosynthesis of N-linked glycosylation. J Cell Biochem 115:754-762.2014).

Whitton P, Curzon G (Anxiogenic-like effect of infusing 1-(3-chlorophenyl) piperazine (mCPP) into the hippocampus. Psychopharmacology (Berl) 100:138-140.1990).

Yamazaki T, Komuro I, Kudoh S, Zou Y, Shiojima I, Mizuno T, Takano H, Hiroi Y, Ueki K, Tobe K, et al. (Angiotensin II partly mediates mechanical stress-induced cardiac hypertrophy. Circ Res 77:258-265.1995).

Yang T, Espenshade PJ, Wright ME, Yabe D, Gong Y, Aebersold R, Goldstein JL, Brown MS (Crucial step in cholesterol homeostasis: sterols promote binding of SCAP to INSIG-1, a membrane protein that facilitates retention of SREBPs in ER. Cell 110:489-500.2002).

Young AJ, Johnson S, Steffens DC, Doraiswamy PM (Coenzyme Q10: a review of its promise as a neuroprotectant. CNS Spectr 12:62-68.2007).

**Ringraziamenti**

Il dottorato è sempre stato il mio sogno nel cassetto che, per motivi personali e lavorativi non ho mai realizzato. Probabilmente qualcuno avrà pensato che intraprendere questa avventura a cinquant'anni, avendo già un ruolo nell'accademia, sia stata una pazzia. Io credo invece che non ci sia un limite di età per mettersi in gioco. Il raggiungimento di questo obbiettivo lo devo non solo alla mia caparbietà, ma ad alcune persone che mi hanno sostenuta, guidata, formata e …. che intendo ringraziare UFFICIALMENTE.

Non posso che iniziare dai miei figli: **Mattia e Simone**. Avete sempre creduto in me, mi avete sostenuta, avete sopportato le mie ansie, le mie assenze, i miei nervosismi, senza mai farmi pesare di aver fatto questa scelta bizzarra. Siete i figli che ogni donna desidererebbe avere!!!! Vorrei ringraziare **Valerio**, senza di te non sarei la donna e la mamma che sono.

**Mamma, papà e Giampaolo**, colonne della mia esistenza, radici vitali e costanti punti di riferimento. Se sono arrivata qui, è perchè ho applicato l'insegnamento della nostra famiglia: volere è potere.

**Ruggero, Marilù** e i **cognati** tutti, siete la mia famiglia romana, vi ringrazio per avermi sempre fatta sentire apprezzata, è stato fondamentale per me, non immaginate quanto!

Vorrei ringraziare **Riccarda**, per essermi amica/sorella e perchè lei sola può capire a pieno il perchè di questa mia avventura dottorale.

E poi **Valerie, Federica e Sabina** semplicemente perchè ci siete sempre!!!!

Un grazie particolare a **Maria**, da quel lontano settembre 1988, quando mi introducesti e mi facesti appassionare alla ricerca…. mentore, collega, ma soprattutto amica!

Non posso dimenticare **Anna Trentalance** la Prof., come l'ho sempre chiamata, mi ha insegnato molto e soprattutto mi ha condotto nel fantastico mondo del colesterolo!

Che dire di **Filippo**? Da studente a collega, un continuo confronto costruttivo!

**Laura, Marco S., Veronica**, i miei amatissimi dottorandi e qualcosa di più, anzi molto di più. Sono cresciuta insieme a voi! Grazie!

**Marco F., Manuela, Claudia, Florenzia** vorrei abbracciarvi tutti! Ogni mattina quando entro in dipartimento lo faccio col sorriso perché ci siete voi!!!!

E poi **Viviana**, collega e amica! Mi hai incoraggiata a fare quello che molti hanno definito una inutile stupidaggine. Mi stai sempre vicina nei momenti di allegria ma anche in quelli di sconforto, lavorativi e non. Grazie!

Ultimo, ma non per importanza, **Frank**. Mi hai dato la possibilità di fare questa bellissima esperienza, grazie per i preziosi consigli, per la pazienza e la professionalità che sempre dimostri.